Technische Universität Dresden

Signal Pre-Processing in the Downlink of Spread-Spectrum Communications Systems

(Signalvorverzerrung im Downlink von Spreizspektrum-Nachrichtensystemen)

André Noll Barreto

Der Fakultät Elektrotechnik der Technischen Universität Dresden

zur Erlangung des akademischen Grades eines

Doktoringenieurs

(Dr.-Ing)

vorgelegte Dissertation

ACKNOWLEDGMENTS

I would like to thank my advisor, Prof. Gerhard Fettweis, for his guidance and motivation during the last four years. Thanks also to the whole staff of the Chair for Mobile Communications Systems for the friendly and stimulating work environment, and special thanks to Achim Nahler, Matthias Stege and Ralf Irmer for giving me some important suggestions for the final manuscript.

I would also like to thank Prof. José Roberto Boisson de Marca from PUC in Rio de Janeiro for encouraging me to travel all the way across the Atlantic Ocean for this challenge. Thanks also to Capes in Brazil and to BMBF in Germany for the financial support.

Finally I would like to thank my wife Cintia for the emotional support and my daughter Nina for just being born and filling my life of gladness.

ABSTRACT

The traffic demand in mobile communications systems is expected to increase very rapidly in the near future, especially for downstream applications. This poses the communications engineer with the task of designing systems with increased capacity in order to satisfy future systems requirements.

In this work we investigate some capacity enhancing techniques for the downlink of Code Division Multiple Access (CDMA) systems. These techniques are based on the precoding of the transmitted signal relying on knowledge of the channel impulse response before transmission. This a priori channel state information can be obtained for instance in Time Division Duplexing (TDD) systems, since in this case the same channel is used both in up- and downlink, provided the channel does not change too much within a TDD duplex frame.

Spread spectrum systems provide us with diversity in frequency selective channels and one common method to exploit this diversity is to employ a Rake receiver. If maximum ratio combining is used, this technique amounts to a channel matched reception filter, which, according to the theory, maximises the signal-to-noise ratio at the receiver. If the transmitter has knowledge about the channel state information, then the channel matched filtering can be performed before transmission instead. This pre-filter is called a pre-Rake, and by applying this technique we can dispense with the Rake receiver with no performance loss in the presence of noise, thus simplifying the receiver design. This is particularly useful in the downlink since the complexity can be then transferred from the mobile terminals to the base station, where costs and power consumption are not as critical. Despite the lower mobile station complexity, the pre-Rake can even increase the downlink capacity under certain capacities, particularly in channels with severe multipath distortion and if part of the spreading gain is used for channel coding. The system capacity with a pre-Rake will be analysed here.

Due to the channel matched pre-filtering performed by a pre-Rake the signal power is concentrated where the channel is most favourable, what is similar to the principle of water filling for maximisation of the channel capacity. Because of that, a reduction in the signal-to-noise ratio in the presence of Gaussian noise can be achieved at the receiver if, besides a pre-Rake, the signal is processed at the receiver by a post-Rake, which is similar to a conventional Rake receiver, except that it is matched to the combination of pre-Rake and channel. The performance gain that can be achieved with a post-Rake will be investigated both in a single user and in multiuser scenarios.

With a pre-Rake the pre-distortion is made for each user individually and the multiuser interference is not considered. In the downlink we can however jointly precode the transmitted signal with the goal of reducing or even eliminating the multiuser interference. Several such joint precoding algorithms will be investigated. We will start with linear block precoding techniques that achieve a complete elimination of the multiuser interference. This is however in most cases only possible with a substantial increase in the transmit power or with a reduction of the signal-to-noise ratio. An iterative method that minimises the interference with power constraint was also developed, which yields better results in heavily loaded systems with a noisy channel. We will show that joint precoding can also be performed bitwise with a substantial reduction in complexity and negligible performance loss in comparison to blockwise techniques.

CONTENTS

1. INTRODUCTION

Mobile communications services have been available for several decades, but their use was limited to a few people, due to the capacity restraints imposed by a limited available bandwidth. It was only with the concept of frequency reuse in a cellular system that this basic hurdle could be overcome. The first cellular mobile communications systems were deployed in the early 80's with several different national or regional standards, such as the North-American AMPS (Advanced Mobile Phone System), the British TACS (Total Access Communications System) and the Scandinavian NMT (Nordic Mobile Telephone) [32]. Even though not compatible, all the first generation systems shared the same principles: analog modulation and Frequency Division Multiple Access (FDMA).

The demand for mobile communications services has been increasing rapidly since then, and the analog systems were soon not able to satisfy the new traffic requirements. Second generation systems based on digital modulation were developed and are in operation since the early 90's. These systems not only have a much higher capacity in relation to the analog ones, but also support limited data services, whereas the analog systems were restricted to speech transmission. Most of these second generation systems, such as the North-American IS-136, the European GSM (Global System for Mobile Communications) and the Japanese PDC (Personal Digital Cellular) rely on Time Division Multiple Access (TDMA) combined with FDMA [32], but a system based on spread spectrum techniques and Code Division Multiple Access (CDMA) combined with FDMA was suggested by Qualcomm and adopted as an alternative digital standard (IS-95) [36] in the United States.

CDMA has several advantages compared to orthogonal channel assignment schemes, such as TDMA and FDMA. Some of them are listed below:

- Spread spectrum signals -which are implied by the use of CDMA- are resilient to fading multipath channels, which are characteristic for mobile communications systems. The expanded bandwidth provides us with a means to obtain signal diversity in frequency-selective channels.
- All cells can use the same frequency band and hence a frequency reuse factor nearly equal to one can be achieved. This reduces the need for frequency planning and facilitates the deployment of new base stations.
- CDMA systems have a soft capacity. There is no hard limit on the system capacity, the Quality of Service(QoS) degrades gracefully with an increase in the traffic instead.
- During a telephone call each user is active only part of the time, and the transmission can be suspended when the user is not actively speaking. The use of discontinuous transmission for capacity increase in TDMA or FDMA requires complex channel assignment protocols, and these are not needed in CDMA.
- CDMA can provide a large capacity in a multi-cell environment [17,38]. Even though the first commercial CDMA mobile communications systems (IS-95) could not stand up to its claims of higher capacity in relation to TDMA systems, the use of new techniques such as joint detection, and, as we will see in this work, signal pre-processing can substantially increase the capacity and bring the system performance closer to its theoretical limits.

Due to the advantages listed above, CDMA is the preferred technique for future mobile communications systems, being chosen as the multiple access technique for the third generation system IMT-2000 (International Mobile Telecommunications - 2000) [9,19], scheduled to be deployed in the next few years.

The maximisation of the system capacity is one of the most important issues for the network operators, since it is directly related with the number of active users in the system, and consequently, with the revenue. Systems with large capacity are also needed if the growing demand for mobile communication services, both in terms of number of users and of required data rate, has to be satisfied.

Initial belief was that the downlink capacity in CDMA systems was greater than in the uplink [39], but some more recent studies [42] show that in practice the opposite can be observed, and the downlink can be the limiting link in terms of capacity for CDMA systems. This is due to several facts:

- The importance of downlink power control has been often neglected. Even though the requirements are not as harsh as in the uplink, a more efficient power control scheme is needed in the downlink, since different users are differently affected by the inter-cell interference depending on their position, not to mention the different impairments caused by the different multipath profiles.
- Soft handover may increase the capacity in the uplink, but in the downlink it implies that the same signal can be transmitted from several base stations at the same time, increasing the downlink interference, and hence reducing the capacity [4].
- Multipath propagation reduces the effectiveness of the orthogonal codes usually used for multi-user transmission in the downlink. This tends to be aggravated in future broadband systems, which are likely to have more resolvable multipath components than in current systems.

The imbalance between up- and downlink capacity is made even greater if we consider that, unlike conventional voice telephony, many new services, such as internet browsing and video on demand, are likely to be strongly asymmetrical, and that the traffic in the future tends to be much higher in the downlink, as it can be seen in Fig. 1.1. This implies that particularly the downlink capacity must be increased to accommodate the expected traffic, and the investigation of methods that help us achieve this is the main goal of this work.

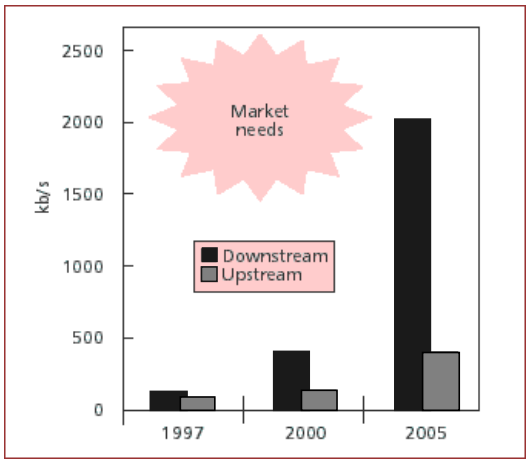

Fig. 1.1 - Capacity Requirements Forecast [9]

In future communication systems the use of multi-user detection is envisaged to increase the capacity, but its use is more likely in the uplink only. The high complexity of this technique implies higher receiver costs and higher power consumption. This is not a serious problem for its implementation at the base station, but makes its implementation prohibitive for a mobile station, where a simple and cheap modem is required. In this work we will concentrate on techniques that require no complex algorithms at the mobile station receivers. Instead, the system complexity will be transferred to the base station, where complexity and power consumption are not such a critical issue. This approach also helps to reduce the overall system cost, since the complexity is concentrated in a few base stations that are active most of the time, as opposed to a system with many costly mobile units that are idle most of the time.

The following paragraphs briefly describe the structure of this work.

In CDMA systems part of the bandwidth expansion can be accomplished using error correcting codes and part of it by multiplying the information signal by a spreading code with larger bandwidth, e.g. with orthogonal Walsh-Hadamard sequences. It is however not clear from the literature to which extent error correcting codes should be employed for signal spreading in order to maximise the capacity. This issue will be addressed in Chapter 2, and the implications from this investigation will be used in the following chapters. It should be noticed here that in this chapter and in this whole work Direct Sequence Spread-Spectrum (DS-SS) only will be examined, but with some modifications the investigations performed herein should also apply to other spread spectrum techniques, such as Frequency Hopping Spread Spectrum (FH-SS) or Multi Carrier Spread Spectrum (MC-SS).

Another technique that has been increasingly popular is Time Division Duplexing (TDD), in which the same carrier is used for both links in different time slots. This is currently employed in the DECT (Digital European Cordless Telecommunication) cordless system [32] and is proposed for one transmission mode of the third generation system IMT-2000 [9,19]. One property of such systems is that, as the same frequency is used, the channel transfer function is nearly the same in both transmission directions, provided the channel does not change too rapidly. This means that the channel estimates obtained upon reception are also valid for transmission, i.e., we know the channel impulse response before transmission. The same can be achieved in Frequency Division Duplex (FDD) systems if the channel state in the downlink is transmitted to the base station via an uplink signalling channel. This is only feasible if the channel changes slowly in order to keep the signalling load to a minimum. This is particularly the case in Wireless Local Loop (WLL) systems, in which the users terminals are fixed or portable.

The a priori channel state information (CSI) can be used to achieve multipath diversity gain using signal pre-processing at the transmitter, instead of employing a Rake receiver at the mobile station. This technique is known as pre-Rake [11,12]. With a pre-Rake transmitter at the base station, the mobile station needs just a conventional integrate-and-dump receiver instead of a more complex Rake receiver, and can be kept simple and cheap; the signal processing is transferred to the base station, where complexity is not such an important issue. Another advantage of the pre-Rake is that capacity increase can be obtained in the downlink under certain circumstances, what is particularly important if the need for higher capacity in the downlink is considered, as discussed above.

In Chapter 3 we will investigate the performance of a system using a pre-Rake both analytically and through simulation. A comparison will be made with a conventional system employing Rake receivers only and we will show that the downlink capacity can be increased with less complexity at the mobile receiver when a pre-Rake is employed at the base station transmitter. However, one major problem with the pre-Rake is that it suffers performance

degradation in fast-changing channels, since the channel estimates used for transmission in the downlink are obtained upon reception in the previous uplink period, and the channel may change in this time interval. The sensitivity of the pre-Rake to time-variant channels will also be investigated and the means to overcome this problem will be proposed.

We will see in Chapter 3 that the performance of the pre-Rake in a single-user environment and ideal channel estimation is the same as with a Rake receiver. With a pre-Rake however, the signal is transmitted with a channel matched pre-filter, and consequently more power is allocated in the frequency ranges where the channel is more favourable. This is in principle similar to the optimum water-filling technique [10], and we can hence expect that a better performance can be obtained with pre-Rake transmission. In order to achieve that, a Rake receiver matched to both the channel and the pre-Rake has to be implemented in the mobile station. We call this receiver a post-Rake. We will examine its performance in Chapter 4, and see that further performance improvements can be obtained this way with low additional complexity at the mobile station.

Besides knowing the channel characteristics before transmission, what we assume for TDD systems, the base station has also knowledge of all the users' signals and codes. We can use this information to shape the transmitted signal such that the system performance is optimised, i.e., we can jointly pre-process the signal from all users. This is a promising approach, which has been investigated in several papers recently [3,8,35,40]. In Chapter 5 joint precoding methods, both blockwise and bitwise, are presented and investigated. We will show that a substantial capacity increase can be reached by theses method with no further complexity at the mobile station.

2. On How to Spread the Signal

In multiple access spread spectrum communications there are basically two ways to increase the signal bandwidth: either with error correcting codes or with conventional spreading, whereas by the latter we understand multiplying the information signal by a spreading signal with larger bandwidth. It has been proven [20,37] that if multi-user detection is employed and no orthogonal spreading is used the signal should be optimally spread entirely by an error correcting code. However, as already mentioned in the Introduction, multi-user detection is somewhat complex for implementation at the mobile station and therefore unsuitable for the downlink.

In the downlink we can make use of the fact that all users from the same cell transmit synchronously and assign to each user one of a set of orthogonal codes, which will be used for signal spreading. These can be obtained for instance from a Hadamard-Walsh matrix[1]. However, due to the multipath propagation typical for the mobile radio channel some of the orthogonality is lost, such that multi-user interference inevitably arises. Furthermore, in cellular systems the signal is also affected by thermal noise and by interference from the neighbouring cells. Users from different cells are not synchronous at chip level and thus we cannot make use of orthogonal sequences for intercell interference reduction. In order to offer some protection against these impairments, some sort of error correcting code should be employed, but this entails a larger transmission rate, and hence a smaller spreading gain is available for orthogonal spreading.

We must therefore reach a compromise between the gains obtained by channel coding and by orthogonal spreading. The IS-95 [36] system, for instance, employs a combination of both methods in the downlink: the data bits are coded with a convolutional code of rate R=1/2 and the coded bits are further spread with orthogonal sequences of length 64 separately in the in-phase and quadrature components, thus achieving a total spreading gain of 128 chips/bit. It is nevertheless not clear from the available literature which is the optimal ratio between channel coding and orthogonal spreading. This problem will be addressed in this chapter, and the optimum parameters obtained here will be employed in the following chapters.

We will start by a short system description in Section 2.1 and follow with a system performance analysis in Section 2.2, both for a single user and in a multi-user environment. Finally in Section 2.3 some results for a multi-user scenario will be presented and commented.

2.1. System Description

2.1.1 Coding and Modulation

We consider a spread spectrum system with bandwidth $W=1/T_c$, where T_c is the period of a complex chip. The processing gain is $G=T_b/T_c$, where T_b is the period of a data bit. The data bits are encoded with a convolutional code of rate R and memory order m_o [27], with $R \geq \frac{1}{G}$;

1. The Hadamard-Walsh matrix H_K provides us with K binary orthogonal sequences of length K, with K a power of 2. Starting by H_1=1, the higher order matrices can be obtained by the following recursive equation: $[H_{2k}] = \begin{bmatrix} H_k & H_k \\ H_k & -H_k \end{bmatrix}$.

and the coded bits are repeated $M=GR$ times. Let $d(i)=\pm 1$ denote the output of this operation. This signal is multiplied by the complex scrambling code $c(i)=\pm 1 \pm j$ to obtain the discrete-time baseband signal:

$$x(i) = \sqrt{\frac{E_c}{2}} d(i)c(i) \tag{2.1}$$

where E_c is the chip energy.

It should be noticed here that this corresponds to the use of two different binary codes $c_R(i)$ and $c_I(i)$ in the in-phase and quadrature components respectively, such that $c(i)=c_R(i)+jc_I(i)$. The transmitter can be visualised in Fig. 2.1.

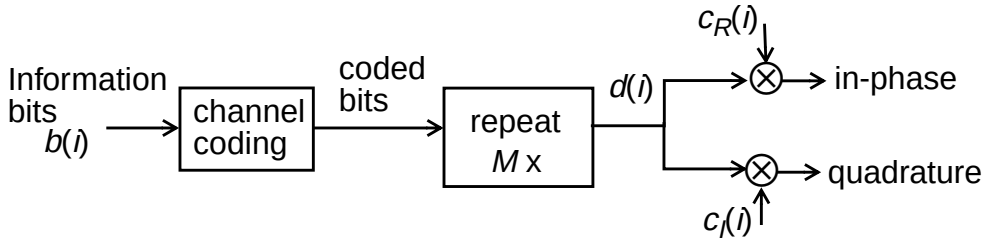

Fig. 2.1 - Transmitter Model

This signal corresponds also to the QPSK modulation (Quaternary Phase-Shift Keying) of the sequence obtained with the multiplication of the coded bits by an equivalent binary spreading sequence.

2.1.2 Channel Model

We will consider a baseband time-variant frequency selective channel model, which is widely used for the modelling of wideband radio communications systems. Considering a channel with bandwidth $W=1/T_c$, the channel impulse response can be given by [31]:

$$h(t;\tau) = \sum_{l=0}^{L-1} g_l(t)\delta(\tau - lT_c) \tag{2.2}$$

where L is the number of resolvable[1] paths with gains $g_l(t)$, which we assume are uncorrelated complex stochastic processes.

Each resolvable path is composed by the sum of a number of time-variant versions of the signal with different amplitudes and phases, which result from different scatterers. The signals with different phases may add up constructively or destructively, and as the mobile moves the phases change, which causes a variation in time of the resulting signal amplitude. This is responsible for the so called fast fading. If the number of such scatterers is large, then the central limit theorem leads to a gaussian process model for the complex gain $g_l(t)$. If the process has zero mean, then the envelope $|g_l(t)|$ is Rayleigh distributed [31,34] with mean $\bar{g}_l$, and the phase $\angle g_l(t)$ is uniformly distributed in the interval $[0,2\pi)$. Besides the Rayleigh fading, the channel may also have one strong line-of-sight (LOS) component, also called specular component, which does not fade, in which case the envelope $|g_l(t)|$ has a Rice distribution [31,34] with parameter K_{Rice}[2].

1. The channel is actually continuous in τ, the resolvable chip-spaced paths from (2.2) arise from the receive filter with bandwidth $W=1/T_c$ [31].

Slow fading will not be considered here, we assume instead that the channel has a fixed delay profile defined by the number of paths, the average power $\bar{g}_l^2$ and the probability distribution (Rayleigh or Rice) of each path.

Throughout the analysis we will be concerned with the discrete-time representation of the signal with sampling interval equal to T_c. We assume that the channel varies slowly in relation to the symbol rate, and, unless otherwise stated, that it remains constant throughout a transmission frame. Ideal synchronisation and channel estimation are also assumed. With these assumptions we can express the channel from (2.2) by the equivalent following time-invariant discrete-time channel model:

$$h(i) = \sum_{l=0}^{L-1} g_l \delta(i-l) \tag{2.3}$$

where we assume that the path gains g_l are independent complex random variables with Rayleigh or Ricean distribution.

We assume that the transmission and reception filters are matched and have unit energy. The filters obey the Nyquist criterion and the signal is ideally sampled, so that no inter-symbol interference arises from the filtering. We can thus assume that, if the complex discrete signal before the transmission filter is $s(i)$, the sampled signal after the reception filter can be given by:

$$r(i) = \sum_{l=0}^{L-1} g_l s(i-l) + \nu(i) \tag{2.4}$$

where $\nu(i)$ is the thermal noise, which is a complex white gaussian variable with complex variance N_0.

The channel can be represented by a tapped delay line, as displayed in Fig. 2.2.

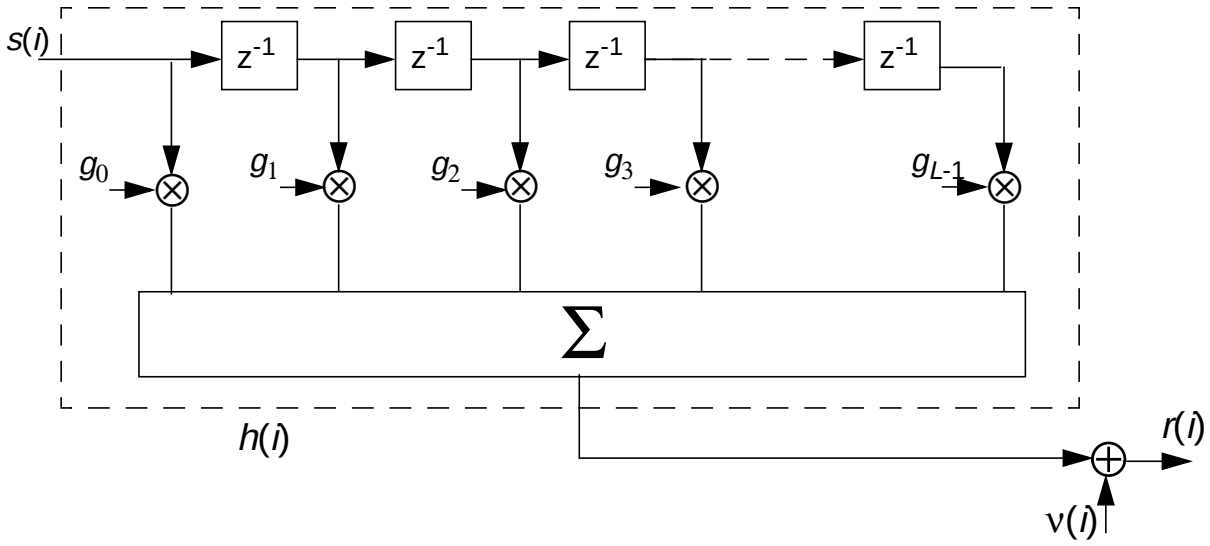

Fig. 2.2 - Multi-path Channel Model

2. The factor K_{Rice} is the power ratio between the LOS component and the Rayleigh component

2.1.3 The Rake Receiver

The channel described above provides the receiver with independently faded copies of the transmitted signal with different time delays, and we can make use of these to obtain signal diversity in fading channels.

This can be done in spread spectrum systems by employing a Rake receiver [31]. In this technique we generate several delayed replicas of the received signal and correlate them with the spreading code. The receiver assumes the form of a tapped delay line and it is depicted in Fig. 2.3. The taps are called Rake fingers and each one of them is synchronised to a channel path. We can neglect the inter-symbol interference caused by the unsynchonised delayed copies of the signal if we assume that the autocorrelation characteristics of the spreading code are nearly ideal[1], what can be taken for granted for large processing gains (see Section 4.2).

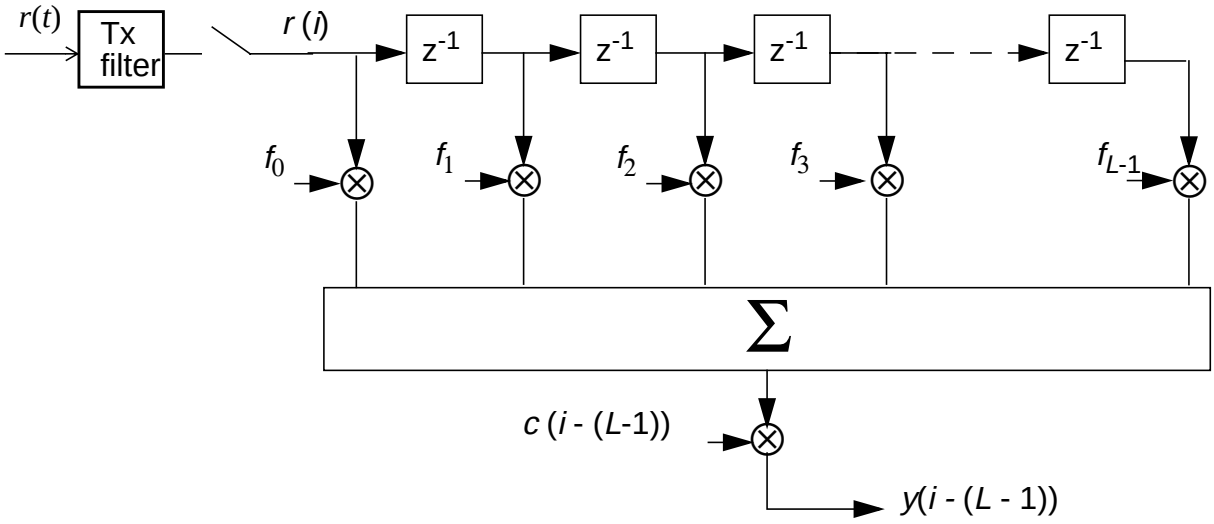

Fig. 2.3 - Rake receiver

There are several different ways in which we can combine the different signals, i.e., several ways to chose the gains f_l of the different Rake fingers. It is well known that the optimum performance in relation to the maximisation of the signal-to-noise ratio can be achieved with maximum ratio combining [31], which corresponds to a channel matched filter. In this case[2] $f_l = g_{(L\text{-}1\text{-}l)}^*$, where g_l^* is the complex conjugate of g_l. Throughout this work we will always consider maximum ratio combining, unless otherwise stated.

In a system with a Rake receiver the modulated signal is transmitted without further processing, i.e., $s(i)=x(i)$. We can thus assume that signal from (2.1) is sent through the channel described in (2.4). The received signal is given by:

---

1. Let $r(\tau)$ be the correlation over G symbols of the code $c(i)$, $r(\tau)=\sum_{i=0}^{G-1}\{\mathrm{Re}[c(i)]\mathrm{Re}[c(i-\tau)]+\mathrm{Im}[c(i)]\mathrm{Im}[c(i-\tau)]\}$.
   The correlation is ideal if $r(\tau) = \begin{cases} 2G & , \text{if } \tau = 0 \\ 0 & , \text{if } \tau \neq 0 \end{cases}$. Nearly ideal correlation means that $r(\tau)<<2G$ if $\tau \neq 0$.
2. The channel matched filtering corresponds to the time-inversion of the complex conjugate channel coefficients

$$r(i) = \sqrt{\frac{E_c}{2}} \sum_{l=0}^{L-1} g_l x(i-l) + \nu(i) = \sqrt{\frac{E_c}{2}} \sum_{l=0}^{L-1} g_l d(i-l)c(i-l) + \nu(i) \quad (2.5)$$

We assume that the receiver can obtain perfect channel estimations and that all resolvable paths are used by the Rake receiver. This assumption implies that the signal phase can be ideally estimated and hence coherent demodulation can be performed. Let $r(i)$ be the sampled received signal and $c(i)$ the complex spreading code. The discrete-time output of a Rake receiver with maximum ratio combining can be expressed by the following equation[1]:

$$y(i) = \sum_{m=0}^{L-1} (g_m^* r(i+m)) \otimes c(i) \quad (2.6)$$

with g_m^* the complex conjugate of g_m. The operator $\otimes$ means that the real and imaginary parts are correlated separately, i.e., given any complex numbers a and b,

$$a \otimes b = \mathrm{Re}[a]\mathrm{Re}[b] + j\mathrm{Im}[a]\mathrm{Im}[b] \quad (2.7)$$

This operation is required since according to the transmission model from Section 2.1.1 we are in fact multiplying the coded bits by two different scrambling sequences in the in-phase and in the quadrature components[2], instead of performing a complex multiplication of the QPSK data signal by a complex code.

Substituting equation (2.5) into (2.6) we obtain the following expression for the Rake receiver output:

$$y(i) = \sqrt{\frac{E_c}{2}} \sum_{m=0}^{L-1} \sum_{l=0}^{L-1} (g_m^* g_l d(i-l+m)c(i-l+m)) \otimes c(i) + \nu_{Rk}(i) \quad (2.8)$$

where

$$\nu_{Rk}(i) = \sum_{m=0}^{L-1} (g_l^* \nu(i+m)) \otimes c(i) \quad (2.9)$$

is the complex gaussian noise component after the Rake receiver with complex variance

$$\mathrm{var}\{\nu_{Rk}\} = N_0 \sum_{m=0}^{L-1} |g_m|^2 \quad (2.10)$$

These expressions will be used in the next Section to obtain the system performance.

---

1. The Rake receiver is usually described by the causal expression $y'(i) = \sum_{m=0}^{L-1} (g_m^* r(i)) \otimes c(i-m)$. The non-causal expression from (2.6) is an alternative way to write the same signal which facilitates the posterior analysis, since the signal integration to be performed later can be then made over the same indices for all Rake fingers.
2. This is the approach taken for instance by IS-95 [36]

2.2. Performance Analysis

In this section we will analyse the performance of a Rake receiver in a multipath channel with white Gaussian noise for the system described above, first for a single user and then in a multi-user environment.

2.2.1 Single User

As already mentioned, we consider a system in which the spreading gain is partially used for coding. Let z be the integration over M=GR chips of the Rake receiver output signal from (2.8), i.e.,

$$z = \sum_{i=0}^{M-1} y(i) \tag{2.11}$$

According to the description in Section 2.1.1, the data bit $d(i)$ is constant during the M integration chips, so that the index i can be removed. By substituting (2.8) into (2.11) the variable z is:

$$z = M\sqrt{\frac{E_c}{2}}\sum_{l=0}^{L-1}|g_l|^2(1+j)d + \nu_{self} + \nu_G, \tag{2.12}$$

where ν_{self} is the self-interference, or inter-symbol interference

$$\nu_{self} = \sqrt{\frac{E_c}{2}}\sum_{i=0}^{M-1}\sum_{l=0}^{L-1}\sum_{\substack{m=0\\ m\neq l}}^{L-1}(g_m^* g_l d(i-l+m)c(i-l+m))\otimes c(i), \tag{2.13}$$

which can be ignored for the large spreading gains common in spread spectrum systems; and ν_G is the complex gaussian noise component

$$\nu_G = \sum_{i=0}^{M-1}\nu_{Rk}(i) \tag{2.14}$$

with variance

$$\mathrm{var}\{\nu_G\} = M\mathrm{var}\{\nu_{Rk}\} = MN_0\sum_{l=0}^{L-1}|g_l|^2. \tag{2.15}$$

To simplify the analysis let d=1. The decision variable v before the decoder will be the sum of the real and complex parts of the integral sum z, i.e.,

$$v = \mathrm{Re}[z] + \mathrm{Im}[z] = \bar{v} + \nu_{dv}, \tag{2.16}$$

where $\bar{v}$ is the mean of the decision variable, which corresponds to desired signal:

$$\bar{v} = M\sqrt{2E_c}\sum_{l=0}^{L-1}|g_l|^2 \tag{2.17}$$

and ν_{dv} is the real-valued noise component of the decision variable, which is the sum of the real and imaginary parts of the complex noise ν, i.e., ν_{dv}=Re[ν_G]+Im[ν_G]. It can be assumed that Re[ν_G] and Im[ν_G] are identically distributed independent random variables, and hence the variance of the real-valued noise ν_{dv} is equal to the complex variance var{ν_G} of the complex noise ν_G, which is given by (2.14).

For a given channel state, which is represented by a certain channel vector $\boldsymbol{g}$=[g_0, g_1,...., g_{L-1}], the bit error probability is a function F_e(.) of the ratio $\frac{\bar{\nu}}{\sqrt{\text{var}\{\nu_G\}}}$, i.e

$$\text{BER}(\boldsymbol{g}) = F_e\left(\frac{\bar{\nu}}{\sqrt{\text{var}\{\nu_G\}}}\right) = F_e(\sqrt{2R\Gamma(\boldsymbol{g})}). \tag{2.18}$$

$\Gamma(\boldsymbol{g})$ is the bit-energy-to-noise-spectral-density ratio after Rake processing:

$$\Gamma(\boldsymbol{g}) = \frac{E_b \sum_{l=0}^{L-1} |g_l|^2}{N_0}, \tag{2.19}$$

where E_b=GE_c is the bit energy.

For a system with no channel coding (R=1) the bit error rate is given by the modified error function Q(.), i.e., F_e(.)=Q(.), with

$$Q(\alpha) = \frac{1}{\sqrt{2\pi}} \int_{\alpha}^{\infty} e^{-x^2/2} dx, \tag{2.20}$$

and we obtain the same result as in [31] for the link performance of an uncoded QPSK system.

When convolutional channel coding is considered, its behaviour can be described by a state diagram and an equivalent trellis. These are represented by the code transfer function [15]

$$T(D, I) = \sum_{d=d_{free}}^{\infty} a_d D^d I^{f(d)}. \tag{2.21}$$

Each term in the above summation represents one path in the decoder trellis that leaves the all-zero state and merges with it again at a given node. The exponent d indicates the Hamming weight of the coded sequence and the exponent $f(d)$ stands for the Hamming weight of the information bit sequence that corresponds to the represented path. The coefficient a_d is also known as complete path enumerator, and indicates the number of times that paths with the same coefficients may occur. d_{free} is the minimum free distance of the code and it denotes the minimum Hamming distance of a path that returns to its original state.

An analytical solution for the bit error rate with convolutional codes is not possible, but a good approximation to the bit error rate function F_e(.) at high signal-to-noise ratios (SNR) can be obtained by the union bound [15]:

$$F_e(\sqrt{2R\Gamma(\boldsymbol{g})}) \le \sum_{d=d_{free}}^{\infty} \zeta_d Q(\sqrt{2dR\Gamma(\boldsymbol{g})}), \tag{2.22}$$

where the coefficients ζ_d are obtained by taking the derivative of the code transfer function in relation to I for I=1:

$$\left.\frac{d}{dI}T(D,I)\right|_{I=1} = \sum_{d=d_{free}}^{\infty} a_d f(d) D^d = \sum_{d=d_{free}}^{\infty} \zeta_d D^d . \tag{2.23}$$

This upper bound is very tight for high SNRs but it is however too pessimistic for low SNRs, and for this latter situation there is to our knowledge no reliable approximation to the bit error rate. Since we are dealing with a Rayleigh-faded environment, low SNRs will occur with a certain probability, so that an accurate calculation of the bit error rate is also needed for this case.

The following approach has to be taken instead. For low SNR values the error function can be obtained by simulation and approximated by a polynomial. Since reliable simulation results are difficult to obtain for very low bit error rates, for SNR values beyond a threshold Γ_{Thresh} the union bound can be used. An example for a maximum free distance convolutional code of rate R=1/8 and memory order m_o=8 can be seen in Fig. 2.4, where a 6-th order fitting polynomial was used. The code generator polynomials, its distance spectrum and the fitting polynomial are given in Appendix A. It should be noticed that the threshold beyond which the union bound can be accurately used was obtained empirically, and it depends not only on the code parameters (rate, memory order) but also on the numbers of terms taken from the distance spectrum. This threshold is also given in Appendix A.

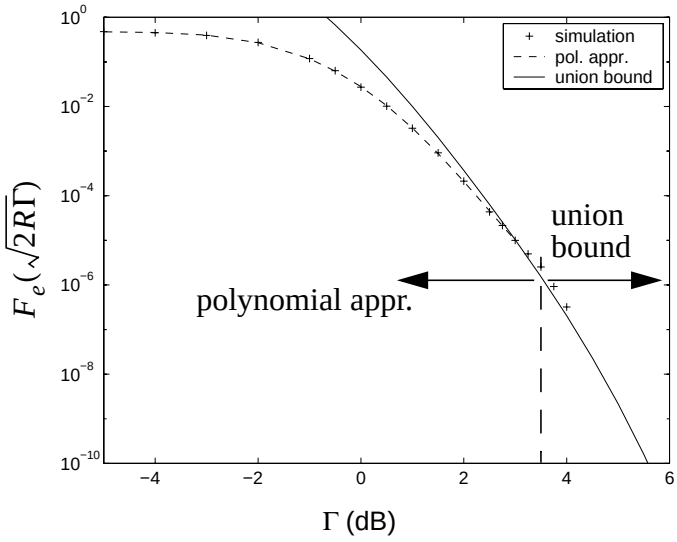

Fig. 2.4 - Performance of a Convolutional Code (R=1/8, m=8)

The above analysis provides us with the instant bit error rate for a particular channel state. If we know the channel probability distribution $p(\boldsymbol{g})$ we can obtain the average bit error probability by performing the following integration:

$$\overline{\mathrm{BER}} = \int p(\boldsymbol{g})\mathrm{BER}(\boldsymbol{g})d\boldsymbol{g}. \tag{2.24}$$

The analytical solution of (2.24) is not feasible, unless no coding is considered, in which case the solution is given in [31]. For a more general solution we should take a semi-analytical approach. The path gains g_l are zero-mean independent complex random variables, and the

power delay profile is such that the average power at the receiver is equal to the transmitted power. Then, according to the desired power delay profile, the path gains are randomly chosen and the instant signal-to-noise ratio is obtained from equation (2.19). This is mapped to an instant bit error rate, e.g. as in Fig. 2.4. This procedure can be repeated many times and the results should be averaged to obtain the mean bit error rate.

In Fig. 2.5 we see that the results obtained through this procedure are very similar to the ones from simulation. We have considered a system with error correcting code like in Fig. 2.4, processing gain G=128 chips/bit, and two different channel models. The first model corresponds to a severe multipath environment, with six chip-spaced multipaths, which are all Rayleigh faded, and the mean path gains decay exponentially with the delay. The second model has only two multipaths of same average power, but the first path has a strong LOS component and is Ricean distributed with factor K_{Rice}=10dB. The channel delay profiles are given in Table 2.1. Fig. 2.5 also shows the results for an additive white gaussian noise (AWGN) channel and for a Rayleigh faded channel without diversity.

delay	0	T	$2T$	$3T$	$4T$	$5T$
severe multipath, 6 paths	$\bar{g}_0^2$ = 0,35 (0dB) Rayleigh	$\bar{g}_1^2$ = 0,24 (-1.6dB) Rayleigh	$\bar{g}_2^2$ = 0,17 (-3.2dB) Rayleigh	$\bar{g}_3^2$ = 0,11 (-4.8dB) Rayleigh	$\bar{g}_4^2$ = 0,08 (-6.4dB) Rayleigh	$\bar{g}_5^2$ = 0,05 (-8.0dB) Rayleigh
strong LOS component, 2 paths	$\bar{g}_0^2$ = 0,5 Rice (K_{Rice}=10dB)	$\bar{g}_0^2$ = 0,5 Rayleigh				

Table 2.1 - Channel Delay Profile

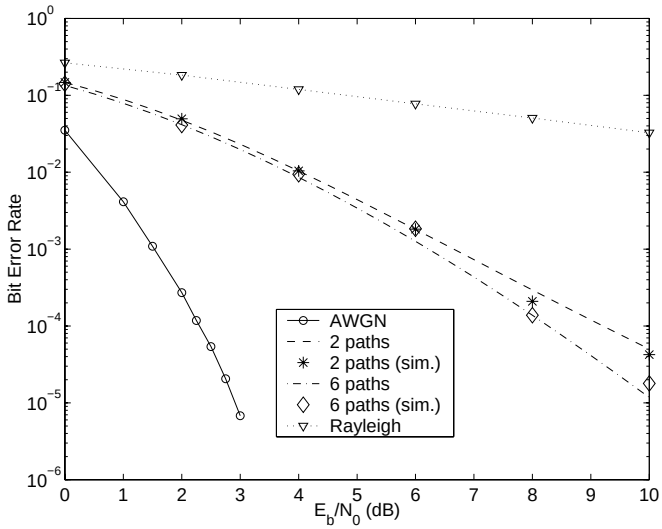

Fig. 2.5 - Single User Performance with a Rake receiver

2.2.2 Multi-user Environment

In this section we extend the analysis from the previous section to a multi-user environment. Unlike the single user analysis, which was valid for both up- and downlink, the multi-user analysis will be performed for the downlink only, where synchronous transmission can be assumed.

The transmitted signal is the sum of the modulated signal of all users. Assuming that the same power is allocated to every user, the transmitted signal is

$$s(i) = \sum_{k=0}^{K-1} x_k(i) = \sqrt{\frac{E_c}{2}} \sum_{k=0}^{K-1} d_k(i) c_k(i), \tag{2.25}$$

where K is the number of users. d_k, c_k and x_k are respectively the information symbol, the scrambling code and the modulated signal from user k, as defined in Section 2.1.1.

Let $g_{k,l}$ be the complex gain of the l-th path of the channel from the base station to the mobile user k. The received signal at user p is:

$$\begin{aligned} r_p(i) &= \sum_{l=0}^{L-1} g_{p,l} s(i-l) + \nu(i) \\ &= \sqrt{\frac{E_c}{2}} \sum_{k=0}^{K-1} \sum_{l=0}^{L-1} g_{p,l} d_k(i-l) c_k(i-l) + \nu(i) \end{aligned} \tag{2.26}$$

With no loss at generality we will investigate the performance of user 0. The operation of the Rake receiver described by equation (2.6) is the same as for a single user environment, and once again the signal is integrated over M symbols as in (2.11). The integrated signal is however now given by

$$z_0 = M \sqrt{\frac{E_c}{2}} \sum_{l=0}^{L-1} |g_{0,l}|^2 (1+j) d + \nu_{self} + \nu_{mu} + \nu_G, \tag{2.27}$$

where ν_{self} is the self-interference given by (2.13) and ν_G the white gaussian noise with variance given by (2.15). Additionally, we have now the multi-user interference:

$$\begin{aligned} \nu_{mu} = \sqrt{\frac{E_c}{2}} \sum_{i=0}^{M-1} \sum_{k=1}^{K-1} \sum_{l=0}^{L-1} \sum_{\substack{m=0 \\ m \neq l}}^{L-1} (g_{0,m}^* g_{0,l} d_k(i-l+m) c_k(i-l+m)) \otimes c_0(i) \\ + \sqrt{\frac{E_c}{2}} \sum_{i=0}^{M-1} \sum_{k=1}^{K-1} \sum_{l=0}^{L-1} (|g_{0,l}|^2 d_k(i) c_k(i)) \otimes c_0(i) \end{aligned} \tag{2.28}$$

As in Section 2.2.1, the channel coefficients $g_{k,l}$ are assumed to be constant during a frame, so that the randomness in the interference comes only from the signal components $(d_k(i-l+m) d_k(i-l+m)) \otimes c_0(i)$. It should be noticed that the summation terms in (2.13) and (2.28) are not statistically independent, which complicates the analysis. These terms are statistically dependent owing to the fact that several summation terms share the same signal components if they have the same delay $\lambda = l-m$. It is a common but non-negligible mistake to ignore this dependency. In order to obtain independent terms in the summations let us define the complex scrambled sequence

$$a_k(i) \equiv d_k(i)c_k(i)\,. \tag{2.29}$$

Then we can rearrange the interference components as

$$\nu_{self} = \sqrt{\frac{E_c}{2}} \sum_{i=0}^{M-1} \sum_{\substack{\lambda=-(L-1) \\ \lambda \neq 0}}^{L-1} \sum_{l-m=\lambda}^{l,m} (g_{0,m}^{*} g_{0,l} a_0(i-\lambda)) \otimes c_0(i) \tag{2.30}$$

and

$$\nu_{mu} = \sqrt{\frac{E_c}{2}} \sum_{i=0}^{M-1} \sum_{k=1}^{K-1} \left[\sum_{\substack{\lambda=-(L-1) \\ \lambda \neq 0}}^{L-1} \sum_{l-m=\lambda}^{l,m} (g_{0,m}^{*} g_{0,l} a_k(i-\lambda)) \otimes c_0(i) + \sum_{l=0}^{L-1} ((|g_{0,l}|^2 a_k(i))) \otimes c_0(i) \right] \tag{2.31}$$

Now the terms inside the summation over λ have all different delays, and we can assume that the asynchronous terms corresponding to a non-zero delay ($\lambda \neq 0$) are independent for different values of i. For the synchronous terms we must consider whether orthogonal sequences are used or not. If we employ orthogonal sequences, then the summation over M symbols of the synchronous term $\sum_{l=0}^{L-1} ((|g_{0,l}|^2 a_k(i))) \otimes c_0(i)$ in (2.31) is equal to zero.

With these considerations, and assuming that random codes are used, the variance of the interference terms can be expressed as (see Appendix B)

$$\mathrm{var}\{\nu_{self}\} = ME_c \sum_{\substack{\lambda=-(L-1) \\ \lambda \neq 0}}^{L-1} \left| \sum_{l-m=\lambda}^{l,m} g_{0,m}^{*} g_{0,l} \right|^2 \tag{2.32}$$

and

$$\mathrm{var}\{\nu_{mu}\} = (K-1)\mathrm{var}\{\nu_{self}\} + \alpha(K-1)ME_c \left[\sum_{l=0}^{L-1} |g_{0,l}|^2 \right]^2, \tag{2.33}$$

where α is the orthogonality factor, with $\alpha=0$ if the codes are orthogonal over M complex symbols and $\alpha=1$ otherwise. We have assumed that orthogonal codes behave like random codes if not synchronised, which is reasonable if the orthogonal codes are multiplied by a further random scrambling code, what we assume throughout this work.

We can assume that the self-interference and the multi-user interference are Gaussian random variables, which, based on the central limit theorem [29], is a good approximation for high processing gains (high G, hence high M) and a large number of users K. In analogy to a white noise process we may then define the power spectral density of the interference I_0, which, since ν_{self} and ν_{mu} are independent, is equal to:

$$I_0 = \frac{\frac{\mathrm{var}\{\nu_{self}\} + \mathrm{var}\{\nu_{mu}\}}{L-1}}{M \sum_{l=0} |g_{0,l}|^2} \tag{2.34}$$

The bit error rate can now be obtained as in a single user scenario, from equations (2.18) and (2.19), but this time substituting the noise density N_0 by N_0+I_0, i.e.

$$\Gamma(\boldsymbol{g}) = \frac{E_b \sum_{l=0}^{L-1} |g_l|^2}{N_0 + I_0} \tag{2.35}$$

The accuracy of the above analysis can be confirmed from Fig. 2.7 to Fig. 2.9 in the next section, where some of the semi-analytical results are compared with simulation results. In these simulations the signals of the interfering users have been really generated and not approximated by white gaussian noise.

2.3. Results

As mentioned previously, we must find a compromise between conventional spreading and channel coding. The use of error correcting codes usually involves bandwidth expansion, but this is not a major drawback in spread spectrum systems since the available bandwidth is much larger than the signal bandwidth anyway. Furthermore, such codes make the signal more resilient to noise or to the inter-cell interference, and the code performance increases as the coding rate is reduced.

Suppose we have a code of rate R that transmits with any desired error rate at the channel capacity [10], i.e.,

$$R = C = \frac{1}{2}\log_2\left(1 + \frac{E_{bc}}{N}\right) = \frac{1}{2}\log_2\left(1 + \frac{RE_b}{N}\right) \tag{2.36}$$

where E_b is the bit energy, E_{bc} the energy of a coded bit and N the noise variance. We can rewrite (2.36) to obtain the minimum signal to noise ratio required for error free transmission at a particular rate:

$$\left(\frac{E_b}{N}\right)_{min} = \frac{2^{2R}-1}{R} \tag{2.37}$$

The result from (2.37) is plotted in Fig. 2.6a, where we can see that a reduction of the coding rate brings a great performance gain at high rates. Nearly 2dB can be gained for instance if we reduce the rate from R=1 to R=1/2, but further halvings in the coding rate will bring smaller gains, e.g., less than 0.1 dB if we reduce the rate from R=1/16 to R=1/32. The same can be observed in practical coding schemes, as in Fig. 2.6b, where the performances in an AWGN channel of convolutional codes with different rates are compared. The performance improves significantly if we reduce the rate from R=1 to R=1/2, but the improvement is negligible if we change the rate from R=1/8 to R=1/256. Those results were obtained through simulation, apart from the case without coding (R=1), for which the exact bit error rate can be obtained analytically. All codes have maximum free distance and similar complexity, i.e. the same memory order m_o=8. The generator polynomial for all the codes are given in Appendix A.

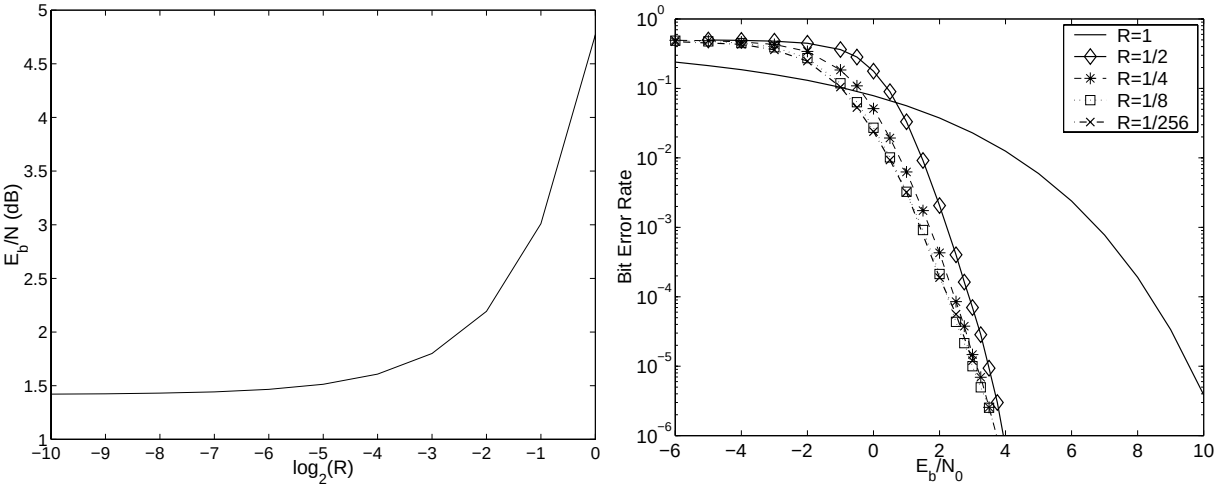

a) minimum SNR required for error free transmission

b) Performance of convolutional codes

Fig. 2.6 - Performance gain with coding

In Figs. 2.7 to 2.9 we show some performance results obtained both through the analysis from Section 2.2 and through computer simulation, which can validate the semi-analytical results. In the computer simulations we have assumed that the channel is constant during a block of 500 bits. Furthermore, the channel gains are independent between the blocks.

In Fig. 2.7 results are shown for both channels described in Table 2.1 and for different coding rates with spreading factor G=128. It has been shown in [14] that a greater capacity can be achieved if the whole bandwidth spread is used for channel coding, and this behaviour can also be observed here, i.e., the best results are achieved with low coding rates. We can however notice that very little can be gained if the code rate is reduced beyond R=1/8, as seen by the comparison with a code of rate R=1/256, which is the minimum rate achievable with the system parameters (G=128 and QPSK modulation).

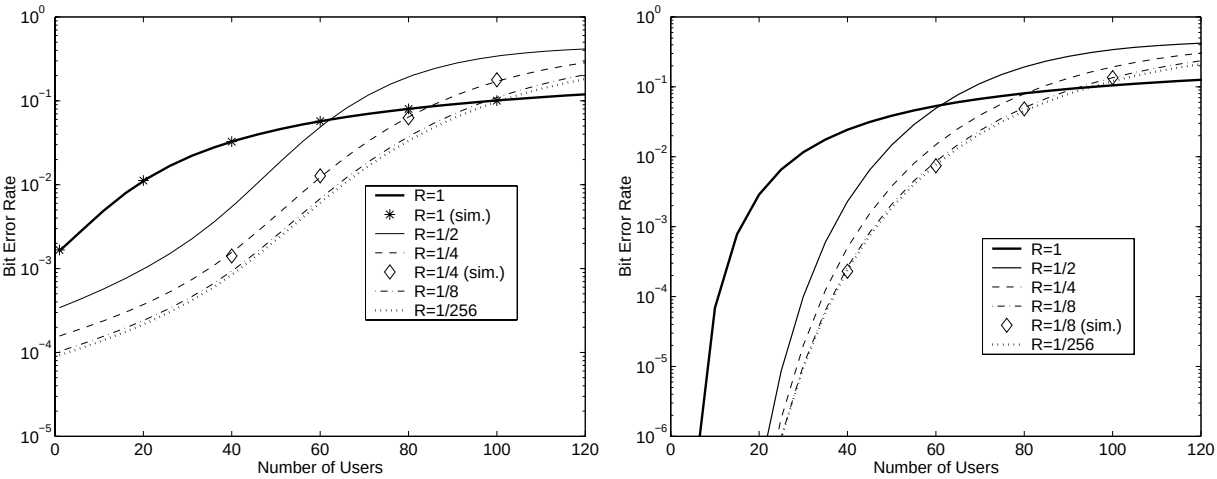

a) strong LOS channel, E_b/N_0=9dB

b) severe multipath channel, no noise

Fig. 2.7 - System performance with non-orthogonal random codes

The analysis so far did not take orthogonal spreading into account though. It is well known that one way to reduce the intra-cell interference in the downlink is to employ orthogonal sequences for spreading. The number of orthogonal sequences that can be generated is however limited by the processing gain available after channel coding; i.e., the number of available orthogonal sequences is at most equal to the number of real-valued chips per coded bit. This means that the use of low rate channel coding has one disadvantage: the lower the coding rate, the smaller is the spreading factor available for orthogonal coding. The increase in the number of orthogonal sequences can however bring about a greater capacity gain than the corresponding reduction in the coding rate, which, as already seen, may result in a negligible performance gain if the coding rate is already low. Nevertheless, systems with low-rate codes are more robust in noisy channels, or when the interference comes from other sources that cannot be orthogonalised, like from other cells or from overlay systems.

This depends on which channel we are considering. In an AWGN channel full orthogonality between the different sequences can be guaranteed, but the wireless channel, specially in broadband communications, is usually characterised by multi-path propagation, in which case much of the orthogonality is lost. This can be seen in (2.33), where the first term of the interference variance denotes the interference caused by orthogonality loss in multi-path propagation. By examining equations (2.32) and (2.33) it can also be noticed that the more severe the multipath distortion is, the less orthogonality can be preserved.

In Fig. 2.8 and Fig. 2.9 we have analysed the system performance for both channels from Table 2.1 and for channel coding rates from R=1 to R=1/8 (convolutional codes, m_o=8), with a processing gain G=128. We have considered that the whole excess bandwidth not used by the convolutional codes is employed for spreading with orthogonal codes. Note that the spreading is made before QPSK modulation, so that, considering the in-phase and the quadrature components, we have a maximum of K_{ort}=2GR orthogonal sequences of length 2GR. Unlike in the IS-95 standard [36], the number of users is here not limited to the number of available sequences. One of the good aspects of CDMA is the soft capacity, so that it would be nice not to have a hard limit on the number of active users in a cell. We have considered that if there are less orthogonal sequences than the total number of users, these are divided into groups of at most K_{ort} orthogonal users and to each group a different scrambling code is assigned. Thus, users belonging to the same group are orthogonal to each other, but not in relation to users from other groups. This approach has also been taken for instance in [33]. We have considered that the orthogonal sequences are Hadamard-Walsh ones and that the scrambling sequences are randomly generated.

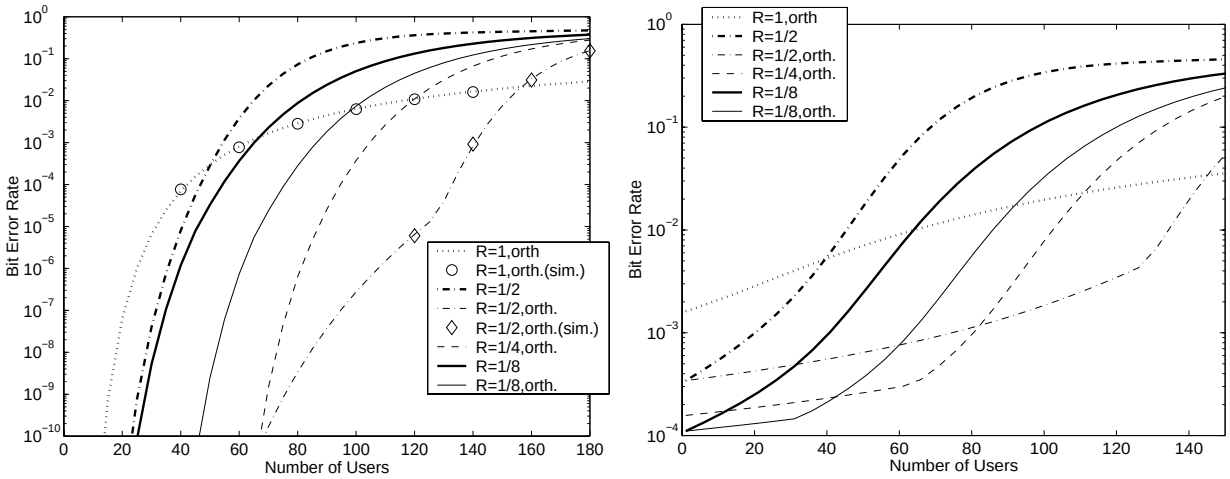

a) no noise *b) E_b/N_0=9dB*

Fig. 2.8 - System performance with orthogonal sequences (channel with strong LOS)

We can observe in Fig. 2.8a that for the channel with strong LOS-component if no noise is present the best approach is undoubtedly to code with a relatively high rate channel code (R=1/2) and use the rest of the excess bandwidth for orthogonal sequences. This was expected, as most of the orthogonality is preserved in this system and the resilience to noise provided by the channel coding is not needed in this case. This situation is however not realistic, the use of CDMA is only reasonable in terms of capacity in multi-cell systems with a low frequency reuse factor, so that a great amount of inter-cell interference is likely to be present, not to mention the additive thermal noise. We assume that the inter-cell interference behaves like gaussian noise, and in Fig. 2.8b a system with noise (E_b/N_0=9dB) was investigated. In this case the advantage of the code with rate R=1/2 is not so significant and, depending on the desired bit error rate, a lower rate code (R=1/4) may be preferable.

We have also included in Fig. 2.8 for the sake of comparison some results if orthogonal codes are not used (for R=1/2 and R=1/8), i.e., the coded bits are spread by a random sequence only. We can see that with this channel model a substantial performance gain is obtained when orthogonal codes are used, specially for high coding rates, as in this case more orthogonal sequences are available.

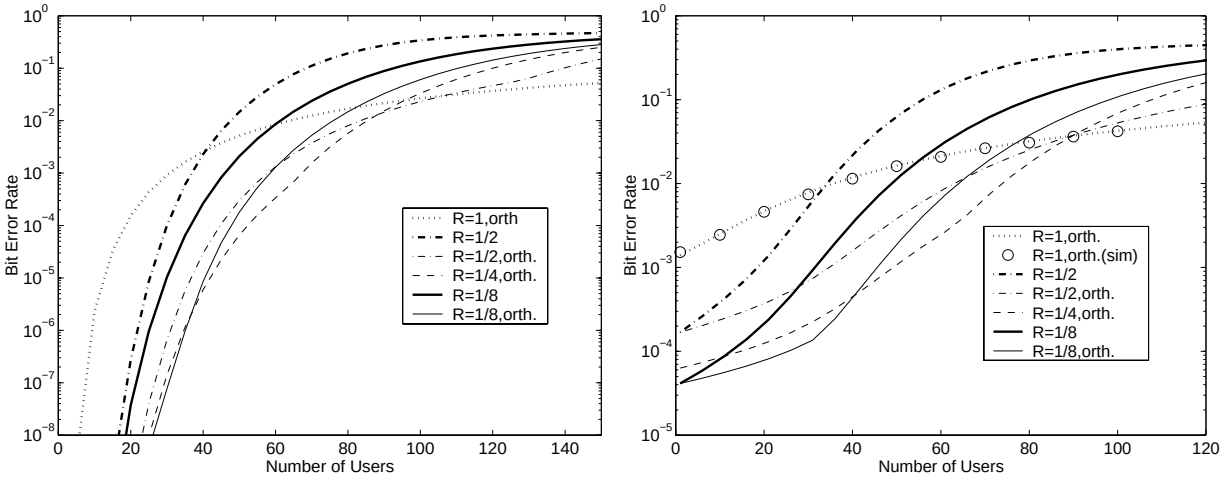

a) no noise *b) E_b/N_0=9dB*

Fig. 2.9 - System performance with orthogonal sequences (severe multipath channel)

In Fig. 2.9 the results for a channel with severe multi-path propagation are shown. We can observe that in this case there is less gain to be obtained from orthogonal codes and a lower rate channel coding should be employed. A code with rate R=1/8 offers superior performance when few users are active and the bit error rate (BER) is low, but at the error rates of interest in practice (10^{-4}<BER<10^{-2}) the system with channel coding of rate R=1/4 outperforms the other possibilities, both with or without noise.

2.4. Summary of Chapter 2

In this chapter we have examined the performance of a direct-sequence spread spectrum system that employs a Rake receiver in a frequency selective channel. We have proposed a semi-analytical method to obtain the bit error rate considering error correcting codes, and based on this we have enquired into the trade-off between channel coding and orthogonal spreading with the goal of maximising the system capacity.

According to the above investigation we infer that a coding scheme with R=1/4 and 64 orthogonal codes is the optimum for the described system with a spreading factor of G=128 symbols/bit and for the suggested channels. This system will be the one considered throughout this work, and these parameters are the ones to be considered when the performance of a Rake receiver is investigated later on.

The results obtained herein are not meant to be definitive, the optimum trade-off depends on the system parameters, such as spreading gain, modulation and coding scheme; on the channel and on the quality requirements. Nevertheless, a similar study can be easily carried out for a different system and for a different environment by following the analysis from Section 2.2.

3. THE PRE-RAKE

As mentioned in the Introduction, it is possible to know the channel characteristics at the base station before transmission. This information can be either obtained by means of a signalling channel or directly from the uplink channel estimates in case of TDD systems, where the same channel is used both in up- and in downlink.

In spread spectrum systems, the simplest way to make use of this information is by means of a pre-Rake, which was first proposed by Esmailzadeh and Nakagawa [11,12], and consists of performing the Rake processing before transmission instead of using a Rake receiver. On account of this, one of the greatest advantages of the pre-Rake when applied to the downlink is that the mobile station receiver can be very simple, not requiring any Rake processing. A great deal of the transmission complexity is transferred to the base station, where costs and power consumption are not a critical issue. Despite that, the same performance can be achieved as with a conventional Rake receiver in a single user environment. The second great advantage of a pre-Rake over a Rake receiver is that it can provide a higher capacity under certain conditions. This is particularly the case when, instead of employing orthogonal spreading, the available spreading gain is partially used for channel coding, which has been previously ignored in the literature [12]. This case will be investigated closely in this chapter.

We will start by a short description and single user performance analysis of the pre-Rake in Section 3.1 and follow with a system analysis with multi-user interference in Section 3.2. In all of these steps the performance comparison of the pre-Rake with a Rake receiver will be stressed. We will then in Section 3.4 investigate the susceptibility of the pre-Rake performance to channel estimation errors, particularly in a fast changing channel in a TDD system, and discuss some ways to overcome this problem.

3.1. The Pre-Rake: Description and Performance Analysis

We consider the same direct-sequence spread spectrum system described in Section 2.1, but now the signal is pre-processed at the transmitter by a pre-Rake, which will be described in this section.

The principle of the pre-Rake is analogous to the one of the Rake receiver. With a pre-Rake the transmitted signal consists of the sum of several versions of the modulated signal with different delays, which compensate for the multipath profile of the transmission channel. The operation of a pre-Rake can be seen in Fig. 3.1. A pre-Rake with maximum ratio combining is, like a Rake receiver, a channel matched filter, but here, based on a priori channel state information, the matched filtering is made before transmission. In this case, if ideal path estimations are available, the tap gains are $f_l = g_l^*$, where g_l^* is the complex conjugate of the channel path gain g_l. Other combining schemes can also be employed with a pre-Rake but these will not be considered in this work. For an analysis of these different schemes please refer to [23].

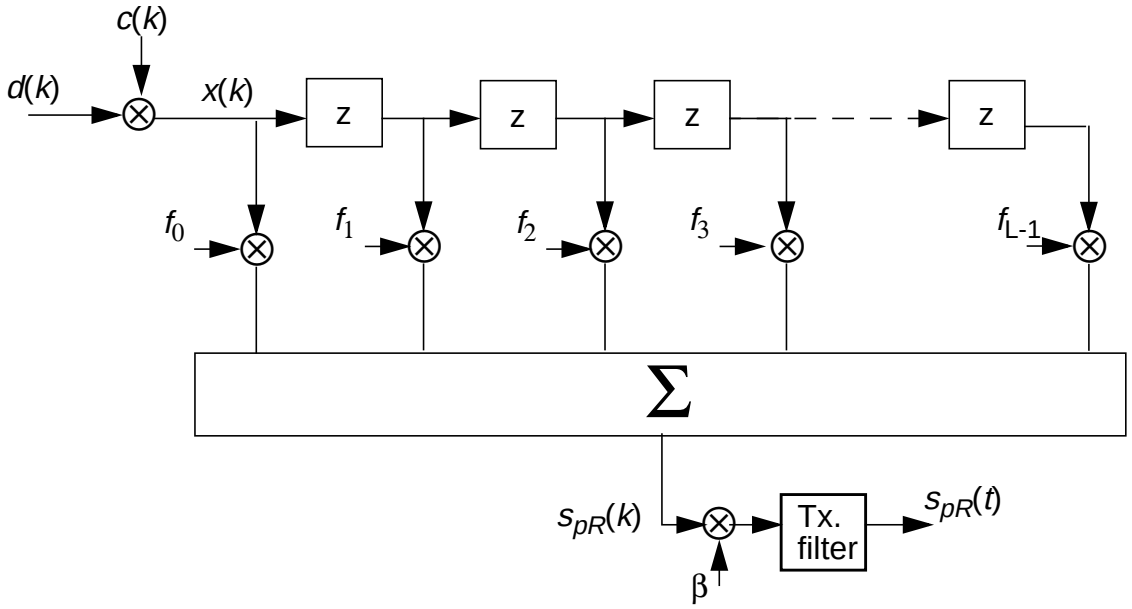

Fig. 3.1 - The pre-Rake

Considering again the channel model given by (2.4), whose parameters we assume are known before transmission, the output of a pre-Rake with maximum ratio combining can be described by the following equation[1]:

$$s_{pR}(i) = \beta \sum_{m=0}^{L-1} f_m x(i+m) = \beta \sum_{m=0}^{L-1} g_m^* x(i+m) \tag{3.1}$$

where $x(i)$ is the coded and modulated signal given by (2.1) and β is a normalisation factor to make sure that the transmitted power be the same as for conventional transmission. Suppose we want the same transmit power as in the system described in Section 2.2.1, then the factor β is given by:

$$\beta = \frac{1}{\sqrt{\sum_{l=0}^{L-1} |g_l|^2}} \tag{3.2}$$

The signal is sent through the channel described by (2.4) and the same assumptions from Section 2.1.2 are made. The received signal is now given by:

$$\begin{aligned} r_{pR}(i) &= \beta \sum_{m=0}^{L-1} \sum_{l=0}^{L-1} g_m^* g_l x(i+m-l) + \nu(i) \\ &= \beta \sqrt{\frac{E_c}{2}} \sum_{m=0}^{L-1} \sum_{l=0}^{L-1} g_m^* g_l d(i+m-l) c(i+m-l) + \nu(i) \end{aligned} \tag{3.3}$$

1. The non-causality of the pre-Rake described by Fig. 3.1 and (3.1) is not a problem for the transmitter, since we can assume that all the data bits and the complete spreading sequence of a frame are known before transmission. Anyway, an equivalent causal system can be obtained if we substitute $x(i)$ for $x'(i)=x(i-L+1)$ in (3.1), and change the integration intervals in the subsequent equations.

Now suppose we correlate the spreading code directly with the received signal obtained with a pre-Rake, without employing a Rake receiver. To facilitate the comparison with the Rake receiver analysis from Chapter 2, we can divide equation (3.3) by the normalisation factor β. This will of course not affect the results since both the noise and the desired signal are multiplied by the same factor. With this scaling, we have the following signal after the correlator:

$$y(i) = \sqrt{\frac{E_c}{2}} \sum_{m=0}^{L-1} \sum_{l=0}^{L-1} (g_m^* g_l d(i-l+m) c(i-l+m)) \otimes c(i) + \nu_{pR}(i) \tag{3.4}$$

where the noise component is:

$$\nu_{pR}(i) = \frac{\nu(i)}{\beta} = \sqrt{\sum_{l=0}^{L-1} |g_l|^2}\ \nu(i) \tag{3.5}$$

We can notice that, apart from the noise component, the signal expressed in equation (3.4) is exactly the same as the one after the Rake receiver in (2.8). We can also observe that the variance of the noise component is the same as with a Rake receiver, i.e.,

$$\mathrm{var}\{\nu_{pR}\} = \mathrm{var}\{\nu(i)\} \sum_{l=0}^{L-1} |g_l|^2 = N_0 \sum_{l=0}^{L-1} |g_l|^2 = \mathrm{var}\{\nu_{Rk}\} \tag{3.6}$$

We can thus conclude that the performance with a pre-Rake is the same as with a Rake receiver for a single user and ideal channel estimation. This can be confirmed by simulations, as it can be seen in Fig. 3.2, where transmission with a convolutional code of rate R=1/4 and memory order m_o=8 was considered for both channels described in Table 2.1. The analytical results shown in Fig. 3.2 were obtained through the analysis performed for a Rake receiver in Section 2.2.1, and the simulation results were obtained considering a pre-Rake. We can see that there is a great accordance between the simulated performance with a pre-Rake and the analytical values expected for either a conventional Rake receiver or a pre-Rake.

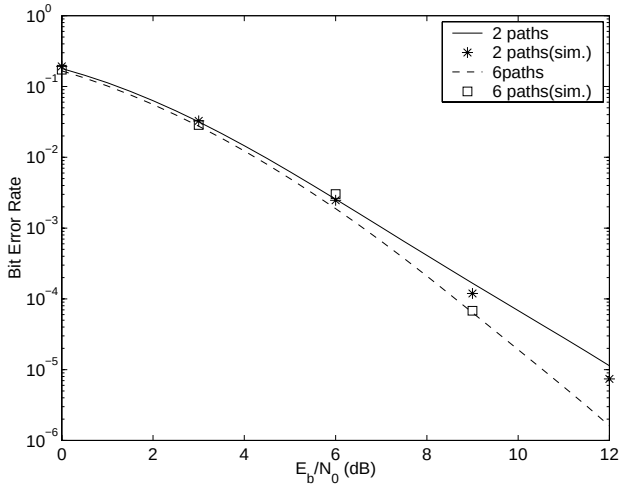

Fig. 3.2 - Pre-Rake performance, single user

With conventional transmission and a Rake receiver the signal goes through two different linear systems: the multipath channel and the Rake receiver, which performs a channel matched filtering. By doing this we can obtain after a Rake receiver the sum of all multipath

signals, where each path is weighted according to its strength. With a pre-Rake at the transmitter the same linear operations are performed, but in a different order, and thus we obtain the same signal. The concept of a pre-Rake is depicted in Fig. 3.3. With pre-Rake pre-processing the receiver needs only to synchronise to the strongest peak of the received signal and decode it. As we shall see in Chapter 4, this is not yet the optimal decoding scheme, but with this very simple receiver we can achieve the same performance of a conventional Rake receiver, which requires a much more complex mobile unit receiver. The pre-Rake implies of course extra complexity in the transmitter, but, as already mentioned, this is not such an important issue in the downlink.

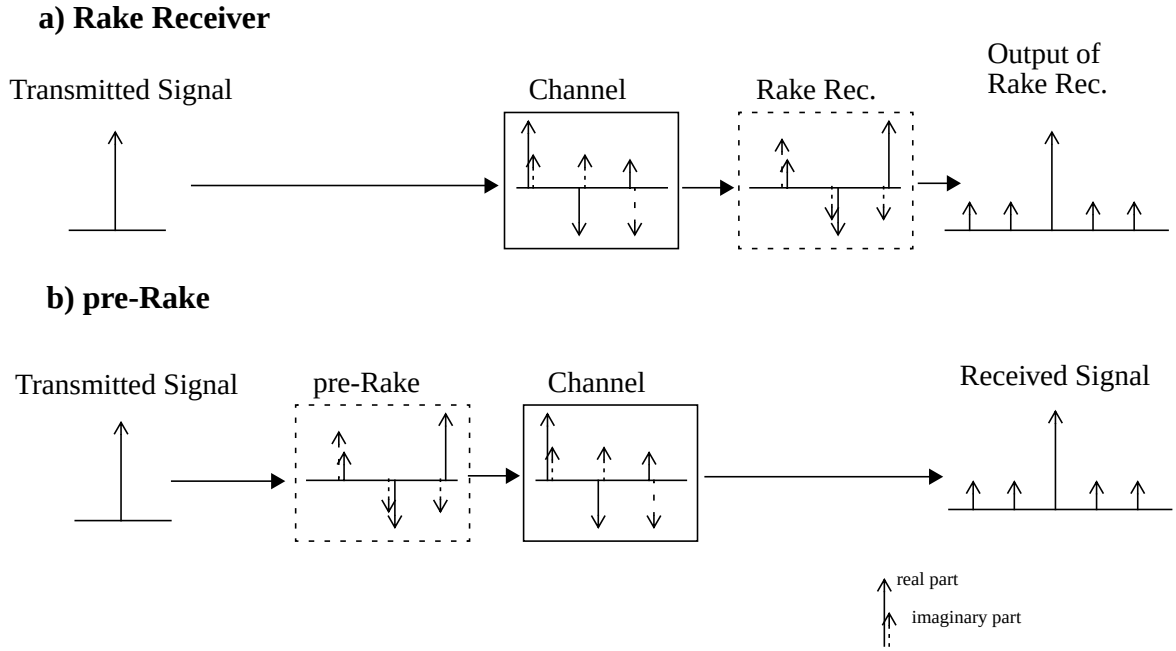

Fig. 3.3 - The pre-Rake principle

3.2. Multi-user System Analysis

An analysis similar to the one made for a Rake receiver in Section 2.2.2 can be carried out for the downlink with a pre-Rake, but in this case the channel impulse response is matched at the transmitter for each user. Each user has a different channel, and consequently a different pre-Rake processing. We have now the following transmitted signal for user k:

$$s_k(i) = \beta_k \sum_{m=0}^{L-1} g_{k,m}^{*} x_k(i+m), \tag{3.7}$$

where β_k is the normalisation factor for user k

$$\beta_k = \frac{1}{\sqrt{\sum_{l=0}^{L-1} |g_{k,l}|^2}} \tag{3.8}$$

The total transmitted signal is the sum of the signal of all users:

$$s_{pR}(i) = \sum_{k=0}^{K-1} \beta_k \sum_{m=0}^{L-1} g_{k,m}^{*} x_k(i+m) \tag{3.9}$$

We again consider the performance of user 0 only. The received signal for user 0 is

$$r_{0,pR}(i) = \sum_{k=1}^{K-1} \beta_k \sum_{l=0}^{L-1} g_{0,l} s_{pR}(i-l) + \nu(i) \tag{3.10}$$

If we multiply the received signal by $1/\beta_0$ to facilitate the analysis, and despread the signal by correlating it with the scrambling code $c_0(i)$, the following is obtained:

$$\begin{aligned} y_{0,pR}(i) &= \frac{1}{\beta_0} \sum_{k=0}^{K-1} \beta_k \sum_{l=0}^{L-1} (g_{0,l} s_{pR}(i-l)) \otimes c_0(i) + \nu(i) \otimes c_0(i) \\ &= \frac{1}{\beta_0} \sqrt{\frac{E_c}{2}} \sum_{k=0}^{K-1} \beta_k \sum_{l=0}^{L-1} \sum_{m=0}^{L-1} (g_{k,m}^{*} g_{0,l} d_k(i-l+m) c_k(i-l+m)) \otimes c_0(i) + \nu_{pR}(i) \end{aligned} \tag{3.11}$$

This signal is integrated over M symbols and we obtain

$$z_{0,pR} = M \sqrt{\frac{E_c}{2}} \sum_{l=0}^{L-1} |g_{0,l}|^2 (1+j) d + \nu_{self} + \nu_{mu,pR} + \nu_{G,pR} \tag{3.12}$$

It can be easily verified that the self-interference is the same as with a Rake receiver in (2.13). In Section 3.1 the thermal noise component $\nu_{G,pR}$ was already shown to have the same variance as with a Rake receiver. The multi-user interference however is completely different from the one with a Rake receiver. Reminding the definition $a_k(i) \equiv d_k(i) c_k(i)$, the multi-user interference is now given by:

$$\begin{aligned} \nu_{mu,pR} = \sqrt{\frac{E_c}{2}} \sum_{i=0}^{M-1} \sum_{k=1}^{K-1} \frac{\beta_k}{\beta_0} \Bigg[& \sum_{\substack{\lambda=-(L-1) \\ \lambda \neq 0}}^{L-1} \sum_{\substack{l,m \\ l-m=\lambda}} (g_{k,m}^{*} g_{0,l} a_k(i-\lambda)) \otimes c_0(i) \\ & + \sum_{l=0}^{L-1} (g_{k,l}^{*} g_{0,l} a_k(i)) \otimes c_0(i) \Bigg] \end{aligned} \tag{3.13}$$

As in Section 2.2.2, we consider the possibility of employing orthogonal sequences. The variance of the interference is obtained in Appendix C and it is given by:

$$\mathrm{var}\{\nu_{mu,pR}\} = M E_c \sum_{k=1}^{K-1} \frac{\beta_k^2}{\beta_0^2} \left[\sum_{\substack{\lambda=-(L-1) \\ \lambda \neq 0}}^{L-1} \left| \sum_{\substack{l,m \\ l-m=\lambda}} g_{k,m}^{*} g_{0,l} \right|^2 + \alpha_k \left| \sum_{l=0}^{L-1} g_{k,l}^{*} g_{0,l} \right|^2 \right] \tag{3.14}$$

with the orthogonality factor

$$\alpha_k = \begin{cases} 1 & \text{, if } c_0(i) \text{ and } c_k(i) \text{ are not orthogonal} \\ \sin^2\left(\angle \sum_{l=0}^{L-1} g_{k,l}^* g_{0,l} \right) & \text{, if } c_0(i) \text{ and } c_k(i) \text{ are orthogonal} \end{cases} \tag{3.15}$$

where $\angle a$ is the phase of the complex number a.

With the result from (3.14), and assuming that the interference behaves like white gaussian noise, we can obtain the bit error rate as described in Section 2.2 for a Rake receiver. For a particular channel configuration given by the complex channel gains $g_{k,l}$, $0 \le k < K$ and $0 \le l < L$, we obtain the power spectral density of the interference

$$I_0 = \frac{\mathrm{var}\{\nu_{self}\} + \mathrm{var}\{\nu_{mu,pR}\}}{M \sum_{l=0}^{L-1} |g_{0,l}|^2} \tag{3.16}$$

and the signal-to-noise ratio

$$\Gamma_{pR}(\boldsymbol{g}) = \frac{E_b \sum_{l=0}^{L-1} |g_{0,l}|^2}{N_0 + I_{0,pR}} \tag{3.17}$$

We proceed like in Section 2.2 and, according to a given channel delay profile, obtain the bit error rate based on randomly generated channel coefficients. This time however we need to generate the channel coefficients not only from the desired user, as for a Rake receiver, but also from every interfering user.

To confirm the validity of the above analysis, it can be seen that some of the results displayed in Fig. 3.4 and Fig. 3.5 are in great accordance with simulation results.

3.3. Performance Results

A comparison between the multi-user performance with a Rake receiver and with a pre-Rake is displayed in Fig. 3.4 and Fig. 3.5. The same channel (see Table 2.1) and transmission parameters as in Section 2.2 were considered and are the same for every user. We further assume that the channels of all users have the same power delay profile, but the instant channel coefficients from different users are independent. This is a reasonable assumption, since users which are at least a few wavelengths λ_c apart from each other can be assumed to have an independent fast fading. At 1,8GHz for example, $\lambda_c \approx 17$cm, for higher frequencies the wavelength is even less. The results for a Rake receiver shown in these figures were obtained considering a convolutional code of rate R=1/4 and 64 orthogonal codes for a spreading factor G=128 symbols/bit, which we determined in Section 2.3 to be the optimum scheme for the investigated system configuration.

In Fig. 3.4 we can see the system performance for a system with the 2-path channel model with strong line-of-sight (LOS) component and in Fig. 3.5 the 6-path severe multipath channel is considered. It can be seen in both figures that the performance with a pre-Rake is much better than the one with a Rake receiver if no orthogonal sequences are employed. We can also see that the use of orthogonal sequences brings about little performance gain if a pre-Rake is used, what was expected, since the signals from different users are pre-processed by different

filters, and this destroys a great deal of the orthogonality. In a system with little multi-path distortion (Fig. 3.4) much of the orthogonality can be however preserved if a pre-Rake is not employed, and in this situation the highest capacity can be achieved with a conventional Rake receiver and orthogonal codes. Nevertheless, when only a pre-Rake is used the mobile stations are less complex, and this may justify the use of a pre-Rake also in this situation, in which the cost and power savings may be worth the small capacity loss.

As described in Section 2.3, more users can be supported than there are codes available, as we separate the users into groups of $K_{ort}=2GR$ orthogonal users, and scramble each group with a different code.

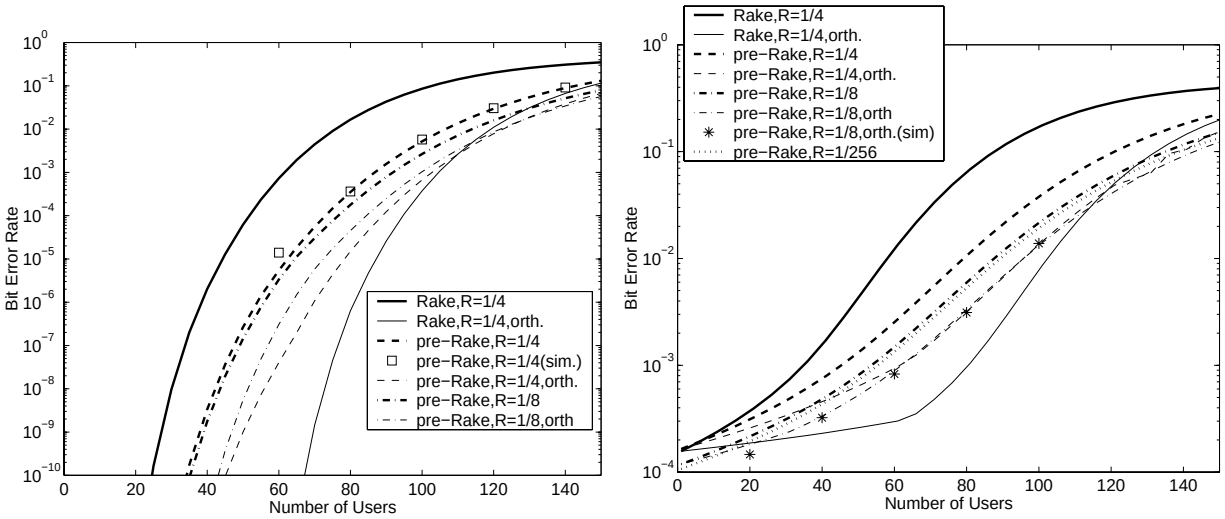

a) no noise *b) $E_b/N_0=9dB$*

Fig. 3.4 - Pre-Rake Performance in a Multi-User Environment (2 path channel)

In a channel with severe multipath distortion however, much of the orthogonality is lost also with conventional transmission. In this situation the capacity that can be obtained with a pre-Rake is significantly higher than the one with a Rake receiver, since not much gain can be obtained from orthogonal spreading in this channel when Rake receivers are used with conventional transmission, as we can see in Fig. 3.5. As already mentioned, the capacity gain achieved with orthogonal sequences compared to non-orthogonal sequences is rather small with a pre-Rake. This implies that with a pre-Rake lower rate codes should be used, which offer a better performance in the presence of noise, and this can be confirmed in both Fig. 3.4 and Fig. 3.5. Nevertheless, as already observed in Section 2.3 little gain can be obtained by utilising the whole spreading gain for channel coding (e.g., with R=1/256 with G=128 and QPSK) instead of a code with moderate rate R=1/8, as we can also see in Fig. 3.4 and Fig. 3.5. This implies that despite the relatively small gain that can be obtained by using orthogonal sequences with a pre-Rake, these should still be employed, for they bring more benefits than to use the excess bandwidth for lower rate channel coding.

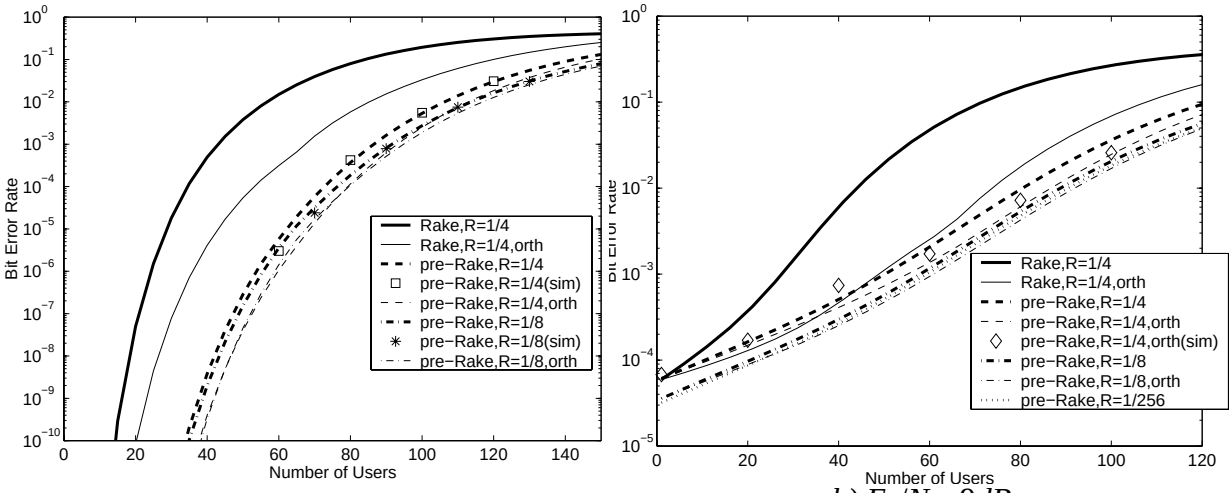

a) no noise *b) E_b/N_0=9dB*

Fig. 3.5 - Pre-Rake Performance in a Multi-User Environment (6 path channel)

The larger capacity achieved with a pre-Rake is due to the reduction in the interference caused by the channel matched pre-filtering. The reason for this interference reduction can be better understood through Fig. 3.6. With a Rake receiver both the desired and interfering signals go through the same channel and the same Rake processing, and consequently they are both received with the same strength before despreading[1]. This is however not so with a pre-Rake. In this case the signal from each user is pre-processed by a different pre-Rake, which is matched to the respective channel impulse response. The signal from the desired user is matched to its channel, so that its signal is received with maximum power. There is however a mismatch between the pre-Rake filtering of an interfering signal and the desired user channel, and, hence, the interfering signals are received with less power.

In [12] the conclusion reached was that the capacity with a Rake receiver is superior to the one with a pre-Rake if orthogonal spreading sequences are employed, since most of the orthogonality is lost with pre-Rake processing. In that paper however, the use of error-correcting codes for part of the spreading has been ignored. Channel coding is nevertheless essential in order to mitigate the effects of thermal noise and out-of-cell interference, and we have seen here that if channel coding is considered the number of orthogonal codes available decreases proportionally to the coding rate, and hence the capacity gain obtained with orthogonal spreading is considerably diminished. Under these conditions the use of the pre-Rake can increase the capacity compared to a more conventional system with Rake receivers, as we have shown here. These results stress the importance of the analysis developed Section 2.2.1, which allows for a simplified investigation considering also error correcting codes as part of the signal spreading.

1. The ratio of desired to interfering signal will be increased by the processing gain *G* after despreading.

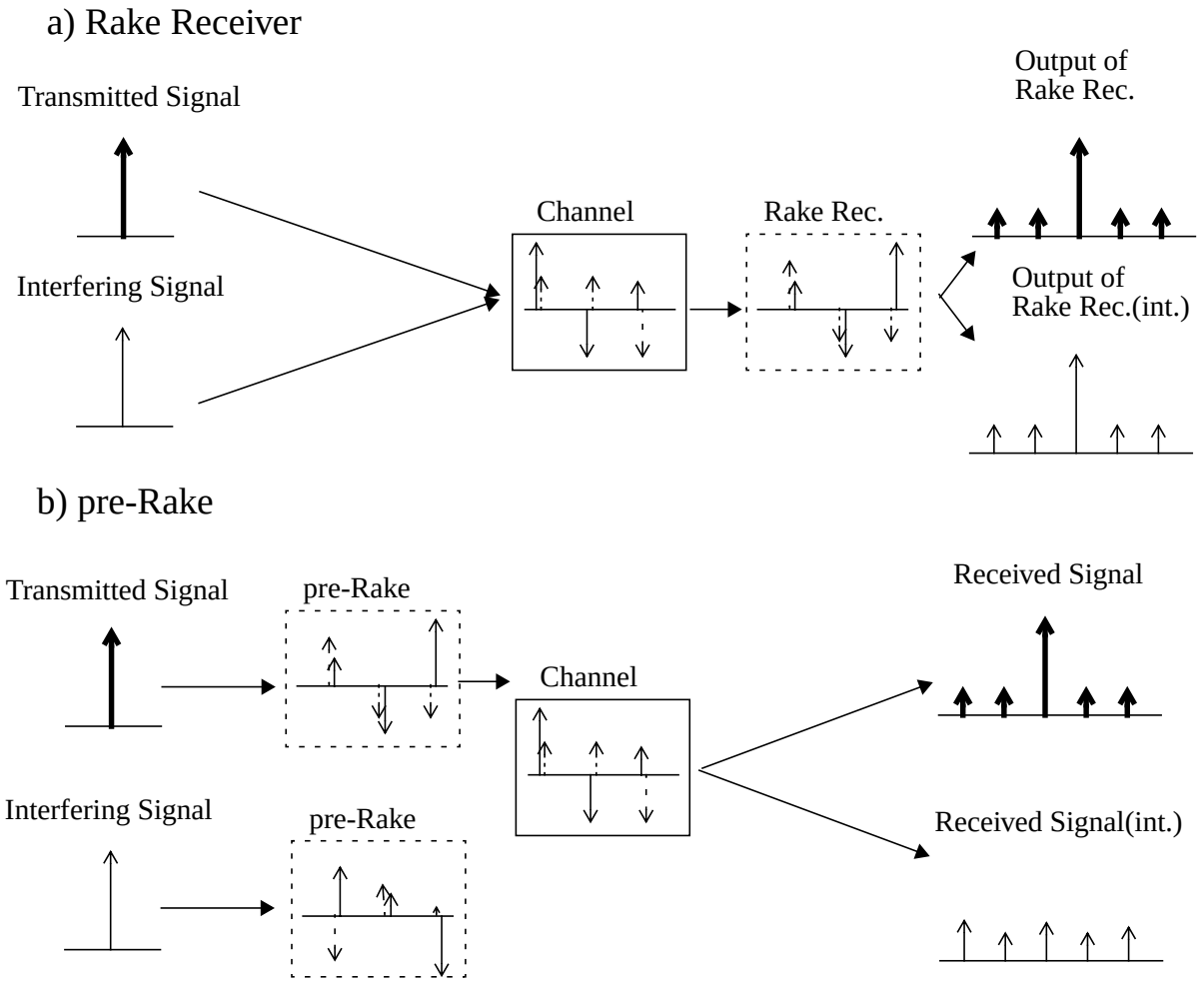

Fig. 3.6 - Multi-user interference reduction with a pre-Rake

3.4. The pre-Rake with Channel Estimation Errors

It was shown in the previous section that under certain conditions a significant capacity increase can be obtained in the downlink with a pre-Rake instead of a Rake receiver, provided ideal channel estimation is available before transmission. In this section the impact of imperfect channel estimation on the performance is examined.

3.4.1 Sensitivity of pre-Rake to Channel Estimation Errors

One question that may arise is whether the pre-Rake is more sensitive to estimation errors than a conventional Rake receiver. To answer that question let us consider a single user system, where the channel estimates for the *l*-th path are given by $\hat{g}_l$, and that the same estimates are employed both for a Rake receiver and a pre-Rake.

We will first consider a system with a Rake receiver. The received signal is the one given by (2.5), and the Rake processing with non-ideal channel estimates will give us the following signal:

$$
\begin{aligned}
y'(i) &= \sum_{m=0}^{L-1} (\hat{g}_m^* r(i+m)) \otimes c(i) \\
&= \sqrt{\frac{E_c}{2}} \sum_{m=0}^{L-1} \sum_{l=0}^{L-1} (\hat{g}_m^* g_l d(i-l+m) c(i-l+m)) \otimes c(i) + \nu'_{Rk}(i)
\end{aligned}
\tag{3.18}
$$

where $\nu'_R(i)$ is the gaussian noise component of variance

$$
\mathrm{var}\{\nu'_{Rk}(i)\} = N_0 \sum_{l=0}^{L-1} |\hat{g}_l|^2 \tag{3.19}
$$

Now suppose that the same channel estimates are available for a pre-Rake at the transmitter. As in Section 3.1 the transmitted signal will be given by

$$
s'_{pR}(i) = \beta' \sum_{m=0}^{L-1} \hat{g}_m^* x(i+m) \tag{3.20}
$$

where β' is the normalising factor, which is now

$$
\beta' = \frac{1}{\sqrt{\sum_{l=0}^{L-1} |\hat{g}_l|^2}} \tag{3.21}
$$

As in Section 3.1, we divide the received signal by β' to make the comparison easier. The signal after the code descrambling is

$$
y'(i) = \sqrt{\frac{E_c}{2}} \sum_{m=0}^{L-1} \sum_{l=0}^{L-1} (\hat{g}_m^* g_l d(i-l+m) c(i-l+m)) \otimes c(i) + \nu'_{pR}(i), \tag{3.22}
$$

which is identical to the signal after a Rake receiver from (3.18), apart from the noise component. But the variance of $\nu'_{pR}(i)$ is

$$
\mathrm{var}\{\nu'_{pR}(i)\} = \mathrm{var}\left\{\frac{\nu(i)}{\beta'}\right\} = N_0 \sum_{l=0}^{L-1} |\hat{g}_l|^2, \tag{3.23}
$$

which is the same as the noise variance after a Rake receiver.

We can hence deduce that a system with a pre-Rake has the same sensitivity to channel estimation errors as the Rake receiver. The issue of the Rake receiver performance with realistic channel estimation has already been studied extensively in the literature [2,26] and is not the subject of our work. We would just like to point out here that if the channel estimates obtained in the uplink are good enough for the Rake receiver, the same performance can be expected if they are used for the pre-Rake in the downlink, provided of course the channel characteristics remain the same. In the next section we will investigate the behaviour of a pre-Rake if the channel changes between the uplink and the downlink period.

3.4.2 Performance in Time-Variant Channels

In Section 3.4.1 we have assumed that the same erroneous channel estimates were available for both a Rake receiver and a pre-Rake. This is however mostly not the case. Due to the time-variability of the mobile radio channel, the estimation errors are usually larger for a pre-Rake than for a Rake receiver.

In TDD systems the channel is estimated by the base station upon reception in the uplink period, and this estimation is used for the pre-Rake processing in the downlink. However, the wireless channel is usually time-variant in mobile communications systems, so that the channel estimates obtained in the uplink are not necessarily up-to-date during the downlink period. This means that, even if ideal channel estimation can be performed on reception, it is unlikely that the channel impulse response will be known exactly before transmission. The error in the channel state information used for transmission pre-distortion depends on how quickly the channel changes. The cause for the time variations in the channel was briefly described in Section 2.1.2, and these are evidenced by a Doppler broadening of the transmit signal [34] with maximum frequency shift of

$$f_d = \frac{V}{\lambda_c} \tag{3.24}$$

where V is the mobile velocity and λ_c the carrier wavelength. The frequency f_d is known as the Doppler spread of the channel, and it gives a measure of how quickly the channel changes; the greater the Doppler spread, the greater is the rate of change in the channel. As it can be inferred from (3.24) the channel varies more rapidly at high velocities and high carrier frequencies.

The coherence time is a measure of the time duration over which the channel is nearly invariant and it is proportional to the inverse of the Doppler spread $T_{coh} \sim 1/f_d$. There are several definitions in the literature for the coherence time, we will consider here the one proposed in [32]:

$$T_{coh} = \frac{0,423}{f_d} \tag{3.25}$$

The estimation error depends on the time delay δ_T between the uplink channel estimation and the Rake pre-processing in the downlink. If the delay is short enough ($\delta_T << T_{coh}$), then there is a high correlation between the uplink and the downlink channel. This delay is a system design parameter and it depends basically on the TDD duplex frame duration[1]. For a good performance of the pre-Rake it is desirable that the TDD duplex frames be as small as possible in order to minimise the delay between estimation upon reception in the uplink and transmission in the downlink. This is also consistent with the need to keep the transmission delay short for real-time applications. On the other hand we should bear in mind that each frame has an overhead consisting of guard intervals and synchronisation sequences, and in short frames this overhead can be quite large compared to the amount of useful information. If this is taken into consideration, the TDD frame should be as long as possible in order to minimise the efficiency loss due to this overhead. When choosing the system parameters we

1. A TDD duplex frame is the minimum frame size containing at least one uplink and one downlink period, plus the necessary guard intervals.

must therefore reach a compromise between these two conflicting requirements, and to do that, we must investigate the effect on the pre-Rake performance of imperfections in the channel estimation due to time varying channels.

In the results presented below in this section we have used the following parameters: carrier frequency f_c=5GHz, symbol rate $1/T_c$=18,162 Mbauds and a TDD frame duration T_{TDD}=1,5ms with equal length uplink and downlink frames. The coding (R=1/8, m_o=8) and the processing gain (G=128) are the same as in Section 3.3, and the same coding scheme was used both with a Rake receiver and with a pre-Rake. Accounting for guard intervals and a training sequence, and considering that the same channel has to be used for both up- and downlink, we achieve a net data rate of 64kbps, with 96 data bits (12228 chips) being transmitted in each direction during a TDD frame. The TDD frame structure is shown in Fig. 3.7, with a training sequence being sent at the middle of an uplink or downlink period. The parameters above were taken from the *Integrated Broadband Mobile System* (IBMS) project [7], which is targeted at microcells (up to 300m cell radius) and moderate velocities. The results shown below should nevertheless apply to any TDD system if the values are normalised to its relevant parameters.

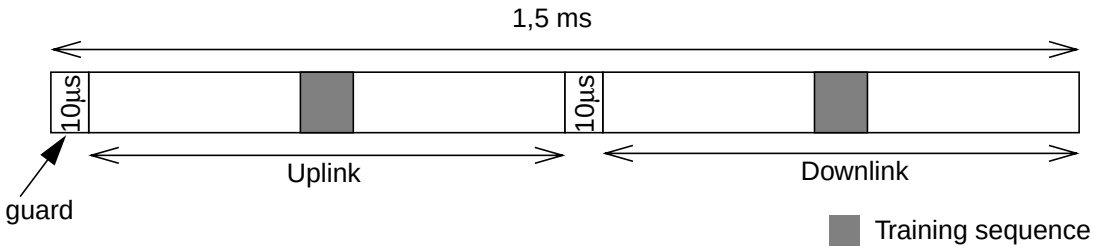

Fig. 3.7 - TDD Frame Structure

An analytical solution for the performance in time-variant channels would be intractable and we decided for a simulation approach. We have assumed that, based on the training sequence, the channel can be ideally estimated at the uplink. The channel considered is the 6-path Rayleigh fading channel model from Table 2.1 with a signal-to-noise ratio E_b/N_0=9dB, but this time we consider a moving mobile station with a classical Doppler spectrum [34] at various velocities. The results are shown in Fig. 3.8, with the x-axis normalised to T_{TDD}/T_{coh}, which is proportional to the velocity.

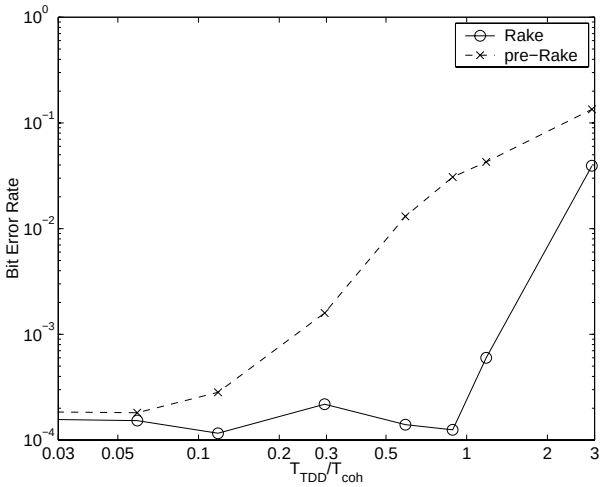

Fig. 3.8 - Link performance in a 6-path time-varying channel

We can see in Fig. 3.8 that with a pre-Rake the performance deteriorates rapidly even at low velocities since the uplink channel coefficients are not up-to-date at the downlink period. We observe also that even a system with a Rake receiver and perfect channel estimation is affected at high velocities, particularly if $T_{TDD}/T_{coh}>1$, although to a lesser extent. This is so because the channel is estimated in the middle of a transmission frame and the estimates are employed for the whole frame. The channel may however change within a single downlink period, such that the estimates are less accurate for the bits far from the training sequence.

The results displayed in Fig. 3.8 have been obtained with simulation over ten different time varying channels[1] with 2.000.000 bits for each channel. Considering the amount of simulated bits and the bit error rate obtained ($\sim 10^{-4}$) it does not seem likely that the fluctuations in the bit error rate observed in Fig. 3.8 for low velocities with a Rake receiver are caused by simulation imperfections. These fluctuations can be perhaps explained by the use of convolutional codes with large memory order (m_o=8). The codes employed here are non-terminated, i.e. the decoding is not made on a frame-by-frame basis, and we have employed a Viterbi decoder with decoding delay $5m_o$ bits, which according to [31] is the required delay for nearly optimum decoding. This means that at the decoding process many of the initial bits in a frame are influenced by bits in the previous frames, and this provides us with a certain amount of time diversity. Even though rapid channel variations pose a difficulty for the channel estimation, they bring about more time diversity, and this may compensate for the performance loss caused by channel estimation errors when these are not very significant, causing the fluctuations seen in Fig. 3.8.

The performance deterioration of a pre-Rake at high velocities can be however avoided to a certain extent if we try to predict the channel characteristics in the downlink based on the previous uplink channel estimates. A theoretical analysis of the predictability of the channel coefficients can be found in Appendix D. One way to perform this prediction is to implement an RLS (Recursive Least Squares) adaptive Kalman algorithm, which will be briefly recalled in Appendix E as applied to our particular application, following the description in [18,31].

The results with prediction can be seen in Fig. 3.9, where it can be observed that the system copes much better with a changing environment if a prediction filter is employed, and a performance similar to the one obtained with a Rake receiver can be obtained with a pre-Rake for low velocities (low values of T_{TDD}/T_{coh}). Nevertheless, it was shown in Appendix D that reliable prediction can only be obtained if $T_{TDD}f_d \leq 0{,}5$. Hence, from (3.25) it follows that for $T_{TDD}/T_{coh} > 1{,}182$ an efficient prediction cannot be performed, which can be confirmed from the results displayed in Fig. 3.9.

1. Each channel corresponds to a different seed of the random number generator

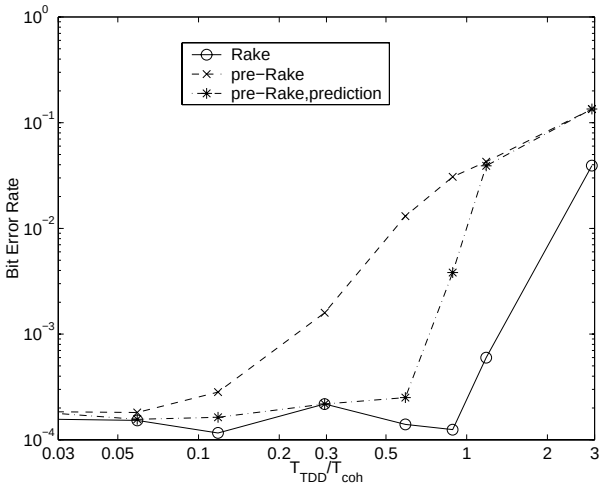

Fig. 3.9 - Link performance in a 6-path time-varying channel with channel prediction

The above RLS-based channel prediction scheme is however not the optimum one. The fading in multipath propagation is due to the superposition of multiple complex sinusoids, and this knowledge about the physical nature of the fading process can be used to devise prediction methods that perform better than the conventional Kalman algorithm approach, for instance in [1,21]. The investigation of these methods is however beyond the scope of this work. Our goal here is to demonstrate the feasibility of a pre-Rake even in time-variant channels, which was done using a Kalman predictor. The use of these newer methods should further improve the performance compared to the one shown here.

Another way to reduce the impairments caused by estimation errors in variable channels is to move the training sequence in the uplink closer to the downlink period, so that the time delay between channel estimation and transmission is reduced. This has a major drawback in that the uplink performance deteriorates, since the channel may change between the beginning of the uplink transmission and the estimation. An alternative is to include an extra training sequence, which will be used for the pre-Rake only, as depicted in Fig. 3.10. Unlike the original training sequence, which is used for synchronisation and channel parameter acquisition, the pre-Rake training sequence can be used for channel updating only, which reduces its length and processing complexity. This implies a small loss in the ratio of user information to signalling overhead, but the results can be significantly improved this way in fast changing channels. It must be however mentioned that this configuration requires that the extra training sequence be demodulated and the channel updated in a very short time, at most before the next downlink period. It remains an open question whether available signal processors are fast enough to perform these tasks in real time.

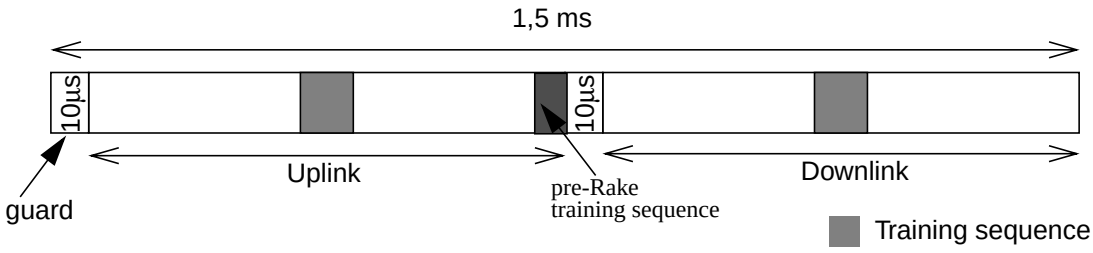

Fig. 3.10 - TDD Frame structure with extra training sequence

In Fig. 3.11 the performance results obtained with the configuration from Fig. 3.10 are displayed, both with and without a channel predictor. It can be observed that the performance improves substantially if the channel coefficients estimated at the end of the downlink frame are used instead of the ones obtained at the middle of the frame. We can also see that in this case the theoretical limits discussed in Appendix D apply as well and no reliable prediction can be made if T_{TDD}/T_{coh}>1,182.

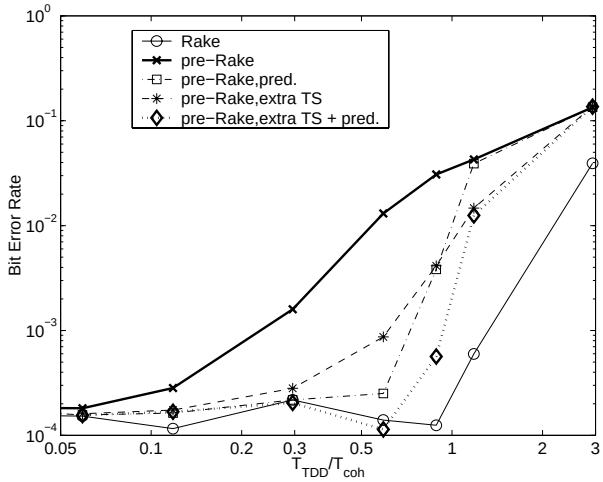

Fig. 3.11 - Link performance in a 6-path time-varying channel with extra training sequence

In Fig. 3.12, the system capacity is shown if all the users have a velocity of 5m/s (T_{TDD}/T_{coh}=0,2955) with the 6-path channel model from Table 2.1 and a signal-to-noise ratio of E_b/N_0=9dB. The system parameters are the same as the ones employed throughout this section, i.e., convolutional coding with parameters R=1/8 and m_o=8, and processing gain G=128. The results indicate that the capacity with a pre-Rake and neither channel prediction nor extra training sequence is substantially reduced compared to the one that can be obtained with channel prediction. This means that measures to counteract the time-variability of the channel are necessary if we want to use the pre-Rake to obtain a higher capacity in mobile communications systems.

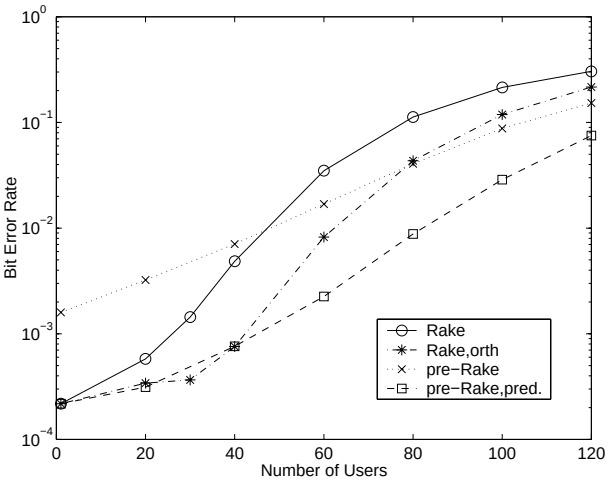

Fig. 3.12 - Capacity in a 6-path time-variant channel

In the above analysis we have considered that the same channel estimate was used during the whole transmission period. The performance can be further improved if the channel estimates are updated during this period, i.e., the channel predictor can make more precise predictions for the first samples in a frame than for the end of the frame, as demonstrated in Appendix D.

The above investigation was carried out for a TDD system, but the essence of it would also apply for a FDD system where the channel state information is obtained through a feedback loop. In this case however the time delay between estimation and transmission depends on how frequently the channel state information is signalled.

3.5. Summary of Chapter 3

In this chapter we have presented the signal pre-processing with a pre-Rake, which can be performed if channel state information is available before transmission. We have analysed its performance and came to the conclusion that a downlink capacity increase can be reached with a pre-Rake in certain environments; even though the mobile station receiver can be less complex in this technique compared to one with a conventional Rake receiver. This capacity gain is particularly significant in channels with severe multi-path propagation.

We have also investigated the performance of this technique in case imprecise channel estimates are available, specially in the case of time-variant channels. Some countermeasures to overcome this problem were suggested and the feasibility of the pre-Rake also in such channels was demonstrated.

4. THE POST-RAKE

In Chapter 2 we have investigated a system with a Rake receiver, which is used in spread spectrum systems to make use of the signal diversity provided inherently by multi-path propagation. In Chapter 3 the pre-Rake was seen to be an alternative technique that, when employed in the downlink, transfers the Rake processing, and hence a great part of the system complexity, to the base station. This scheme provides us with the same performance obtained with a Rake receiver in a single user environment and larger capacity under certain circumstances, with the additional advantage of needing less complex mobile station receivers.

In this chapter we will see that if a pre-Rake is used upon transmission, and larger complexity is allowed at the mobile stations, a post-Rake can be used in addition. It is similar to a conventional Rake receiver and is the optimal receiver in terms of maximising the signal-to-noise ratio if a pre-Rake is employed at the transmitter.

A qualitative analysis will be made in Section 4.1, which will provide us the motivation for the use of a post-Rake. It will be better described and analysed in a single user environment in Section 4.2; and its use to alleviate the performance loss of a pre-Rake in time-variant channels will be briefly investigated in Section 4.3. The analysis in case of multi-user interference will follow in Section 4.4 and some performance results will be shown and interpreted in Section 4.5.

4.1. Motivation

Suppose we have no pre-processing at the transmitter, a channel[1] with frequency response $H(f)$ and additive white Gaussian noise. Then a Rake receiver with maximum ratio combining and ideal channel estimation corresponds to a channel matched filter $H^*(f)$ (see Fig. 4.1), which according to the theory [31] maximises the signal-to-noise ratio. The Rake receiver is hence the optimal receiver in terms of the maximisation of signal-to-noise ratio in channels with white noise, if no pre-processing is made at the transmitter.

The pre-Rake is also a channel matched filter, but the filtering occurs before transmission, and, as seen in Chapter 3, the performance of this technique in the presence of white noise with no further processing at the receiver is the same as with a Rake receiver, provided ideal channel knowledge is available beforehand.

As already mentioned, the signal-to-noise ratio can be maximised with a matched filter at the receiver, but this has not been considered so far in the pre-Rake implementation found in the literature [11,12], where no further signal processing was considered at the receiving mobile station. We can however increase the signal-to-noise ratio with added complexity at the receiver. If pre-Rake filtering is performed at the transmitter, the optimal receiver is also a matched filter, yet not one matched to the channel only, as in a conventional Rake receiver, but to the combination of channel and pre-Rake, as shown in Fig. 4.1. This filtering, which we call a post-Rake[2], maximises the signal-to-noise ratio when a pre-Rake is employed. A better performance can be thus obtained in relation to a simple pre-Rake, and, since the error rate of the latter is equal to the one of a Rake receiver in presence of white noise, the use of a pre- and a post-Rake can also improve the link performance compared to a conventional Rake receiver.

1. The channel described by $H(f)$ corresponds to the concatenation of transmit filter, radio channel and receive filter, corresponding to the discrete-time channel model described in Section 2.1.
2. Throughout this chapter, whenever a post-Rake is mentioned, the use of a pre-Rake is also implied.

The reason for the better performance with a pre- and a post-Rake is that, with channel-matched pre-filtering, the signal power is concentrated at the frequency ranges where the channel is most favourable. The principle behind channel matched transmission is similar to the concept of water-filling [16], i.e., we should not waste signal power where the channel is bad, but rather concentrate it where we know that the signal will get through with little noise. Real water-filling[1] would be more difficult to implement, as this would require the transmitter to have knowledge of the noise level at the receiver.

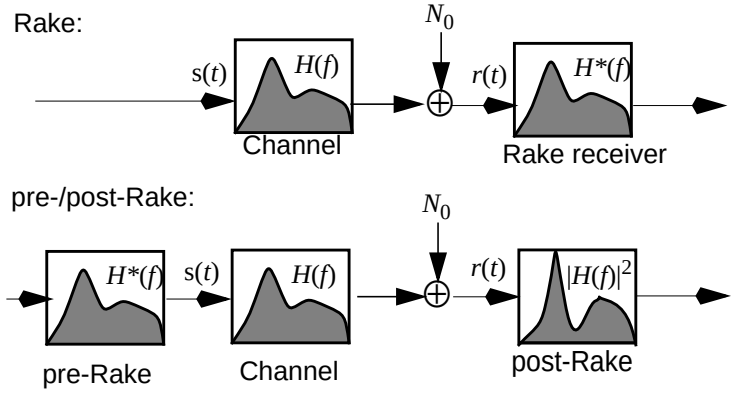

Fig. 4.1 - Concept of a pre/post-Rake (frequency domain)

This can also be visualised in the time domain, as in Fig. 4.2a. At the output of the Rake receiver several delayed copies of the desired signal are available. The independent noise samples at the receiver input also go through the Rake receiver, i.e., the Rake receiver acts like a noise 'colouring' filter, such that noise samples with different delays are mutually correlated at the output of a Rake receiver. Due to this, no further noise diversity can be obtained from the Rake output. The delayed signal copies only cause inter-symbol interference to the strongest signal at the middle of the Rake response, and cannot contribute to increase the signal-to-noise ratio.

The same does not happen if a pre-Rake is employed, as we can see from Fig. 4.2b. Upon reception we have the same delayed versions of the signal as after a Rake receiver, but the noise components are independent on the different delayed signals. This means that these can still be used to obtain noise diversity, what is optimally achieved by means of a post-Rake, which is nothing but a conventional Rake receiver matched to the combination of pre-Rake and channel impulse response. The optimum post-Rake is slightly more complex than an

1. For water-filling the power spectral density of the transmitted signal has to be [16]:

$$S_{Tx}(f) = \begin{cases} B - \dfrac{N_0}{|H(f)|^2} & , f \in F_b \\ 0 & , f \notin F_b \end{cases},$$

where F_b is the range of f for which $N_0/|H(f)|^2 \leq B$, and B is the solution to

$$P = \int_{f \in F_b} \left[B - \frac{N_0}{|H(f)|^2} \right] df ,$$

where P is the available power.

optimum conventional Rake receiver, since it requires more fingers to fully exploit the available multipaths, but most of the added system complexity is at the base-station, where a pre-Rake is employed, and where complexity is not such an important issue.

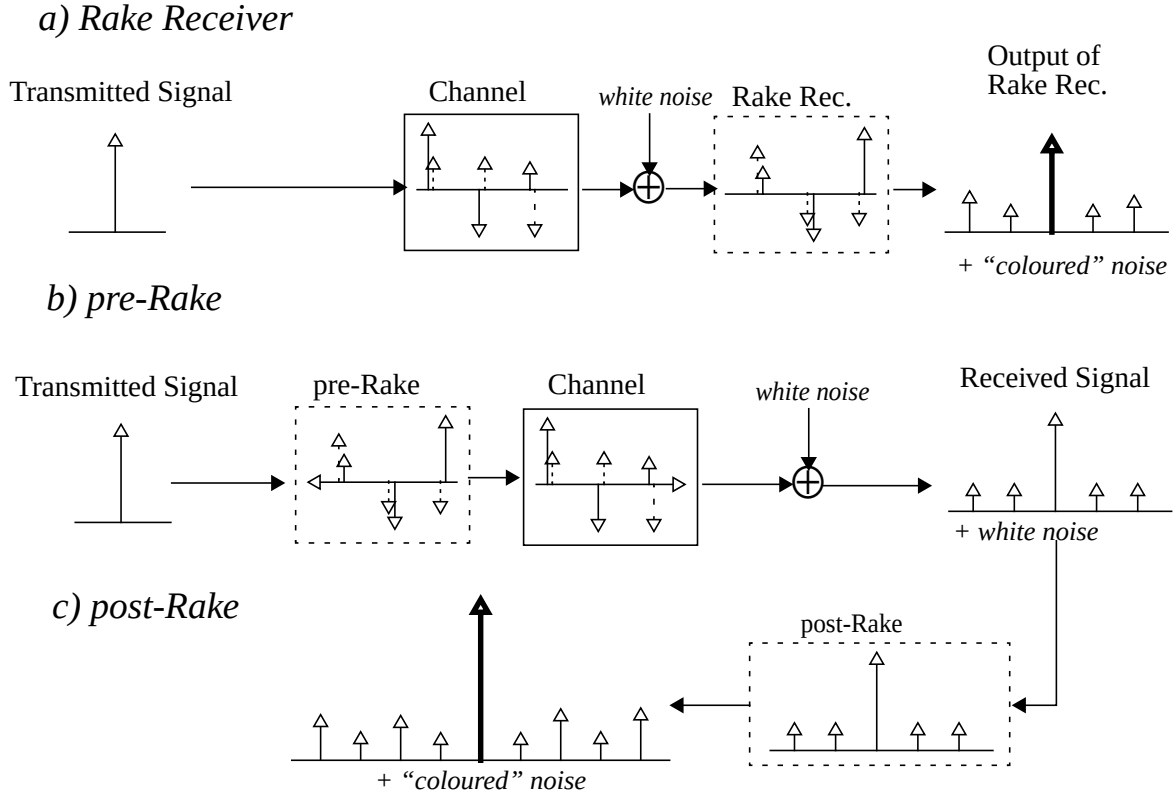

Fig. 4.2 - Concept of a pre/post-Rake (time domain)

4.2. System description and performance analysis (single user)

We will consider the same system model already described in Section 2.1. We assume that the transmission is made with an ideal pre-Rake with perfect channel estimation. The received signal was given in (3.3), but it will be repeated here for our convenience:

$$r_{pR}(i) = \beta\sqrt{\frac{E_c}{2}}\sum_{m=0}^{L-1}\sum_{l=0}^{L-1} g_m^* g_l d(i+m-l)c(i+m-l) + \nu(i) \tag{4.1}$$

where β is the normalising factor

$$\beta = \frac{1}{\sqrt{\sum_{l=0}^{L-1}|g_l|^2}}. \tag{4.2}$$

To make the analysis simpler, the signal from (4.1)can be divided by β with no influence at the results and we obtain:

$$r'_{pR}(i) = \sqrt{\frac{E_c}{2}}\sum_{m=0}^{L-1}\sum_{l=0}^{L-1} g_m^* g_l d(i+m-l)c(i+m-l) + \frac{1}{\beta}\nu(i) \tag{4.3}$$

In order that signal components with same delay be in the same summation term, which facilitates the analysis, the signal $r_{pR}'(i)$ from (4.3) can be alternatively written as:

$$r'_{pR}(i) = \sqrt{\frac{E_c}{2}} \sum_{\lambda=-L+1}^{L-1} \gamma_\lambda d(i-\lambda)c(i-\lambda) + \frac{1}{\beta}\nu(i) \tag{4.4}$$

where

$$\gamma_\lambda = \sum_{\substack{l,m \\ l-m=\lambda}} g_m^* g_l \tag{4.5}$$

This signal contains $2L$-1 delayed versions of our desired signal $d(k)c(k)$ with independent noise samples. It is as if the signal had been transmitted over a channel with $2L$-1 paths, with the difference that the path gains are no longer independent. In the conventional pre-Rake approach only the signal corresponding to λ=0 is used, and its delayed versions contribute to the inter-symbol interference only. We can however increase the signal-to-noise ratio through noise diversity by employing a post-Rake that optimally combines (i.e., with maximum ratio combining for maximum signal-to-noise ratio) the $2L$-1 delayed versions of the signal, exactly as with a normal Rake receiver.

Analogous to the expression for a Rake receiver from (2.6), the post-Rake processing can be expressed by the following equation:

$$\begin{aligned} y_{pRp}(i) &= \left(\sum_{\mu=-L+1}^{L-1} \gamma_\mu^* r'(i+\mu) \right) \otimes c(i) \\ &= \sqrt{\frac{E_c}{2}} \left(d \sum_{\lambda=-L+1}^{L-1} \left| \sum_{\substack{l,m \\ l-m=\lambda}} g_m^* g_l \right|^2 + \sum_{\substack{p=-2(L-1) \\ p\neq 0}}^{2(L-1)} \left(\sum_{\substack{\lambda,\mu \\ \lambda-\mu=p}} \gamma_\mu^* \gamma_\lambda a(i-p) \right) \otimes c(i) \right) + \\ &\quad + \frac{1}{\beta} \sum_{\mu=-L+1}^{L-1} (\gamma_\mu^* \nu(i+\mu)) \otimes c(i) \end{aligned} \tag{4.6}$$

with $a(i)=d(i)c(i)$.

This signal is integrated over M chips and we obtain thus

$$z_{pRp} = M\sqrt{2E_c} \sum_{\mu=-L+1}^{L-1} |\gamma_\mu|^2 (1+j)d + \nu_{self,\,pRp} + \nu_{G,\,pRp} \tag{4.7}$$

Where $\nu_{G,pRp}$ is the Gaussian noise component after a pre- and a post-Rake

$$\nu_{pRp} = \frac{1}{\beta} \sum_{i=0}^{M-1} \sum_{\mu=-L+1}^{L-1} (\gamma_\mu^* \nu(i+\mu)) \otimes c(i)\,, \tag{4.8}$$

whose complex variance is given by

$$\mathrm{var}(\nu_{G,\,pRp}) = MN_0 \sum_{l=0}^{L-1} |g_l|^2 \sum_{\mu=-L+1}^{L-1} |\gamma_\mu|^2\,; \tag{4.9}$$

and $\nu_{self,pRp}$ is the self-interference

$$\nu_{self,\,pRp} = \sqrt{\frac{E_c}{2}} \sum_{i=0}^{M-1} \sum_{\substack{p=-2(L-1) \\ p\neq 0}}^{2(L-1)} \left(\sum_{\substack{\lambda,\,\mu \\ \lambda-\mu=p}} \gamma_\mu^* \gamma_\lambda a(i-p) \right) \otimes c(i) \tag{4.10}$$

which, as we assume large spreading factors, will be ignored at this stage.

The decision variable will be the sum of the real and imaginary parts of z_{pRp}, and, as done in Section 2.2.1, we can obtain from (4.7) and (4.9) the ratio of bit-energy to noise variance after the post-Rake processing, which is

$$\Gamma_{pRp} = \frac{E_b \sum_{\mu=-L+1}^{L-1} |\gamma_\mu|^2}{N_0 \sum_{l=0}^{L-1} |g_l|^2} = \frac{E_b \sum_{\mu=-L+1}^{L-1} \left| \sum_{\substack{l,\,m \\ l-m=\mu}} g_m^* g_l \right|^2}{N_0 \sum_{l=0}^{L-1} |g_l|^2} \tag{4.11}$$

With the expression from (4.11) we can proceed with the semi-analytical approach proposed in Section 2.2.1 to obtain the bit error rate with a post-Rake.

We can recall from Section 2.2.1 that the signal-to-noise ratio with either a conventional Rake receiver or a pre-Rake only is

$$\Gamma_{Rake} = \frac{E_b \sum_{l=0}^{L-1} |g_l|^2}{N_0} = \frac{E_b \left(\sum_{l=0}^{L-1} |g_l|^2 \right)^2}{N_0 \sum_{l=0}^{L-1} |g_l|^2} \tag{4.12}$$

Now, since

$$\sum_{\mu=-L+1}^{L-1} \left| \sum_{\substack{l,\,m \\ l-m=\mu}} g_m^* g_l \right|^2 = \left(\sum_{l=0}^{L-1} |g_l|^2 \right)^2 + \sum_{\substack{\mu=-L+1 \\ \mu\neq 0}}^{L-1} \left| \sum_{\substack{l,\,m \\ l-m=\mu}} g_m^* g_l \right|^2 \geq \left(\sum_{l=0}^{L-1} |g_l|^2 \right)^2, \tag{4.13}$$

it follows readily from equations (4.11) to (4.13) that $\Gamma_{pRp} \geq \Gamma_{Rake}$ for any channel configuration $\boldsymbol{g}$ and, consequently, the bit error rate is always smaller with the combination of a pre-Rake and a post-Rake than with either a conventional Rake receiver or a pre-Rake only.

It could be argued that the same processing performed by a post-Rake with a pre-Rake could be made after a conventional Rake receiver, but we should recall that the matched filter is the optimum receiver in the presence of noise and maximises the signal-to-noise ratio [31]. The Rake receiver with maximum ratio combining is already a matched filter and, if another filter is applied to it, the combined filter will no longer be optimum. Thus the application of a post-Rake to a Rake receiver will only increase the signal-to-noise ratio (and the inter-symbol interference) and make the performance worse.

The results obtained through the above analysis are shown in Fig. 4.3 for both channels of Table 2.1, with a spreading gain of G=128 and for different coding rates: R=1/4 for the 2-path channel with strong LOS component and R=1/8 for the 6-path severe multipath channel, both convolutional codes with memory order m_o=8. It can be seen that the results are very similar to the ones obtained through simulation, which indicates the accuracy of the analysis carried out above for the proposed system parameters. We can see in this figure that the performance with

a pre- and a post-Rake is much better than the one with a conventional Rake receiver (or a pre-Rake only) for the proposed scenarios, which confirms the performance gains we expected from the above analysis. We can also notice that this gain is much more pronounced in a severe multipath environment, in which about 2dB performance gain can be achieved. This was also expected, because, as we can see in Fig. 4.2, the better performance with a post-Rake results from the use of the delayed versions of the received desired signal to obtain noise diversity, and these arise from the multipath propagation.

The complexity of an optimal post-Rake is slightly greater than the one of an optimal conventional Rake receiver, since $2L$-1 fingers are required instead of just L. Nevertheless, in a post-Rake the weakest fingers correspond to the signal obtained by the multiplication of the weakest paths with the pre-Rake fingers with lowest gains, and thus tend to concentrate little of the signal energy. A post-Rake with the same complexity as an optimum Rake receiver (i.e., with only L paths) can also be very effective and yield a significant performance gain, as displayed in Fig. 4.3. We can observe that the performance loss is little if the L-1 weakest fingers are discarded, specially in a severe multipath environment.

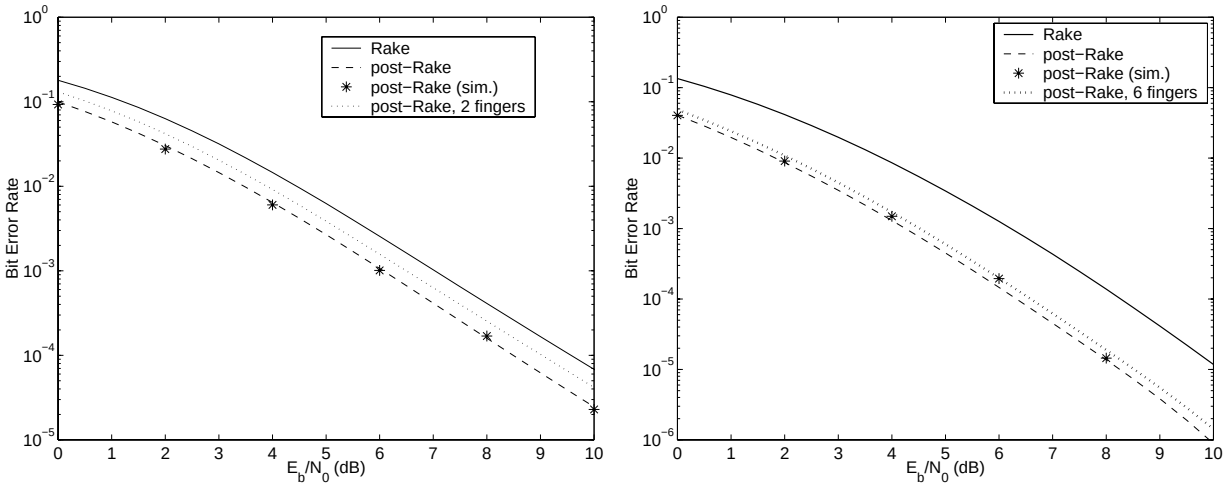

a) 2 path channel, R=1/4 *b) 6 path channel, R=1/8*

Fig. 4.3 - Performance of a pre/post-Rake (single user)

We have so far ignored the self-interference, which is negligible for large spreading gains. However one of the drawbacks of the combination of a pre- and a post-Rake is that the ratio of desired signal energy to inter-symbol interference decreases compared to a system with a single Rake processor.

From the expression for the self-interference in (4.10) we can obtain its variance, as done in Section 2.2. It is

$$\mathrm{var}\{\nu_{self,\,pRp}\} = ME_c \sum_{\substack{p=-2(L-1)\\ p\neq 0}}^{2(L-1)} \left| \sum_{\substack{\lambda,\,\mu\\ \lambda-\mu=p}} \gamma_\mu^* \gamma_\lambda \right|^2 \tag{4.14}$$

In Fig. 4.4 we plot the average ratio of signal-energy to self-interference variance Γ_{self} for both a conventional Rake receiver (or a pre-Rake only) and the combination of a pre- and a post-Rake, considering both proposed channel models; and it can be seen that the self-interference is much more significant if a post-Rake is employed, being about 4,5dB higher in a severe multi-path environment. Nevertheless, as assumed so far, it can be noticed that the inter-

symbol interference is of little relevance with the system parameters we are using (G=128) and it is usually much less than the thermal noise. It may however make a difference for very low processing gains, particularly in environments with high signal-to-noise ratio. In this case however, our approximation of the self-interference to Gaussian noise by the central limit theorem is not good enough, and our approach to obtain the bit error rate cannot be applied. If the inter-symbol interference is noticeable, it can be dealt with by employing the Viterbi algorithm [31] instead of Rake receiver (or a post-Rake) to obtain optimum results.

Even though the inter-symbol interference is mostly irrelevant in a single-user environment, the fact that it increases with a post-Rake will have its implications in a multi-user environment, as we shall see in Section 4.4.

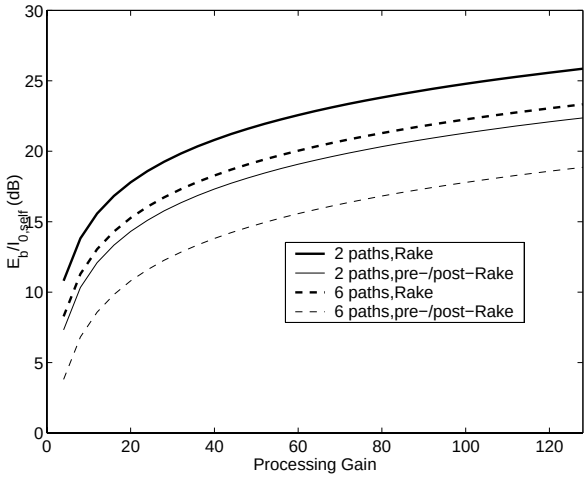

Fig. 4.4 - Effect of the self-interference

4.3. Post-Rake in Time-Variant Channels

We have seen in Section 3.4.2 that the performance of a pre-Rake suffers in a time-variant environment, due to the time delay between channel estimation in the uplink and transmission in the downlink. In this case the post-Rake can also be used to alleviate this impairment, what is shown in Fig. 4.5. The same TDD frame structure from Fig. 3.7 was considered and we assume that each user transmits its own training sequence in the downlink, which is also pre-distorted by the pre-Rake. The processing gain (G=128), the coding scheme (R=1/8, m=8) and the channel (6 paths, Rayleigh fading with classical Doppler spectrum, f_c=5GHz, E_b/N_0=9dB) are the same as in Section 3.4.2. Additionally, we assume that the channel can be ideally estimated upon reception of the training sequence, but, as the channel changes, these estimations may be not up-to-date for the rest of the frame. In the downlink this means that the combination of pre-Rake and channel can be estimated and this information can be used to compensate for the erroneous pre-Rake distortion.

The results from Fig. 4.5 demonstrate the above assumption, and we can see that part of the performance loss of a pre-Rake caused by the channel variability can be compensated by the use of a post-Rake, and that even at relatively high speeds the use of a pre-Rake becomes feasible, with performance approaching the one obtained with a conventional Rake receiver. Recalling that the ratio T_{TDD}/T_{coh} is proportional to the velocity, we can see that at low velocities the performance with a pre- and a post-Rake is much better than the one with either a Rake receiver or a pre-Rake, as obtained in the previous section, but this performance gain disappears at higher velocities. The techniques proposed in 3.4.2 to reduce the transmission

estimation errors in time-variant channels (prediction, extra training sequence) have not been considered here, but we can expect them to bring a substantial performance improvement in the case of a post-Rake too. The variations in the BER observed in the curve for the Rake receiver are possibly due to the use of convolutional codes with large memory order, as explained in Section 3.4.2.

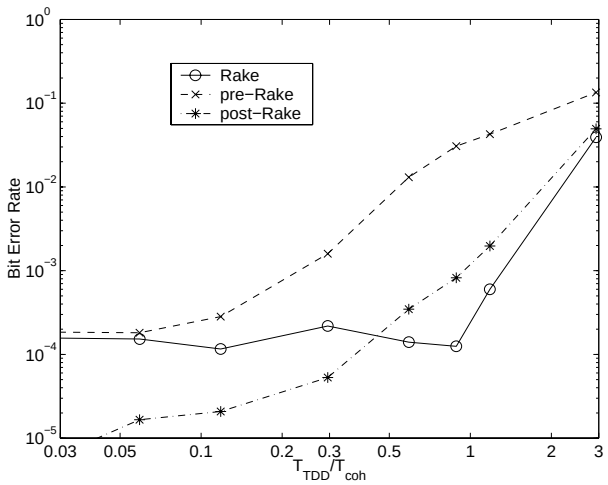

Fig. 4.5 - Performance with a post-Rake in a time-variant channel

4.4. Performance analysis in a multi-user environment

An analysis similar to the one made for a single-user can be made for the downlink in a multi-user environment. We follow an analysis like the one performed for a pre-Rake only in Section 3.2. The received signal was already obtained in that section, but it will be repeated here for our convenience. With no loss at generality, we consider the signal at user 0, and the signal is divided by the normalising factor β_0 to make the analysis easier.

$$\begin{aligned} r_{0,\,pR}'(i) &= \frac{1}{\beta_0}\sqrt{\frac{E_c}{2}}\sum_{l=0}^{L-1} g_{0,\,l}\, s_{pR}(i-l) + \frac{1}{\beta_0}\nu(i) \\ &= \sqrt{\frac{E_c}{2}}\sum_{k=0}^{K-1}\frac{\beta_k}{\beta_0}\sum_{l=0}^{L-1} g_{0,\,l}\sum_{m=0}^{L-1} g_{k,\,m}^{*}\, d_k(i+m-l)\,c_k(i+m-l) + \frac{1}{\beta_0}\nu(i) \end{aligned} \tag{4.15}$$

We now proceed to the analysis considering both a pre- and a post-Rake. Reminding that $a_k(i)=d_k(i)c_k(i)$, the received signal will be rewritten as

$$r_{0,\,pR}'(i) = \sqrt{\frac{E_c}{2}}\sum_{k=0}^{K-1}\frac{\beta_k}{\beta_0}\sum_{\lambda=-L+1}^{L-1}\left(\sum_{\substack{l,\,m \\ l-m=\lambda}} g_{k,\,m}^{*}\, g_{0,\,l}\right) a_k(i-\lambda) + \frac{1}{\beta_0}\nu(i) \tag{4.16}$$

This is processed by a post-Rake matched to the combination of pre-Rake and channel as in (4.6) and we obtain:

$$
\begin{aligned}
y_{pRp}(i) \;=\; & \sqrt{\frac{E_c}{2}} d_0 \sum_{\lambda=-L+1}^{L-1} \left| \sum_{\substack{l,m \\ l-m=\lambda}} g^*_{0,m} g_{0,l} \right|^2 + \\
& + \sqrt{\frac{E_c}{2}} \sum_{\substack{p=-2(L-1) \\ p\neq 0}}^{2(L-1)} \left(\sum_{\substack{\lambda,\mu \\ \lambda-\mu=p}} \gamma^*_{0,\mu}\gamma_{0,\lambda} a_0(i-p) \right) \otimes c_0(i) \\
& + \sqrt{\frac{E_c}{2}} \sum_{k=1}^{N-1} \frac{\beta_k}{\beta_0} \sum_{p=-2(L-1)}^{2(L-1)} \left(\sum_{\substack{\lambda,\mu \\ \lambda-\mu=p}} \gamma^*_{k,\mu}\gamma_{0,\lambda} a_k(i-p) \right) \otimes c_0(i) \\
& + \frac{1}{\beta_0} \sum_{\mu=-L+1}^{L-1} (\gamma^*_{0,\mu} \nu(i+\mu)) \otimes c_0(i)
\end{aligned}
\tag{4.17}
$$

where

$$
\gamma_{k,\mu} \;=\; \sum_{\substack{l,m \\ l-m=\mu}} g^*_{k,m} g_{0,l} \tag{4.18}
$$

The first term in (4.17) corresponds to the desired signal, the second to the self-interference, the third to the multi-user interference and the fourth to the white Gaussian noise. The post-Rake output is summed over *M* symbols, and we obtain the same signal as in (4.7), plus the multi-user interference:

$$
z_{pRp} \;= M\sqrt{2E_c} \sum_{\mu=-L+1}^{L-1} |\gamma_{0,\mu}|^2 (1+j)d + \nu_{self,\,pRp} + \nu_{mu,\,pRp} + \nu_{pRp} \tag{4.19}
$$

The variance of the Gaussian noise component was already given in (4.9) and of the self-interference in (4.14). The variance of the multi-user interference component can be obtained as in Appendix C and it is given by

$$
\begin{aligned}
\mathrm{var}\{\nu_{mu,\,pRp}\} \;=\; ME_c \sum_{k=1}^{K-1} \frac{\beta_k^2}{\beta_0^2} \Bigg[& \sum_{\substack{p=-2(L-1) \\ p\neq 0}}^{2(L-1)} \left| \sum_{\substack{\lambda,\mu \\ \lambda-\mu=p}} \gamma^*_{k,\mu}\gamma_{0,\lambda} \right|^2 \\
& + \alpha_k \left| \sum_{\lambda=-L+1}^{L-1} \gamma^*_{k,\lambda}\gamma_{0,\lambda} \right|^2 \Bigg]
\end{aligned}
\tag{4.20}
$$

where α is the orthogonality factor

$$
\alpha_k \;=\; \begin{cases} 1 & \text{, if } c_0(i) \text{ and } c_k(i) \text{ are not orthogonal} \\ \sin^2\left(\angle \sum_{\lambda=-L+1}^{L-1} \gamma^*_{k,\lambda}\gamma_{0,\lambda} \right) & \text{, if } c_0(i) \text{ and } c_k(i) \text{ are orthogonal} \end{cases} \tag{4.21}
$$

with $\angle a$ the phase of the complex number *a*.

As in Section 2.2, we can also define the interference power spectral density $I_{0,\,pRp}$, which is now given by:

$$I_{0,\,pRp} = \frac{\mathrm{var}\{\nu_{self,\,pRp}\} + \mathrm{var}\{\nu_{mu,\,pRp}\}}{M \sum_{l=0}^{L-1} |g_{0,\,l}|^2 \sum_{\mu=-L+1}^{L-1} \left| \sum_{\substack{l,\,m \\ l-m=\mu}} g^*_{0,\,m} g_{0,\,l} \right|^2} \tag{4.22}$$

and the signal-to-noise ratio

$$\Gamma_{pRp}(\boldsymbol{g}) = \frac{E_b \sum_{\mu=-L+1}^{L-1} \left| \sum_{\substack{l,\,m \\ l-m=\mu}} g^*_{0,\,m} g_{0,\,l} \right|^2}{(N_0 + I_{0,\,pRp}) \sum_{l=0}^{L-1} |g_{0,\,l}|^2} \tag{4.23}$$

Based on the above equation and on the interference variance from (4.14) and (4.20) we can proceed like in Section 2.2 to obtain the bit error rate. Once again the semi-analytical results fit the simulation results very closely, as we can see from the figures displayed in Section 4.5, in which some semi-analytical results are compared to ones obtained through simulation.

It is not evident from the above equations, but it can be shown that the multi-user interference with a post-Rake increases compared to a system with a pre-Rake only. As we have seen in Section 4.2, the signal-to-noise ratio improves when a post-Rake is used, whereas the inter-symbol interference increases, which can be neglected for a single user. But that also means that the inter-symbol interference caused by the other users also increases, what is depicted in Fig. 4.6, and for a great number of users this becomes important.

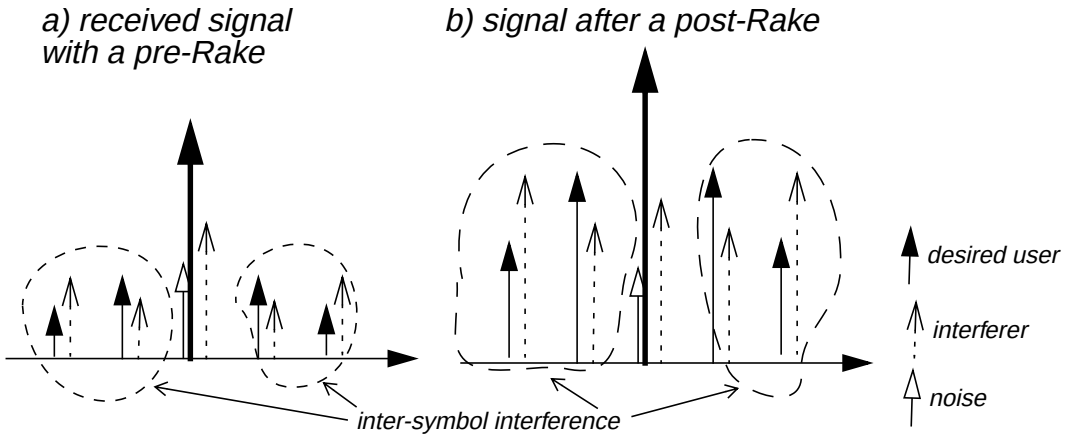

Fig. 4.6 - Multi-user interference with a post-Rake

To obtain quantitative results that demonstrate the explanation above we have separated the multi-user interference ($\nu_{mu,pR}$ with a pre-Rake only and $\nu_{mu,pRp}$ with a post-Rake) into two components: one due to the synchronous interference with non-orthogonal sequences, corresponding to the terms multiplied by the orthogonality factor α_k in (3.14) and (4.20); and one due to the multi-user inter-symbol interference, which corresponds to the asynchronous terms on $\lambda \neq 0$ in (3.14) and on $p \neq 0$ in (4.20). The signal-to-interference ratios in a 6-path channel for the these two kinds of interference were obtained separately and plotted in Fig. 4.7. We can see that the multi-user inter-symbol interference is responsible for most of the

signal impairment caused by the other users, and this is higher when a post-Rake is used, whereas the synchronous component of the interference is about the same either with or without a post-Rake. The difference seems rather small, about 1dB at most, but this can have a significant influence on the bit error rate, as we can see for instance in Fig. 2.6b. The effect of this on the capacity will be seen in the next section.

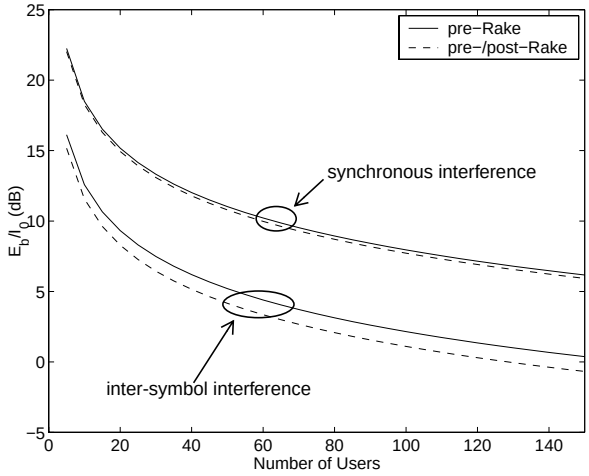

Fig. 4.7 - Effect of multi-user inter-symbol interference with a post-Rake

4.5. Results

As done in the previous chapters, we can use equations (4.20) to (4.23) to calculate the ratio of the signal energy to noise-plus-interference and, based on that, obtain the bit error rate. Some performance results with a post-Rake are shown in Fig. 4.8 and in Fig. 4.9 and are compared with those obtained either with a Rake receiver or with a pre-Rake only. We have considered a system with a processing gain G=128 and with both channel models described in Table 2.1. Convolutional codes with memory order m_o=8 are employed. When a conventional Rake receiver is used, a coding rate of R=1/4 is considered, for the reasons explained in Chapter 2. When a pre-Rake is employed, either with or without a post-Rake, a coding rate of R=1/8 is considered, as proposed in Chapter 3. The same considerations concerning the optimum trade-off between orthogonality and channel coding made in Chapter 3 for a pre-Rake apply when a post-Rake is used since the use of a post-Rake does not change the behaviour of pre-Rake with orthogonal spreading.

The results shown in Fig. 4.8 were obtained considering a signal-to-noise ratio of E_b/N_0=9dB. We can see that for a small number of users the performance with a post-Rake is much better than either with a Rake receiver or with a pre-Rake only. This is due to the fact that the combination of a pre- and a post-Rake increases the signal-to-noise-ratio, as demonstrated in Section 4.2, and hence the performance is improved when Gaussian noise is dominant. For a large number of users however, the performance deteriorates slightly in relation to a pre-Rake only or to a conventional Rake receiver. This is due to the increase in the inter-symbol interference caused by the other users, which was expounded in the previous section. This interference becomes more significant with the increase in the number of users and it eventually outweighs the better performance of a post-Rake in the presence of noise. The same applies both for the 6-path channel with severe multipath distortion and for the 2-path channel

with strong line-of-sight component, but for the former the performance gain with a post-Rake is much more significant if few users are active, as it was expected from the single user performance results from Section 4.2.

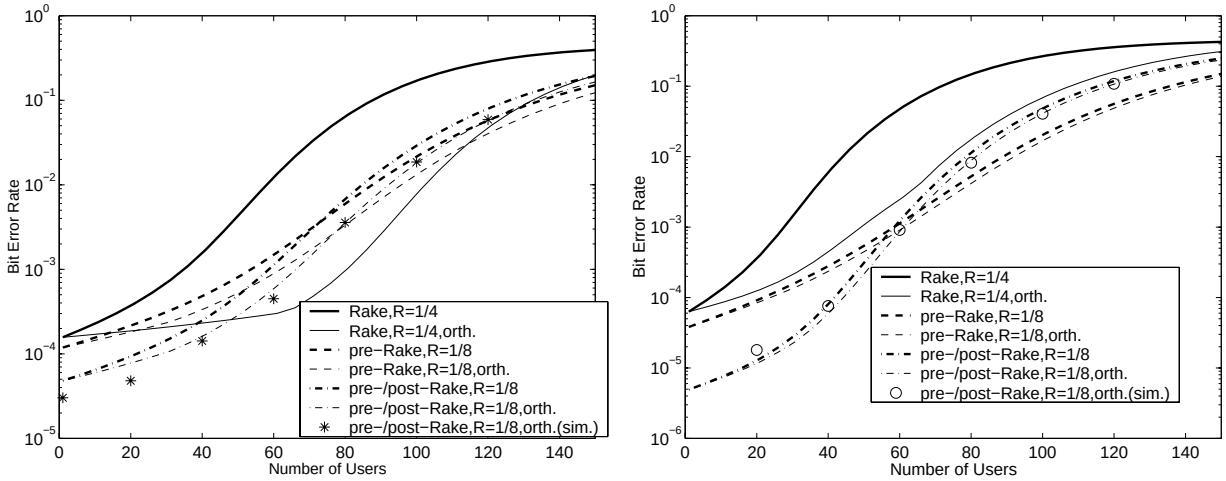

a) 2-path channel *b) 6-path channel*

Fig. 4.8 - Performance of a pre/post-Rake in a multi-user environment (E_b/N_0=9dB)

In Fig. 4.9 we consider a noisier channel, with signal-to-noise ratio of E_b/N_0=6dB. We can see that in this case the post-Rake is the best technique in a larger region than in Fig. 4.8, due to resilience of this technique against noise. We can see that under these circumstances the use of a pre- and a post-Rake may be the only alternative that allows the achievement of a reasonably low bit error rate.

Furthermore, from both Fig. 4.8 and Fig. 4.9 we can notice that, as with a pre-Rake only, little can be gained by the use of orthogonal spreading sequences with the combination of a pre- and a post-Rake, particularly in an environment with severe multi-path distortion.

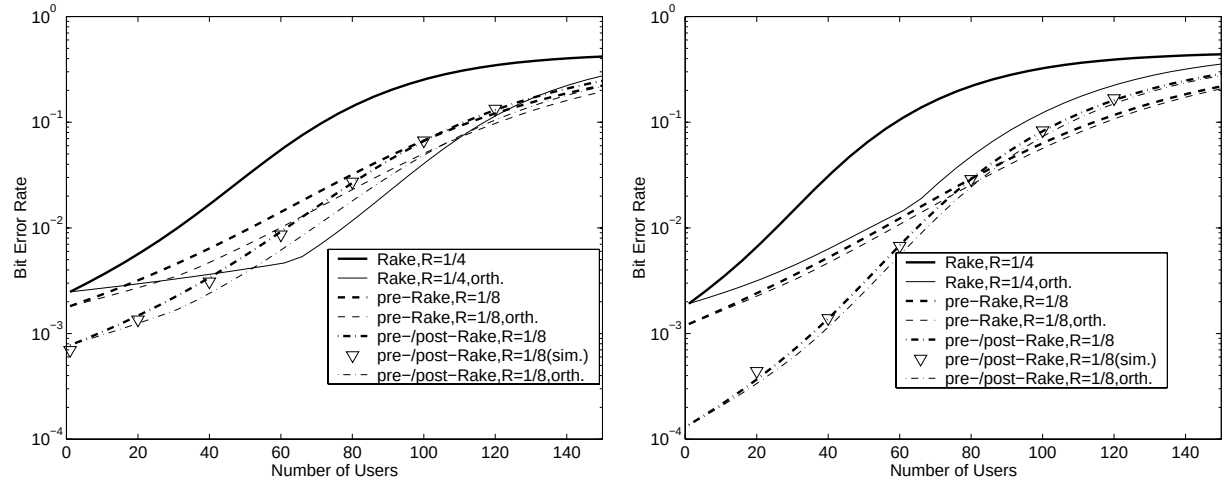

a) 2-path channel *b) 6-path channel*

Fig. 4.9 - Performance of a pre/post-Rake in a multi-user environment (E_b/N_0=6dB)

Unlike in the other chapters, where a noiseless channel has also been investigated, this situation has not been considered here. It is however clear that due to the increase in the multi-user interference caused by a post-Rake, its use in such an environment would only bring about a performance worsening. However, as already pointed out, this situation is unrealistic, since noise is unavoidable and it may come from several sources; not only from the thermal noise, but also from interference caused by the other cells and by overlay networks, if we assume that these can be modelled as white Gaussian noise. A more detailed investigation of the system capacity considering a realistic modelling of these other interference sources is yet to be carried out.

The increase in the multi-user interference with a post-Rake could be possibly tackled by the implementation of a multi-user multi-path detection scheme [28] instead. With the use of a pre-Rake the signal energy is concentrated on the good parts of the channel, as seen in Section 4.1, and a better performance in the presence of noise can be achieved; whereas the multi-user multi-path detector might be able to cancel out the multi-user interference, which increases with a post-Rake. Due to the above considerations, we presume that the use of a pre-Rake should bring some performance gain when multi-user detection is employed, nevertheless with a significant increase in the receiver complexity. The investigation of such techniques is however beyond the scope of this work.

Even though a greater capacity cannot always be achieved with a post-Rake, this technique offers more resilience against noise if few users are active, and this can be used to reduce the transmit power of the base stations, which consequently is reflected in a lower interference for the other cells or overlaying systems. The low sensitivity to noise attained with the combination of a pre- and a post-Rake also means that a greater range can be attained with this technique, what is particularly useful in areas with light traffic.

4.6. Summary of Chapter 4

We have proposed in this chapter a new technique which involves a pre-Rake at the transmitter and a post-Rake at the receiver. We have seen that this technique largely increases the signal-to-noise ratio at the receiver and hence the performance in the presence of Gaussian noise. In comparison to the use of a Rake receiver or to a pre-Rake only, the price to pay for the noise reduction with a post-Rake is an increase in the multi-user interference, but in many situations this is likely to be more than compensated by the good performance in noisy channels. The use of a post-Rake is particularly favourable where a low bit error rate is required with a relatively small number of users.

The complexity of the post-Rake receiver is equivalent to the one of a conventional Rake receiver, except that more fingers are required for optimal detection. These extra fingers can however be discarded with no significant performance loss.

From the results shown in this and in the previous chapters we can reach the conclusion that there is not a single optimum technique among the ones investigated: conventional Rake receiver, pre-Rake and post-Rake. The choice depends on the particular environment, on the traffic load, and on the required quality of service, and should be made adaptively.

5. JOINT SIGNAL PRECODING

In the previous chapters we have analysed techniques in which each user is processed individually. It is nonetheless known that a substantial capacity increase can be achieved if the users are jointly detected upon reception [28]. However, as mentioned in the Introduction, multiuser detection is somewhat complex for implementation at a mobile station and should therefore be avoided to save costs and power. In the downlink, if channel state information is available a priori, an alternative solution is to jointly pre-distort the signal before transmission with the goal of reducing the interference. Some approaches to this problem for a single path channel were proposed in the literature [40,41], but are not of practical significance in a typical multipath wireless channel. In [40] the issue of joint precoding was dealt with considering also a multipath channel, but the use of Rake receivers at the mobile stations was required for a reasonable performance. In [35] a joint precoding scheme similar to zero-forcing multiuser detection was proposed which dispenses with the use of a Rake receiver at the mobile stations and achieves high system capacity with low-cost mobile terminals. Further joint precoding schemes were proposed recently in [3,8].

In this chapter we will investigate in depth the use of joint precoding for capacity maximisation in the downlink of CDMA systems. The concept of joint precoding in direct-sequence spread spectrum systems will be clarified in Section 5.1.

In Section 5.2 a few existing methods of linear block precoding will be reviewed and some modifications of them will be proposed. We will also derive the optimum precoder for complete interference elimination, and a precoding method for power constrained systems will be suggested.

The block precoding methods have a complexity that increases polynomially not only with the number of users but also with the block size, which makes their use limited to systems with short data blocks. In Section 5.3 a joint precoding method will be proposed whose complexity increases linearly with the block size with little performance loss compared to the block precoding techniques.

In Section 5.4 some small modifications of the block precoding algorithms which allow their application to systems employing multiple transmit antennas will be proposed.

5.1. Concept

As we have seen, the basic idea behind the pre-Rake is that in TDD systems we can assume that the channel is known before transmission. We have previously used this fact to pre-distort the signal of each user individually by employing a pre-Rake matched to each user's channel. In a conventional approach, with or without a pre-Rake, the total transmitted signal is the sum of K individually pre-processed signals. We can however do better than that if, besides using the channel state information (CSI), we also employ the knowledge about each user's signal to reduce or even eliminate the multiuser interference by jointly precoding the signal. This concept is depicted in Fig. 5.1. The transmitted signal does not have to be the sum of the signals of different users, but should rather be a signal that optimises a certain performance parameter (e.g., average bit error rate) as a function of the transmitted signals, spreading codes and the channel state information of every user. Supposing we know the channel impulse response of every user before transmission, such a joint precoding scheme can be found for the downlink, as the signals are transmitted synchronously and both the transmitted bits $d_k(i)$ and the scrambling codes $c_k(i)$ of all the users are known by the base station.

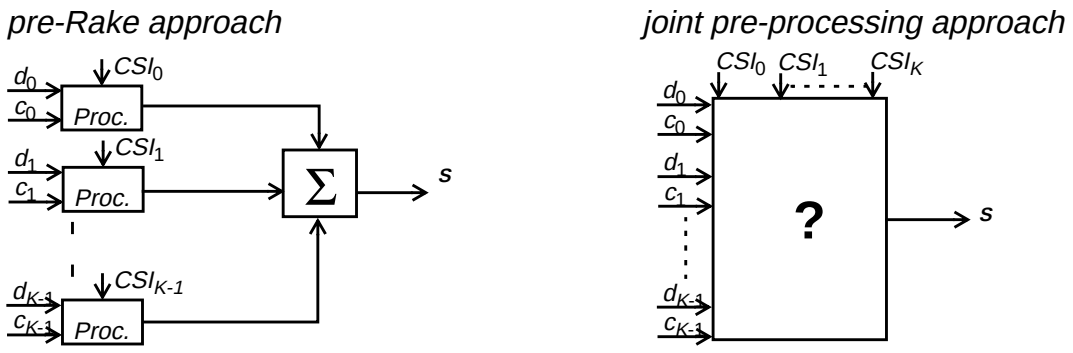

Fig. 5.1 - Joint pre-processing concept

The precoding algorithms may substantially increase the complexity of the transmitting base station, which is however preferable to the use of expensive multiuser detection techniques at the mobile stations. Joint precoding schemes work either with integrate-and-dump[1] or with Rake receivers at the mobile stations and, as we shall see in the following sections, can nonetheless bring about a significant capacity gain compared to systems employing either pre-Rakes or conventional transmission[2] with Rake receivers.

5.2. Block Precoding

In this section we will investigate some joint precoding techniques in which blocks of N bits are simultaneously processed. In Section 5.2.1 a new matrix notation will be introduced to enable a blockwise analysis. Methods which aim at completely eliminating the interference will be investigated in Section 5.2.2 to Section 5.2.4, and a precoding scheme with power constraint will be proposed in Section 5.2.5. Some issues regarding the implementation of the methods investigated here will be briefly analysed in Section 5.2.6

5.2.1 System Model

In order to facilitate the analysis of block precoding techniques it is useful to develop a vector notation for the spread-spectrum system presented in Section 2.1.

We will consider the transmission of a block of N_{inf} information bits, which correspond to $N=N_{inf}/R$ coded bits. Let $\boldsymbol{d}_k$ be the vector of transmitted coded bits of user k

$$\boldsymbol{d}_k = \begin{bmatrix} d_k(0) \\ d_k(1) \\ \cdots \\ d_k(N-1) \end{bmatrix} \tag{5.1}$$

where $d_k(n)=\pm 1$ denotes the n-th bit of user k.

We can also define the vector $\boldsymbol{d}$ containing the bits of all the users:

1. We call integrate-and-dump receiver the conventional spread spectrum receiver in which the received signal is correlated with the scrambling code, integrated and dumped. No Rake receiver is considered in this case.
2. By conventional transmission we understand spectrum spreading without pre-processing as described in Section 2.1.1.

$$\boldsymbol{d} = \begin{bmatrix} \boldsymbol{d}_0 \\ \boldsymbol{d}_k \\ \cdots \\ \boldsymbol{d}_{K-1} \end{bmatrix} \tag{5.2}$$

where K is the number of users.

As in Section 2.1.1 these bits are spread by a complex sequence $c_k(i)$, with $M=GR$ chips per coded bit. Let the vector $\boldsymbol{c}_k(n)$ represent the coding sequence corresponding to the n-th bit of the k-th user:

$$\boldsymbol{c}_k(n) = \begin{bmatrix} c_{k,R}(nM) \\ c_{k,I}(nM) \\ c_{k,R}(nM+1) \\ c_{k,I}(nM+1) \\ \cdots \\ \cdots \\ c_{k,R}(nM+M-1) \\ c_{k,I}(nM+M-1) \end{bmatrix} \tag{5.3}$$

where $c_{k,R}(i)$ and $c_{k,I}(i)$ are respectively the real and imaginary parts of the i-th chip of the spreading sequence $c_k(i)$[1].

The spread signal of user k over one block can be hence given by

$$\boldsymbol{x}_k = \begin{bmatrix} x_{k,R}(0) \\ x_{k,I}(0) \\ x_{k,R}(1) \\ x_{k,I}(1) \\ \cdots \\ \cdots \\ x_{k,R}(NM-1) \\ x_{k,I}(NM-1) \end{bmatrix} = \boldsymbol{C}_k \boldsymbol{d}_k \tag{5.4}$$

where $\boldsymbol{C}_k$ is the $2MN \times N$ block spreading matrix of the k-th user

1. The separation of the real imaginary terms is needed for the following two reasons:
   - to take into account in the matrix notation the operator $\otimes$, defined in (2.7) as the separate multiplication of the real and imaginary parts of two complex numbers. This is straightforward if the real and imaginary components are isolated.
   - in Section 5.2 we will work with gradients to perform some vector optimisations. Let x be a complex number, with x_R and x_I its real and imaginary components respectively. We will employ the energy function $E(x)=|x|^2$, which is not complex differentiable. We can however define the real-valued vector $\boldsymbol{x}=[x_R\ x_I]^{\mathrm{T}}$ and obtain the same energy function $E(\boldsymbol{x})=\boldsymbol{x}^{\mathrm{T}}\boldsymbol{x}$, whose gradient can be easily obtained.

$$\boldsymbol{C}_k = \begin{bmatrix} \boldsymbol{c}_k(0) & 0 & \dots & 0 \\ 0 & \boldsymbol{c}_k(1) & \dots & 0 \\ \dots & \dots & \dots & \dots \\ 0 & 0 & \dots & \boldsymbol{c}_k(N-1) \end{bmatrix}. \tag{5.5}$$

In a system without pre-coding the multiuser transmitted signal vector, separated into real and imaginary parts, is given by

$$\boldsymbol{s} = \sum_{k=0}^{K-1} \boldsymbol{x}_k. \tag{5.6}$$

Now let $\boldsymbol{x}$ be the composite vector of all spread signals

$$\boldsymbol{x} = \begin{bmatrix} \boldsymbol{x}_0 \\ \boldsymbol{x}_1 \\ \dots \\ \boldsymbol{x}_{K-1} \end{bmatrix} = \boldsymbol{C}\boldsymbol{d} \tag{5.7}$$

where $\boldsymbol{C}$ is the $2MNK \times NK$ spreading matrix

$$\boldsymbol{C} = \begin{bmatrix} \boldsymbol{C}_0 & 0 & \dots & 0 \\ 0 & \boldsymbol{C}_1 & \dots & 0 \\ \dots & \dots & \dots & \dots \\ 0 & 0 & \dots & \boldsymbol{C}_{K-1} \end{bmatrix}. \tag{5.8}$$

Also let $\boldsymbol{I}$ be the $2MN \times 2MN$ identity matrix and $\boldsymbol{A}$ be the addition matrix

$$\boldsymbol{A} = [\underbrace{\boldsymbol{I}\boldsymbol{I}\dots\boldsymbol{I}}_{K \text{ times}}]. \tag{5.9}$$

The transmitted signal vector from (5.6) can be alternatively represented by

$$\boldsymbol{s} = \boldsymbol{A}\boldsymbol{x} = \boldsymbol{A}\boldsymbol{C}\boldsymbol{d}. \tag{5.10}$$

The signal $\boldsymbol{s}$ is transmitted through a multipath wireless channel, and the received signal at the k-th user's mobile terminal is given by

$$\boldsymbol{r}_k = \boldsymbol{H}_k\boldsymbol{s} + \underline{\nu}_k \tag{5.11}$$

where $\underline{\nu}_k$ is the real-valued noise vector containing $2MN$ Gaussian distributed independent samples with variance $N_0/2$, and $\boldsymbol{H}_k$ is the $2MN \times 2MN$ matrix[1] representing the transmission channel of user k.

Assuming that the channel is constant during a transmission block, the channel matrix is

1. To simplify the analysis, the channel matrix was truncated such that the receive and transmit blocks have the same length, the samples received after MN chips are thus not taken into account. This will have little influence in the results if the number of paths is small compared to the block size.

$$\boldsymbol{H}_k = \begin{bmatrix} g_{k,0,R} & -g_{k,0,I} & 0 & 0 & \dots & 0 & 0 \\ g_{k,0,I} & g_{k,0,R} & 0 & 0 & \dots & 0 & 0 \\ g_{k,1,R} & -g_{k,1,I} & g_{k,0,R} & -g_{k,0,I} & \cdots & 0 & 0 \\ g_{k,1,I} & g_{k,1,R} & g_{k,0,R} & g_{k,0,R} & \cdots & 0 & 0 \\ \dots & \dots & \dots & \dots & \dots & \dots & \dots \\ 0 & 0 & 0 & 0 & \dots & g_{k,0,R} & -g_{k,0,I} \\ 0 & 0 & 0 & 0 & \dots & g_{k,0,I} & g_{k,0,R} \end{bmatrix} \tag{5.12}$$

where $g_{k,l,R}$ and $g_{k,l,I}$ are respectively the real and imaginary parts of the gain $g_{k,l}$ of the l-th path of user k, according to the channel model from Section 2.1.2.

If we consider a system with integrate-and-dump receivers at the mobile station, i.e., with no Rake receivers, then the decision variable at the decoder input will be obtained by correlating the filtered and sampled signal $r_k(i)$ with the spreading code $c_k(i)$ over M samples. In vector form, the N decision variables of user k are given by

$$\hat{\boldsymbol{d}}_k = \boldsymbol{C}_k^{\mathrm{T}} \boldsymbol{r}_k = \boldsymbol{C}_k^{\mathrm{T}} \boldsymbol{H}_k \boldsymbol{s} + \boldsymbol{C}_k^{\mathrm{T}} \underline{\nu}_k . \tag{5.13}$$

The composite vector with the decision variables of all users can also be obtained using the addition matrix $\boldsymbol{A}$:

$$\hat{\boldsymbol{d}} = \boldsymbol{C}^{\mathrm{T}} \boldsymbol{H} \boldsymbol{A}^{\mathrm{T}} \boldsymbol{s} + \boldsymbol{C}^{\mathrm{T}} \underline{\nu} \tag{5.14}$$

where

$$\boldsymbol{H} = \begin{bmatrix} \boldsymbol{H}_0 & 0 & \dots & 0 \\ 0 & \boldsymbol{H}_1 & \dots & 0 \\ \dots & \dots & \dots & \dots \\ 0 & 0 & \dots & \boldsymbol{H}_{K-1} \end{bmatrix} \tag{5.15}$$

and $\underline{\nu}=[\underline{\nu}_0, \underline{\nu}_1,...,\underline{\nu}_{K-1}]^{\mathrm{T}}$ is the composite noise vector.

By substituting the signal from (5.10) into (5.14) we have the decision variable that is obtained with conventional transmission and no Rake receiver:

$$\hat{\boldsymbol{d}} = \boldsymbol{C}^{\mathrm{T}} \boldsymbol{H} \boldsymbol{A}^{\mathrm{T}} \boldsymbol{A} \boldsymbol{C} \boldsymbol{d} + \boldsymbol{C}^{\mathrm{T}} \underline{\nu} . \tag{5.16}$$

It can be easily verified that a Rake receiver with maximum ratio combining can be represented in the matrix notation as the multiplication by the transpose of the channel matrix $\boldsymbol{H}^{\mathrm{T}}$ before despreading. The decision variable vector with a Rake receiver is hence

$$\hat{\boldsymbol{d}}_{Rake} = \boldsymbol{C}^{\mathrm{T}} \boldsymbol{H}^{\mathrm{T}} \boldsymbol{H} \boldsymbol{A}^{\mathrm{T}} \boldsymbol{s} + \boldsymbol{C}^{\mathrm{T}} \boldsymbol{H}^{\mathrm{T}} \underline{\nu} = \boldsymbol{C}^{\mathrm{T}} \boldsymbol{H}^{\mathrm{T}} \boldsymbol{H} \boldsymbol{A}^{\mathrm{T}} \boldsymbol{A} \boldsymbol{C} \boldsymbol{d} + \boldsymbol{C}^{\mathrm{T}} \boldsymbol{H}^{\mathrm{T}} \underline{\nu} . \tag{5.17}$$

The same applies to a pre-Rake. In this case the transmitted signal is modified by channel matched filtering after spreading, and it is given by

$$\boldsymbol{s}_{pR} = \boldsymbol{A}_{pR} \boldsymbol{H}^{\mathrm{T}} \boldsymbol{C} \boldsymbol{d} \tag{5.18}$$

where $\boldsymbol{A}_{pR}$ is the modified addition matrix

$$\boldsymbol{A}_{pR} = \left[\beta_0 \boldsymbol{I}\ \beta_1 \boldsymbol{I}\ \ldots\ \beta_{K-1}\boldsymbol{I}\right], \tag{5.19}$$

with β_k the normalisation factor given in (3.8).

By substituting (5.18) into (5.14) we obtain the decision variable vector with a pre-Rake

$$\hat{\boldsymbol{d}}_{pR} = \boldsymbol{C}^{\mathrm{T}}\boldsymbol{H}\boldsymbol{A}^{\mathrm{T}}\boldsymbol{s}_{pR} + \boldsymbol{C}^{\mathrm{T}}\underline{\nu} = \boldsymbol{C}^{\mathrm{T}}\boldsymbol{H}\boldsymbol{A}^{\mathrm{T}}\boldsymbol{A}_{pR}\boldsymbol{H}^{\mathrm{T}}\boldsymbol{C}\boldsymbol{d} + \boldsymbol{C}^{\mathrm{T}}\underline{\nu}. \tag{5.20}$$

As seen in Chapter 4, if a pre-Rake is used the optimum receiver in terms of maximising the signal-to-noise ratio is a post-Rake, which is like a Rake receiver, but matched to the combination of pre-Rake and multipath channel. In our vector notation this is equivalent to employing a Rake receiver matched to the combined channel $\boldsymbol{H}\boldsymbol{H}^{\mathrm{T}}$. Considering that the transmitted signal was pre-distorted by a pre-Rake as in (5.18), the decision variable with a post-Rake is given by

$$\begin{aligned}\hat{\boldsymbol{d}}_{pRp} &= \boldsymbol{C}^{\mathrm{T}}\boldsymbol{H}\boldsymbol{H}^{\mathrm{T}}\boldsymbol{H}\boldsymbol{A}^{\mathrm{T}}\boldsymbol{s}_{pR} + \boldsymbol{C}^{\mathrm{T}}\boldsymbol{H}\boldsymbol{H}^{\mathrm{T}}\underline{\nu} \\ &= \boldsymbol{C}^{\mathrm{T}}\boldsymbol{H}\boldsymbol{H}^{\mathrm{T}}\boldsymbol{H}\boldsymbol{A}^{\mathrm{T}}\boldsymbol{A}_{pR}\boldsymbol{H}^{\mathrm{T}}\boldsymbol{C}\boldsymbol{d} + \boldsymbol{C}^{\mathrm{T}}\boldsymbol{H}\boldsymbol{H}^{\mathrm{T}}\underline{\nu}\end{aligned}. \tag{5.21}$$

In this section we have developed a vector notation for the downlink of a direct-sequence spread-spectrum system and applied it to the techniques investigated so far (Rake receiver, pre- and post-Rake). In the following sub-sections we will use this representation to derive some joint pre-processing techniques that help eliminate or reduce the multiuser interference.

5.2.2 Block Precoding by Linear Transformation

One simple way to precode the signal is to multiply the transmitted signal by a transformation matrix $\boldsymbol{T}$. The techniques investigated in this Section take this approach, and their optimisation criterion is to completely eliminate the multiuser and multipath interference. This means that we wish our decision variables to have the same values as they would in a single-user single-path system. Ignoring noise, and assuming a unit gain channel, we want $\hat{d}_k(n) = d_k(n)$ for any $0 \le n < N$ and $0 \le k < K$, or in vector form

$$\hat{\boldsymbol{d}} = \boldsymbol{d}. \tag{5.22}$$

Two methods found in the literature will be presented: the Vojcic-Jang [40] and the Zero-Forcing [35] algorithms. We will also propose some modifications to these algorithms that take into account the use of a pre-Rake or different receiver configurations, such as Rake or post-Rake receivers.

The Vojcic-Jang method

In [40] Vojcic and Jang suggested applying the matrix $\boldsymbol{T}$ to modify the data bit vector $\boldsymbol{d}$ such that

$$\boldsymbol{s}_{VJ} = \boldsymbol{A}\boldsymbol{C}\boldsymbol{d}' = \boldsymbol{A}\boldsymbol{C}\boldsymbol{T}\boldsymbol{d}, \tag{5.23}$$

i.e., we obtain an optimised linear transformation $\boldsymbol{d'}=\boldsymbol{T}\boldsymbol{d}$ of the data bit vector and send the vector $\boldsymbol{d'}$ through a conventional spread spectrum transmitter. This concept is shown in Fig. 5.2.

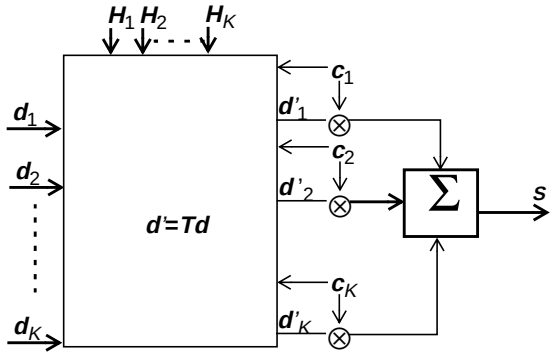

Fig. 5.2 - Concept of Vojcic-Jang precoding

In [40] the application of this technique was proposed either with or without a Rake receiver. Let us first consider the situation without a Rake receiver. In this case, by substituting (5.23) into (5.14) we obtain the decision variable

$$\hat{\boldsymbol{d}}_{VJ} = \boldsymbol{C}^{\mathrm{T}}\boldsymbol{H}\boldsymbol{A}^{\mathrm{T}}\boldsymbol{A}\boldsymbol{C}\boldsymbol{T}\boldsymbol{d} + \boldsymbol{C}^{\mathrm{T}}\underline{\nu}. \tag{5.24}$$

It was shown in [40] that the transformation matrix that minimises the mean square error $J = \mathrm{E}\{\|\hat{\boldsymbol{d}} - \boldsymbol{d}\|^2\}$ is given by

$$\boldsymbol{T}_{VJ} = (\boldsymbol{C}^{\mathrm{T}}\boldsymbol{H}\boldsymbol{A}^{\mathrm{T}}\boldsymbol{A}\boldsymbol{C})^{-1}. \tag{5.25}$$

The $KN \times KN$ matrix $\boldsymbol{C}^{\mathrm{T}}\boldsymbol{H}\boldsymbol{A}^{\mathrm{T}}\boldsymbol{A}\boldsymbol{C}$ represents the cross-correlation matrix between the bits of every user at the decoder input if no precoding is utilized. It can be easily checked that by applying the linear transformation we can eliminate both the multiuser and the multipath interference, and the problem is reduced to the detection of K isolated users in an AWGN channel.

In [40] it was also suggested to employ this technique with a Rake receiver at the mobile station. Now the decision variable can obtained by the substitution of (5.23) into (5.17)

$$\hat{\boldsymbol{d}}_{VJ,\,Rake} = \boldsymbol{C}^{\mathrm{T}}\boldsymbol{H}^{\mathrm{T}}\boldsymbol{H}\boldsymbol{A}^{\mathrm{T}}\boldsymbol{A}\boldsymbol{C}\boldsymbol{T}\boldsymbol{d} + \boldsymbol{C}^{\mathrm{T}}\boldsymbol{H}^{\mathrm{T}}\underline{\nu}. \tag{5.26}$$

This case is similar to the one without a Rake receiver expressed in (5.24), but with a different cross-correlation matrix. The solution is also obtained by inverting this matrix, i.e.,

$$\boldsymbol{T}_{VJ,\,Rake} = (\boldsymbol{C}^{\mathrm{T}}\boldsymbol{H}^{\mathrm{T}}\boldsymbol{H}\boldsymbol{A}^{\mathrm{T}}\boldsymbol{A}\boldsymbol{C})^{-1}, \tag{5.27}$$

and once again the multiuser and the multipath interference are eliminated.

Unfortunately, the price to pay for the total interference elimination is usually an increase in the transmission power. The performance of the above algorithm in a power limited system will be investigated later in this section and compared to other joint block precoding schemes.

The algorithm complexity is another issue of great relevance. The complexity of this and of other block precoding schemes will be briefly examined in Section 5.2.6.

Zero-Forcing Pre-Distortion

Another method of linear pre-distortion was proposed for implementation in the TDD mode of IMT-2000 [35], and, differently from the Vojcic-Jang method, the linear transformation is now applied to the spread signal, i.e., the transmitted signal is given by

$$\boldsymbol{s}_{ZF} = \boldsymbol{ATCd}. \tag{5.28}$$

This concept is depicted in Fig. 5.3 below.

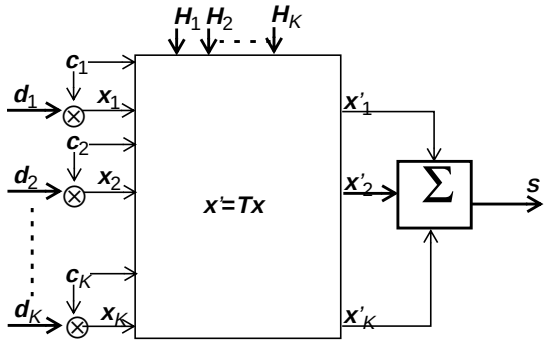

Fig. 5.3 - Concept of zero-forcing precoding

This method was originally proposed considering that no Rake receiver is employed at the mobile stations. In this case, by substituting (5.28) into (5.14) we obtain the vector of decision variables, which is now

$$\hat{\boldsymbol{d}}_{ZF} = \boldsymbol{C}^{\mathrm{T}}\boldsymbol{HA}^{\mathrm{T}}\boldsymbol{ATCd} + \boldsymbol{C}^{\mathrm{T}}\underline{\nu}. \tag{5.29}$$

As suggested in [35], the following transformation matrix can be chosen:

$$\boldsymbol{T}_{ZF} = \frac{1}{\|\boldsymbol{Cd}\|^2}\boldsymbol{A}^{\mathrm{T}}\boldsymbol{AH}^{\mathrm{T}}\boldsymbol{C}(\boldsymbol{C}^{\mathrm{T}}\boldsymbol{HA}^{\mathrm{T}}\boldsymbol{AA}^{\mathrm{T}}\boldsymbol{AH}^{\mathrm{T}}\boldsymbol{C})^{-1}\boldsymbol{dd}^{\mathrm{T}}\boldsymbol{C}^{\mathrm{T}}. \tag{5.30}$$

In the precoder described by the equation above the same operations are made as in a multiuser detector with a zero-forcing block linear equaliser [24], hence the name adopted here for this method.

By substituting (5.30) into (5.28) and making some simplifications we can obtain the transmitted signal with the zero-forcing precoder:

$$\boldsymbol{s}_{ZF} = \boldsymbol{AH}^{\mathrm{T}}\boldsymbol{C}(\boldsymbol{C}^{\mathrm{T}}\boldsymbol{HA}^{\mathrm{T}}\boldsymbol{AH}^{\mathrm{T}}\boldsymbol{C})^{-1}\boldsymbol{d}, \tag{5.31}$$

It can be easily verified that we can completely eliminate the multiuser and the multipath interference with this linear transformation, and thus satisfy (5.22).

Variations on the Vojcic-Jang method

In the original Vojcic-Jang proposal [40] no attempt was made to compensate for the multipath propagation at the transmitter. This can be made for example by employing a pre-Rake. If we modify equation (5.23) to include a pre-Rake without the normalisation factors, we obtain the following transmitted signal

$$\boldsymbol{s}_{VJ,\,pR} = \boldsymbol{AH}^{\mathrm{T}}\boldsymbol{CTd}. \tag{5.32}$$

We will first consider the situation in which no Rake correlator is used at the receiver. In this case, we can substitute (5.32) into (5.14) to obtain the decision variable

$$\hat{\boldsymbol{d}}_{VJ,\,pR} = \boldsymbol{C}^{\mathrm{T}}\boldsymbol{H}\boldsymbol{A}^{\mathrm{T}}\boldsymbol{A}\boldsymbol{H}^{\mathrm{T}}\boldsymbol{C}\boldsymbol{T}\boldsymbol{d} + \boldsymbol{C}^{\mathrm{T}}\underline{\nu}. \tag{5.33}$$

As in the original Vojcic-Jang method described above, we can eliminate the multiuser interference by inverting the correlation matrix, which must now take the pre-Rake into account. The optimal linear transformation is now given by

$$\boldsymbol{T}_{VJ,\,pR} = (\boldsymbol{C}^{\mathrm{T}}\boldsymbol{H}\boldsymbol{A}^{\mathrm{T}}\boldsymbol{A}\boldsymbol{H}^{\mathrm{T}}\boldsymbol{C})^{-1}. \tag{5.34}$$

By substituting (5.34) into (5.32) it can be verified that the transmitted signal obtained with the Vojcic-Jang scheme considering the use of a pre-Rake is exactly the same as the one we got with the zero-forcing method, which is given in (5.31), i.e., the zero-forcing pre-processor is in fact nothing but a pre-Rake applied on an optimised linear transformation of the information bits.

Assuming that a pre-Rake is applied at the base station, we can also consider the use of the matched post-Rake. This will however alter the cross-correlation properties of the signal and hence a different transformation matrix will be required at the transmitter. With this in mind the decision variable with a pre- and a post-Rake can be obtained by substituting (5.32) into (5.21), and it is

$$\hat{\boldsymbol{d}}_{VJ,\,pRp} = \boldsymbol{C}^{\mathrm{T}}\boldsymbol{H}\boldsymbol{H}^{\mathrm{T}}\boldsymbol{H}\boldsymbol{A}^{\mathrm{T}}\boldsymbol{A}\boldsymbol{H}^{\mathrm{T}}\boldsymbol{C}\boldsymbol{T}\boldsymbol{d} + \boldsymbol{C}^{\mathrm{T}}\boldsymbol{H}\boldsymbol{H}^{\mathrm{T}}\underline{\nu}. \tag{5.35}$$

The transformation matrix that eliminates the multiuser interference is again the inverse of the correlation matrix, which is in this case

$$\boldsymbol{T}_{VJ,\,pRp} = (\boldsymbol{C}^{\mathrm{T}}\boldsymbol{H}\boldsymbol{H}^{\mathrm{T}}\boldsymbol{H}\boldsymbol{A}^{\mathrm{T}}\boldsymbol{A}\boldsymbol{H}^{\mathrm{T}}\boldsymbol{C})^{-1}. \tag{5.36}$$

Variations on the Zero-Forcing Method

The pre-coding method proposed in [35] was designed for an integrate-and-dump receiver and did not take into account the possibility of employing Rake processing at the receiver. This can however also be considered. To do this we should compare the decision variable obtained in an integrate-and-dump receiver to the one obtained with a Rake receiver. The former is given by

$$\hat{\boldsymbol{d}} = \boldsymbol{C}^{\mathrm{T}}\boldsymbol{H}\boldsymbol{A}^{\mathrm{T}}\boldsymbol{s} + \boldsymbol{C}^{\mathrm{T}}\underline{\nu}, \tag{5.37}$$

and the latter by

$$\hat{\boldsymbol{d}}_{Rake} = \boldsymbol{C}^{\mathrm{T}}\boldsymbol{H}^{\mathrm{T}}\boldsymbol{H}\boldsymbol{A}^{\mathrm{T}}\boldsymbol{s} + \boldsymbol{C}^{\mathrm{T}}\boldsymbol{H}^{\mathrm{T}}\underline{\nu}. \tag{5.38}$$

We can see that in what concerns the multiuser interference a system with a Rake receiver behaves exactly like one with an integrate-and-dump receiver and an equivalent channel $\boldsymbol{H}'=\boldsymbol{H}^{\mathrm{T}}\boldsymbol{H}$. With this in mind the precoding scheme described by (5.28) and (5.30) can be easily modified to account for the use of a Rake receiver, by considering the equivalent channel $\boldsymbol{H}'$ in the transformation matrix

$$\boldsymbol{T}_{ZF,\,Rake} = \frac{1}{\|\boldsymbol{C}\boldsymbol{d}\|^2}\boldsymbol{A}^{\mathrm{T}}\boldsymbol{A}\boldsymbol{H}^{\mathrm{T}}\boldsymbol{H}\boldsymbol{C}(\boldsymbol{C}^{\mathrm{T}}\boldsymbol{H}^{\mathrm{T}}\boldsymbol{H}\boldsymbol{A}^{\mathrm{T}}\boldsymbol{A}\boldsymbol{A}^{\mathrm{T}}\boldsymbol{A}\boldsymbol{H}^{\mathrm{T}}\boldsymbol{H}\boldsymbol{C})^{-1}\boldsymbol{d}\boldsymbol{d}^{\mathrm{T}}\boldsymbol{C}^{\mathrm{T}}. \tag{5.39}$$

As we have seen, the zero-forcing algorithm for a conventional receiver is basically a pre-Rake with a linear transformation of the transmitted bits. Therefore, we can also consider the use of a post-Rake at each mobile station receiver. Looking into (5.21) we can imply that the same considerations made above for a pre-Rake also apply for a post-Rake, i.e., in terms of

interference the combination of pre- and a post-Rake is equivalent to conventional transmission over the modified channel $\boldsymbol{H'}=\boldsymbol{H}\boldsymbol{H}^{\mathrm{T}}\boldsymbol{H}$. In this case the zero-forcing transformation matrix is

$$\boldsymbol{T}_{ZF,\,pRp} = \frac{1}{\|\boldsymbol{C}\boldsymbol{d}\|^2}\boldsymbol{A}^{\mathrm{T}}\boldsymbol{A}\boldsymbol{H}^{\mathrm{T}}\boldsymbol{H}\boldsymbol{H}^{\mathrm{T}}\boldsymbol{C}(\boldsymbol{C}^{\mathrm{T}}\boldsymbol{H}\boldsymbol{H}^{\mathrm{T}}\boldsymbol{H}\boldsymbol{A}^{\mathrm{T}}\boldsymbol{A}\boldsymbol{A}^{\mathrm{T}}\boldsymbol{A}\boldsymbol{H}^{\mathrm{T}}\boldsymbol{H}\boldsymbol{H}^{\mathrm{T}}\boldsymbol{C})^{-1}\boldsymbol{d}\boldsymbol{d}^{\mathrm{T}}\boldsymbol{C}^{\mathrm{T}}. \quad (5.40)$$

5.2.3 Block Precoding with Minimisation of Transmitted Signal Power

In the previous section we have seen several techniques that enable a complete elimination of both the multiuser and the multipath interference. However, the price to pay for this is usually an increase in the needed transmit power. In real systems, power is a valuable resource, and the optimum technique will be the one that minimises the transmission power while satisfying the requirement of interference cancellation given by (5.22). The methods described in Section 5.2.2 are all based on a linear transformation of the data bits, either spread or not, but, instead of searching for a transformation matrix that modifies the information bits, we can directly search for the signal $\boldsymbol{s}$ that minimises the transmit signal energy of a block

$$E(\boldsymbol{s}) = \boldsymbol{s}^{\mathrm{T}}\boldsymbol{s}, \quad (5.41)$$

with the constraint that the interference is completely eliminated.

We have a set of KN constraints from (5.22). Considering that no Rake receiver is employed at the mobile station, these constraints can be expressed in vector form as follows:

$$\boldsymbol{g}(\boldsymbol{s}) = \hat{\boldsymbol{d}}(\boldsymbol{s}) - \boldsymbol{d} = \boldsymbol{C}^{\mathrm{T}}\boldsymbol{H}\boldsymbol{A}^{\mathrm{T}}\boldsymbol{s} - \boldsymbol{d} = 0. \quad (5.42)$$

This is a constrained minimisation problem, which we prove in Appendix F to be solvable using Lagrange multipliers if $K \leq 2M$. We must thus obtain the vector $\boldsymbol{s}$ that minimises the Lagrange function

$$F(\boldsymbol{s}) = E(\boldsymbol{s}) - \underline{\lambda}^{\mathrm{T}}\boldsymbol{g}(\boldsymbol{s}) = \boldsymbol{s}^{\mathrm{T}}\boldsymbol{s} - \underline{\lambda}^{\mathrm{T}}(\boldsymbol{C}^{\mathrm{T}}\boldsymbol{H}\boldsymbol{A}^{\mathrm{T}}\boldsymbol{s} - \boldsymbol{d}) \quad (5.43)$$

where $\underline{\lambda}$ is the $KN\times 1$ vector of Lagrange multipliers, which can be obtained from the minimisation constraints.

The minimisation of (5.43) can be made by taking the root of the gradient of $F(\boldsymbol{s})$, i.e., we want to find $\boldsymbol{s}$ such that

$$\nabla F(\boldsymbol{s}) = 2\boldsymbol{s} - \boldsymbol{A}\boldsymbol{H}^{\mathrm{T}}\boldsymbol{C}\underline{\lambda} = 0, \quad (5.44)$$

with $\nabla F(\boldsymbol{s})$ being the gradient of $F(\boldsymbol{s})$.

The solution is straightforward:[1]

$$\boldsymbol{s} = \boldsymbol{A}\boldsymbol{H}^{\mathrm{T}}\boldsymbol{C}\underline{\lambda}, \quad (5.45)$$

which is nothing less than a pre-Rake applied on the modified non-binary information signal given by $\underline{\lambda}$. By substituting (5.45) into the constraints from (5.42) we obtain the Lagrange multipliers

$$\underline{\lambda} = \boldsymbol{R}^{-1}\boldsymbol{d} \quad (5.46)$$

1. Actually, $\boldsymbol{s} = \frac{1}{2}\boldsymbol{A}\boldsymbol{H}^{\mathrm{T}}\boldsymbol{C}\underline{\lambda}$, but for our convenience the multiplication term 1/2 can be ignored.

where $\boldsymbol{R}$ is the $KN \times KN$ correlation matrix

$$\boldsymbol{R} = \boldsymbol{R}^{\mathrm{T}} = \boldsymbol{C}^{\mathrm{T}}\boldsymbol{H}\boldsymbol{A}^{\mathrm{T}}\boldsymbol{A}\boldsymbol{H}^{\mathrm{T}}\boldsymbol{C}. \tag{5.47}$$

The vector $\underline{\lambda}$ is also a linear transformation of the data bit vector $\boldsymbol{d}$, similar to the one performed in the Vojcic-Jang proposal considering a pre-Rake at the transmitter. This concept is displayed below in Fig. 5.4.

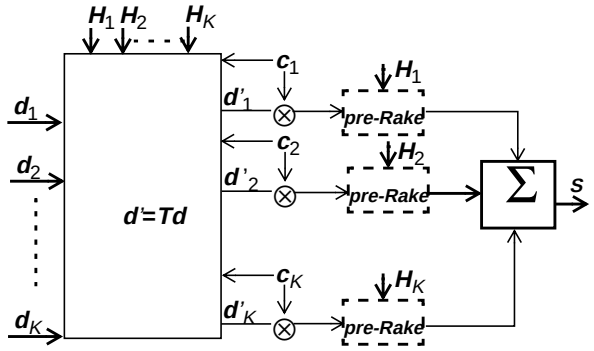

Fig. 5.4 - Block precoding with minimum power

It can also be verified that the transmitted signal expressed by (5.45) is exactly the same as the one obtained with the zero-forcing algorithm, which is thus proved to be the optimum one in terms of power minimisation for interference elimination. The concept displayed in Fig. 5.4 is hence just another way to implement the zero-forcing algorithm.

This approach can provide us with an insight in the operation of the optimum precoder. With knowledge of the cross-correlation between the different bits of all the users, which is a function of the spreading codes and of the channels, these bits can be linearly transformed in order to equalise the interference, i.e., we need a sort of bitwise power control to guarantee that all bits are received with equal amplitude. These transformed bits are then sent through a pre-Rake, which is a channel-matched filter, and optimises the performance in terms of the signal-to-noise ratio.

The same conclusions taken here for a system with integrate-and-dump receivers apply also when a Rake receiver (or a post-Rake) is employed, in which case the channel $\boldsymbol{H}$ in (5.45) and (5.47) should be substituted by the equivalent channel $\boldsymbol{H'}=\boldsymbol{H}^{\mathrm{T}}\boldsymbol{H}$ (or $\boldsymbol{H'}=\boldsymbol{H}\boldsymbol{H}^{\mathrm{T}}\boldsymbol{H}\boldsymbol{H}^{\mathrm{T}}$).

5.2.4 Performance of Linear Block Precoding

All the block precoding algorithms proposed so far in this section can completely eliminate both the multiuser and the multipath interference, i.e., they all satisfy the condition from (5.22). Nevertheless, this is usually achieved at the expense of an increase in the transmit power. In real-life systems power is however usually limited. Let the available energy for a block be E_{blk}. If the signal obtained by precoding as described in Section 5.2.2 and Section 5.2.3 is $\boldsymbol{s}_{pc}$ then the effectively transmitted signal with energy normalised to E_{blk} is

$$\boldsymbol{s}_{tx} = \beta_{norm}\boldsymbol{s}_{pc} \tag{5.48}$$

where β_{norm} is the normalisation factor

$$\beta_{norm} = \sqrt{\frac{E_{blk}}{\boldsymbol{s}_{pc}^{\mathrm{T}}\boldsymbol{s}_{pc}}}. \tag{5.49}$$

This means that, instead of the goal from (5.22), the decision variable at the receiver will be in effect

$$\hat{\boldsymbol{d}} = \beta_{norm}\boldsymbol{d}, \tag{5.50}$$

which means that the signal-to-noise ratio at the decoder input will be altered correspondingly.

This provides us with a method to assess the performance of the several block precoding algorithms, by investigating their performance with normalised power.

We have chosen the block energy to be proportional to the number of users:

$$E_{blk} = KNRE_b \tag{5.51}$$

where E_b is the bit energy. We can thus simplify the comparison with single-user transmission methods, either with or without a pre-Rake, since in these methods, as described in Section 2.1 and Section 3.1, the average block energy is the same as the one given by (5.51).

There is to our knowledge no simple closed form solution for the bit error rate with joint precoding techniques, and performance results had to be obtained through simulation. These are presented in Fig. 5.5 to Fig. 5.9.

It is known that the number of users supported in a spread spectrum system is proportional to its spreading factor. Because of the increased complexity of joint precoding techniques, systems with a processing gain as high as the one used in the previous chapters (G=128) would take too long to be simulated at a high system load. We have thus decided to consider a processing gain G=16 for the simulations whose results are shown here. The number of information bits in a transmission frame must also be kept low because of the algorithm complexity, in our case we chose N_{inf}=20.

In Fig. 5.5 and Fig. 5.6 we have considered a system without channel coding. The results in Fig. 5.5 were obtained with the 2-path channel with strong line-of-sight component described in Table 2.1. In all the results shown in this chapter the channels are assumed to be constant during one frame. The system performance was investigated with two different signal-to-noise ratios, E_b/N_0=9dB and E_b/N_0=12dB. For all configurations orthogonal spreading before the QPSK modulation with random scrambling was considered, such that 32 orthogonal sequences are available.

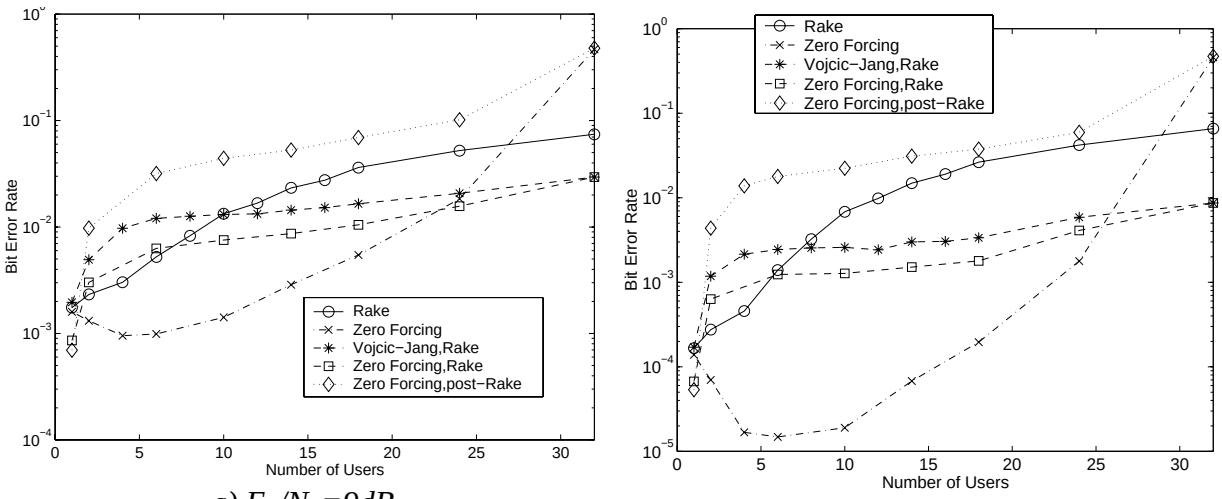

a) E_b/N_0=9dB *b) E_b/N_0=12dB*

Fig. 5.5 - Joint precoding performance (2-path channel, no channel coding)

The bit error rate of the joint block precoding techniques were compared with the one of conventional transmission with a Rake receiver, which, as seen in Chapter 3, yields a greater capacity than a pre-Rake if orthogonal sequences are employed with no channel coding. We can see that the results are in the essence very similar in both channel models. It can also be observed that the use of joint precoding techniques can bring about a substantial capacity increase compared to a non-precoded system.

It is clear in the figures that the zero-forcing precoding with integrate-and-dump receivers is the most efficient if the number of users is small. Starting from the single user case, the transmission quality even improves with an increase in the number of interfering users, eventually reaching a minimum. This happens because the users are differently affected by fading, such that users with favourable fading conditions require less power than ones in a fading trough. Furthermore, the interference is sometimes constructive, such that for some bits different users can 'share' the same transmitted signal and require thus less overall power. With these things in mind, the total available power can be allocated according to the users' needs on a bit-by-bit basis, and not, as in transmission without joint precoding, equally allocated the whole time for all the users. We can construct an interference free signal with energy less than E_{blk}, and by normalising the signal we actually improve the signal-to-noise ratio at the receiver compared to the single user situation. It should be noticed that this is only possible because in our system the total transmit power is proportional to the number of users and hence greater than in the single user case. With a further increase in the number of users the elimination of the multiuser interference with low transmit power becomes more unlikely, and the energy needed to cancel out the interference is rapidly augmented. This means that after normalisation the signal-to-noise ratio gets smaller and smaller, and, eventually, beyond a certain point the advantage of eliminating the interference does not compensate for the worsening in the signal-to-noise level. As the number of users approaches the $2M$ degrees of freedom provided by bandwidth spreading the power required for interference elimination tends towards infinity and the signal-to-noise ratio tends towards zero after normalisation.

Joint precoding with Rake receivers behaves somewhat differently. In order to cancel the interference caused by the initial few additional users in the system the power has to be increased so much that, after normalisation, the signal-to-noise ratio becomes less than in the single-user case or with multiuser transmission. The precoding method can however cope very well with the inclusion of new users, since the code orthogonality facilitates the interference elimination, and it eventually outperforms the Rake receiver with conventional transmission and precoding with integrate-and-dump receivers as the number of users augments. The effect of orthogonal spreading will be investigated with more details later. Nevertheless, zero-forcing joint precoding with integrate-and-dump receivers performs worse than precoding with Rake receivers at high system loads only, and the beneficial effect of reduced interference observed with few users and integrate-and-dump receivers cannot be observed when Rake correlators are employed.

Both the Vojcic-Jang and the zero-forcing precoding algorithms were investigated, and the superior performance of the latter method could be confirmed, as it was expected from the analysis in Section 5.2.3, which shows the optimality of the latter method in terms of power minimisation with interference elimination.

The performance of block precoding with a post-Rake does not bring many benefits, because, as already seen in Chapter 4, the multi-user interference increases this way, which makes the interference elimination scheme require a too high transmit power. For a single user the block precoding scheme does not differ much from conventional transmission, and as expected from the results in Section 4.2, the post-Rake brings about an improvement in the signal-to-noise

ratio. It is interesting to notice that the same happens when zero-forcing precoding is applied with Rake receivers, which can be explained by the fact that in the precoder a sort of pre-Rake matched to the combination of channel and Rake receiver is applied, and this has the same effect of a post-Rake applied to a pre-Rake.

We can also notice that the capacity gain achieved by joint precoding is larger in less noisy channels. This was expected, since the elimination of interference usually involves a worsening of the noise figure at the receiver, but this becomes less important as the signal-to-noise ratio increases. In an ideal channel without noise, error-free transmission is possible with precoding for up to $2M$ users, which cannot be said about conventional single-user techniques.

In Fig. 5.6 the results for the 6-path channel from Table 2.1 are displayed. The results are qualitatively the same as for the 2-path channel, but the intersection points of the curves have changed. The most noticeable difference in relation to the 2-path channel is that the zero-forcing method with Rake receivers is more effective in a severe multipath environment, providing a better performance than conventional transmission also for a few users. This happens because of the enhancement in the signal-to-noise ratio obtained through this technique and explained above. This enhancement, which was also observed in the 2-path channel, becomes more significant with an increase of the multipath diversity, as happens for the post-Rake as shown in Chapter 4.

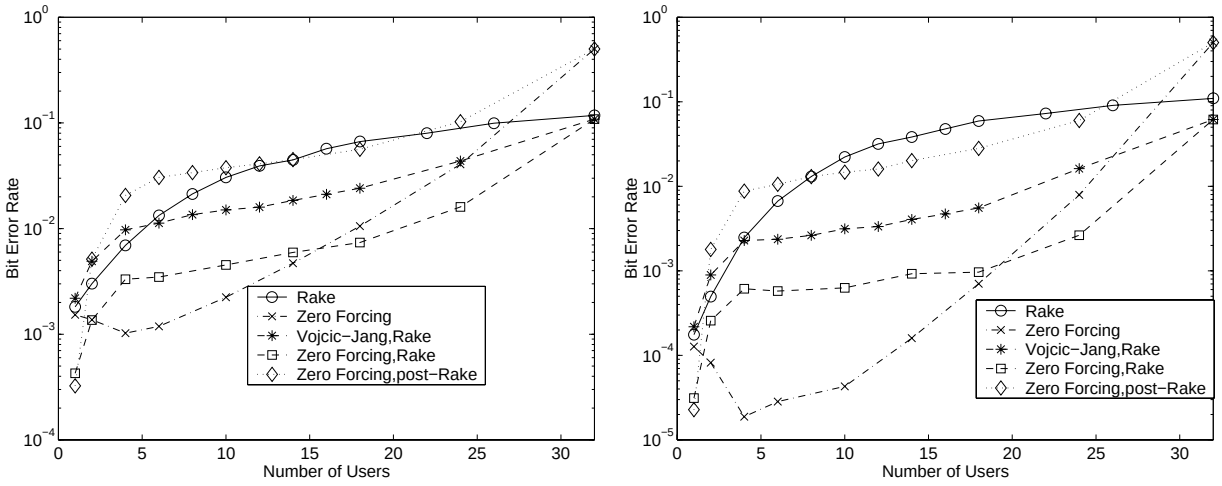

a) E_b/N_0*=9dB* *b)* E_b/N_0*=12dB*

Fig. 5.6 - Joint precoding performance (6-path channel, no channel coding)

In Fig. 5.7 we see the effect of orthogonal codes in the performance of the joint precoding algorithms with different receiver configurations. Since zero-forcing precoding was proven to be superior to the Vojcic-Jang method, only the former will be considered. It can be observed that the use of orthogonal sequences brings a substantial gain if Rake receivers are used, but are not so important with post-Rakes or integrate-and-dump receivers, since these imply the use of a pre-Rake in the precoding, which destroys a great deal of the orthogonality. The advantage brought by the use of orthogonal sequences with Rake receivers explain the superior performance of this receiver configuration with a large system load. This can be easily seen in Fig. 5.7, as with random codes the use of integrate-and-dump receivers brings about the best results with zero-forcing joint precoding in the presence of multiuser interference. The use of a Rake filter lengthens the impulse response of the equivalent channel

(wireless channel and Rake), increasing the inter-bit interference coming from the other users and making the interference elimination more difficult, but we orthogonal sequences this can be compensated by the preservation of the orthogonality if no pre-Rake is employed.

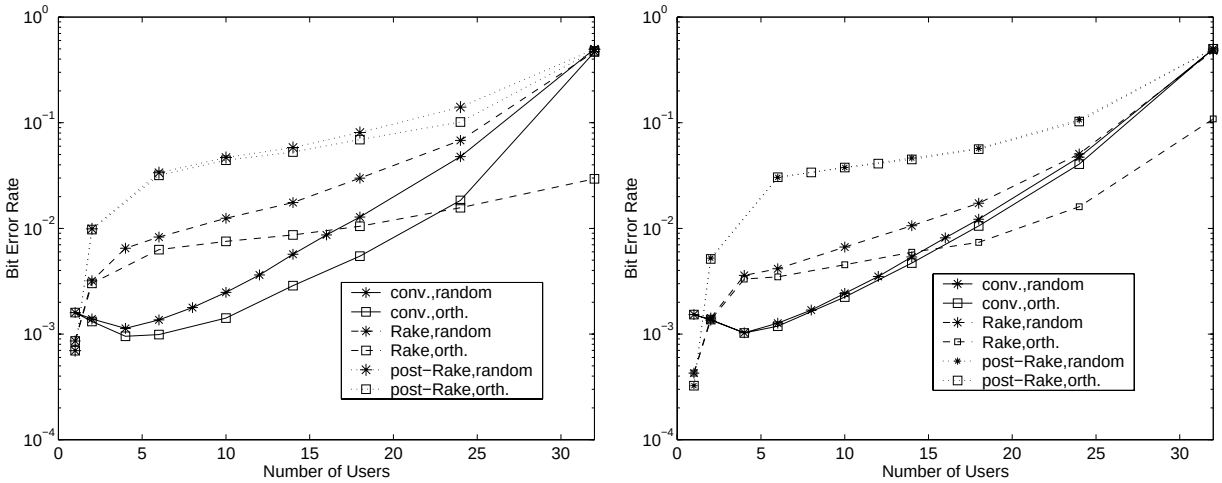

a) 2 paths, E_b/N_0=9dB *b) 6 paths, E_b/N_0=9dB*

Fig. 5.7 - Effect of orthogonal spreading with zero-forcing precoding

If however part of the spreading gain is employed for channel coding, the use of the block precoding algorithms seen so far is not as favourable, as observed in the results shown in Fig. 5.8 and Fig. 5.9. A convolutional code of rate R=1/2 and memory order m_o=8 was used (see Appendix A), which means that only 16 orthogonal codes are available, as opposed to 32 without channel coding. The N_{inf}=20 information bits in each frame correspond now to N=2N_{inf}=40 coded bits pro frame that have to be considered by the joint precoding scheme. The Vojcic-Jang method and the precoding scheme considering a post-Rake have been discarded due to their inferior performance shown in the situation with no error correcting codes.

In Fig. 5.8 the results for a 2-path channel with strong line-of-sight component are displayed. The interruption in the curve corresponding to zero-forcing precoding with integrate-and-dump receivers in Fig. 5.8b means that the bit error rate was too low for precise results to be obtained within the simulated time[1]. Comparing this figure to Fig. 5.5 we can see that the shape of the curves are the same as in the case with no channel coding, but the capacity gain with joint precoding is not as significant. Let us first examine the results with zero-forcing precoding and integrate-and-dump receivers. As in the uncoded system the bit error rate can be reduced with few interfering users compared to a single user system. We have seen however previously that the performance deteriorates rapidly as the number of users approaches the number of degrees of freedom. With R=1/2 convolutional coding we have half as many degrees of freedom as in the uncoded case so that the performance degradation occur with much fewer users. The same applies if a Rake receiver is considered, the fewer degrees of freedom and the smaller number of orthogonal sequences make it more difficult for the precoding algorithm to eliminate the interference with reasonably low power. Differently from

1. The simulations are stopped after 2.500.000 bits or 5000 bit errors, whichever comes first.

the uncoded case, in which there was always a precoding scheme superior to conventional transmission with Rake receivers for up to 2*M* users, with channel coding the precoding schemes suggested so far improve the performance for a small number of users only.

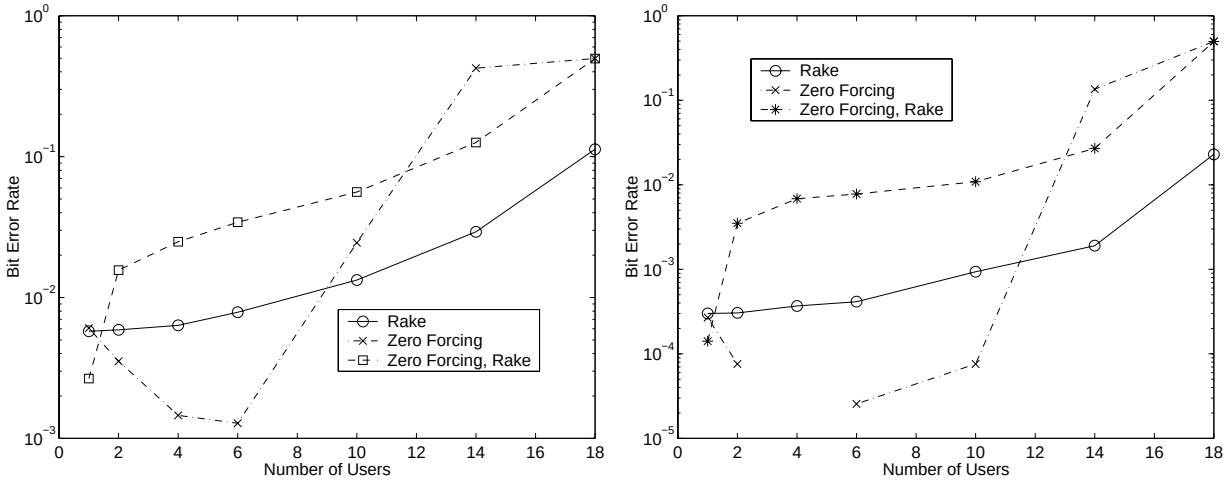

a) E_b/N_0*=6dB* *b)* E_b/N_0*=9dB*

Fig. 5.8 - Joint precoding performance (2-path channel, convolutional coding R=1/2)

Similar results can be obtained if the 6-path channel is considered, as it can be seen in Fig. 5.9, but this time the performance of zero-forcing precoding with Rake receivers is comparatively better. This is so not only because most of the orthogonality is lost in this channel in the case of conventional transmission with Rake receivers, but also because of the improvement in the signal-to-noise ratio obtained with zero-forcing pre-coding employing a Rake receiver, which was also observed in Fig. 5.5 to Fig. 5.8, and is more significant in channels with severe multipath distortion.

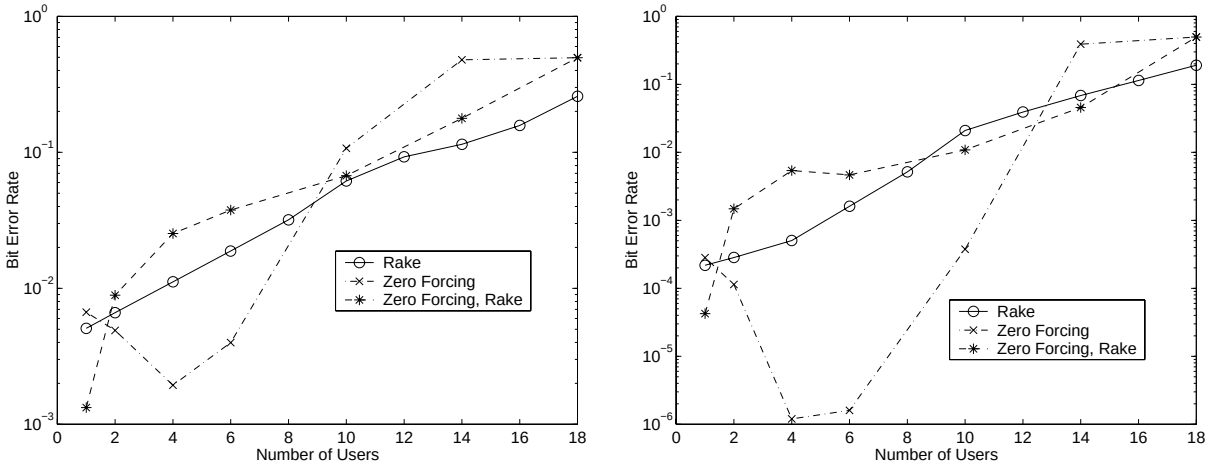

a) E_b/N_0*=6dB* *b)* E_b/N_0*=9dB*

Fig. 5.9 - Joint precoding performance (6-path channel, convolutional coding R=1/2)

5.2.5 Block Precoding with Power Constraint

All the techniques proposed in Section 5.2.2 are able to completely eliminate the multiuser and the multipath interference. However, as seen in the simulation results from Fig. 5.5 to Fig. 5.9, in power limited systems the price to pay for this interference elimination is usually a substantial reduction in the signal to noise ratio, which sometimes is not compensated by the interference cancellation. In order to circumvent this problem we can restate the minimisation problem. In Section 5.2.3 we tried to transform our multiuser multipath system into a single user AWGN system by precoding the signal with minimum transmit power. With power limitation we should instead try to minimise the mean square error caused by interference

$$e = (\boldsymbol{d} - \hat{\boldsymbol{d}})^{\mathrm{T}}(\boldsymbol{d} - \hat{\boldsymbol{d}}) \tag{5.52}$$

with a limitation in the transmit power.

With integrate-and-dump receivers the function to be minimised is

$$e(\boldsymbol{s}) = (\boldsymbol{d}^{\mathrm{T}} - \boldsymbol{s}^{\mathrm{T}}\boldsymbol{A}\boldsymbol{H}^{\mathrm{T}}\boldsymbol{C})(\boldsymbol{d} - \boldsymbol{C}^{\mathrm{T}}\boldsymbol{H}\boldsymbol{A}^{\mathrm{T}}\boldsymbol{s}). \tag{5.53}$$

The power limitation can be expressed by the following constraint:

$$G(\boldsymbol{s}) = \boldsymbol{s}^{\mathrm{T}}\boldsymbol{s} - E_{max} \leq 0 \tag{5.54}$$

where E_{max} is the maximum signal energy allowed in a block.

It holds true for the mean square error that $e(\boldsymbol{s})\geq 0$ and, hence, one approach to this problem is to try to obtain the signal $\boldsymbol{s}^*$ that eliminates the interference (i.e., such that $e(\boldsymbol{s})=0$) with minimum transmit power as done in Section 5.2.3. If the constraint from (5.54) can be satisfied for $\boldsymbol{s}^*$, then the problem is already solved; otherwise we can minimise $e(\boldsymbol{s})$ with the maximum allowed energy, i.e., satisfying the constraint $G(\boldsymbol{s})=0$. This problem can also be solved using Lagrange multipliers. We must now minimise the Lagrange function

$$F(\boldsymbol{s}) = (\boldsymbol{d}^{\mathrm{T}} - \boldsymbol{s}^{\mathrm{T}}\boldsymbol{A}\boldsymbol{H}^{\mathrm{T}}\boldsymbol{C})(\boldsymbol{d} - \boldsymbol{C}^{\mathrm{T}}\boldsymbol{H}\boldsymbol{A}^{\mathrm{T}}\boldsymbol{s}) - \mu(\boldsymbol{s}^{\mathrm{T}}\boldsymbol{s} - E_{max}) \tag{5.55}$$

where μ is the Lagrange multiplier.

The value of $\boldsymbol{s}$ that minimises this function is the root of the gradient of $F(\boldsymbol{s})$. We want $\boldsymbol{s}$ such that:

$$\nabla F(\boldsymbol{s}) = 2\boldsymbol{A}\boldsymbol{H}^{\mathrm{T}}\boldsymbol{C}\boldsymbol{C}^{\mathrm{T}}\boldsymbol{H}\boldsymbol{A}^{\mathrm{T}}\boldsymbol{s} - 2\boldsymbol{A}\boldsymbol{H}^{\mathrm{T}}\boldsymbol{C}\boldsymbol{d} - 2\mu\boldsymbol{s} = 0, \tag{5.56}$$

with $\nabla F(\boldsymbol{s})$ being the gradient of $F(\boldsymbol{s})$.

The transmitted signal $\boldsymbol{s}$ that minimises the mean square error with any given energy E_{max} can be obtained from (5.56) and it is the solution to the following system

$$\begin{aligned}(\boldsymbol{A}\boldsymbol{H}^{\mathrm{T}}\boldsymbol{C}\boldsymbol{C}^{\mathrm{T}}\boldsymbol{H}\boldsymbol{A}^{\mathrm{T}} - \mu\boldsymbol{I})\boldsymbol{s} &= \boldsymbol{A}\boldsymbol{H}^{\mathrm{T}}\boldsymbol{C}\boldsymbol{d} \\ \boldsymbol{s}^{\mathrm{T}}\boldsymbol{s} &= E_{max}\end{aligned}. \tag{5.57}$$

Since the factor μ must also be calculated, a non-linear system with $2MN+1$ variables has to be solved, for which to our knowledge there is no closed form solution.

One alternative to the approach above is to use the method of penalty functions [44]. With this method we define a new function to be minimised which includes a penalty function that approaches infinity if the constraint is not satisfied. Furthermore, the penalty function is

chosen such that the new function be differentiable in order to facilitate the analysis. We can use for instance a square law penalty function, and in this case the new function to be minimised is

$$P(\boldsymbol{s}) = e(\boldsymbol{s}) + \begin{cases} r[G(\boldsymbol{s})]^2 & \text{,if } G(\boldsymbol{s}) > 0 \\ 0 & \text{,if } G(\boldsymbol{s}) \le 0 \end{cases} \tag{5.58}$$

where r is a real valued constant such that $r>0$.

The vector $\boldsymbol{s}^*$ that minimises the error $e(\boldsymbol{s})$ and satisfies the constraint from (5.54) is given by

$$\boldsymbol{s}^* = \min_{\boldsymbol{s}} \lim_{r \to \infty} P(\boldsymbol{s}, r) . \tag{5.59}$$

In our case however it makes sense to consider (5.54) to be a weak constraint, i.e., a block with energy slightly higher than E_{max} might be acceptable if this results in a much smaller mean square error. The value of the square law penalty function $r[G(\boldsymbol{s})]^2$ grows very rapidly with an increase in the signal energy beyond E_{max} even for moderate values of r, so that the minimisation of $P(\boldsymbol{s})$ is very unlikely to yield a signal with energy much higher than E_{max}. We can thus ignore the limit in (5.59) and consider r to be a parameter that determines how strict the power limitation is.

The optimum $\boldsymbol{s}^*$ that minimises $P(\boldsymbol{s})$ can be found by obtaining the root of its gradient

$$\nabla P(\boldsymbol{s}) = 2\boldsymbol{A}\boldsymbol{H}^{\mathrm{T}}\boldsymbol{C}\boldsymbol{C}^{\mathrm{T}}\boldsymbol{H}\boldsymbol{A}^{\mathrm{T}}\boldsymbol{s} - 2\boldsymbol{A}\boldsymbol{H}^{\mathrm{T}}\boldsymbol{C}\boldsymbol{d} + \begin{cases} 4r(\boldsymbol{s}^{\mathrm{T}}\boldsymbol{s} - E_{max})\boldsymbol{s} & \text{,if } G(\boldsymbol{s}) > 0 \\ 0 & \text{,if } G(\boldsymbol{s}) \le 0 \end{cases} \tag{5.60}$$

If $G(\boldsymbol{s}^*)>0$, then $\boldsymbol{s}^*$ is the root of a cubic equation over $\Re^{2MN}$, for which to our knowledge there is no closed form solution. The roots of the gradient given in (5.60) can be obtained numerically, but the efficiency of numerical algorithms to obtain roots of a function is usually very sensitive to the choice of an initial value [30]. Instead, we should try to minimise the function $P(\boldsymbol{s})$ numerically, for instance through the conjugate gradient method [44], which is an iterative method that converges quadratically to the function minimum. The application of this technique to the optimisation problem above is described in Appendix G.1.

In communications systems the minimisation must be performed in real-time and we have to define then a maximum number of iterations I of the numerical algorithm that can be executed in the available time with the available processing power.

The complexity of the algorithm depends basically on the number of chips per coded bit M, since we must optimise a vector $\boldsymbol{s}$ with $2MN$ dimensions. We can however devise an algorithm which depends upon the number of users instead, which may be preferable if these are few. We have seen in Section 5.2.3 that the optimum algorithm in terms of power minimisation with interference elimination consists of a pre-Rake applied on a modified data vector $\underline{\lambda}$

$$\boldsymbol{s} = \boldsymbol{A}\boldsymbol{H}^{\mathrm{T}}\boldsymbol{C}\underline{\lambda} . \tag{5.61}$$

We may imply that this is also the case if we want to minimise the mean square error with limited power, and instead of searching for the optimum vector $\boldsymbol{s}$ of dimension $2MN$, we can optimise the vector $\underline{\lambda}$ of dimension KN, such that the transmit signal is given by (5.61).

By substituting (5.61) into (5.53) and (5.54) we obtain the mean square error

$$e(\underline{\lambda}) = (\boldsymbol{d}^{\mathrm{T}} - \underline{\lambda}^{\mathrm{T}}\boldsymbol{R}^{\mathrm{T}})(\boldsymbol{d} - \boldsymbol{R}\underline{\lambda}) \tag{5.62}$$

and the power constraint

$$G(\underline{\lambda}) = \underline{\lambda}^{\mathbf{T}}\boldsymbol{R}\underline{\lambda} - E_{max} \leq 0 \tag{5.63}$$

as a function of $\underline{\lambda}$, where $\boldsymbol{R}$ is the symmetric correlation matrix given in (5.47).

As with the direct optimisation of $\boldsymbol{s}$, there is to our knowledge no simple solution for the minimisation of (5.62) with the power constraint from (5.63). However, we can again optimise the function numerically. As in (5.58), let us define the penalty function

$$P(\underline{\lambda}) = e(\underline{\lambda}) + \begin{cases} r[G(\underline{\lambda})]^2 & ,\text{if } G(\underline{\lambda}) > 0 \\ 0 & ,\text{if } G(\underline{\lambda}) \leq 0 \end{cases}. \tag{5.64}$$

The gradient of $P(\underline{\lambda})$ is given by

$$\nabla P(\underline{\lambda}) = 2\boldsymbol{R}^{\mathrm{T}}\boldsymbol{R}\underline{\lambda} - 2\boldsymbol{R}\boldsymbol{d} + \begin{cases} 4r(\underline{\lambda}^{\mathrm{T}}\boldsymbol{R}\underline{\lambda} - E_{max})\boldsymbol{R}\underline{\lambda} & ,\text{if } G(\underline{\lambda}) > 0 \\ 0 & ,\text{if } G(\underline{\lambda}) \leq 0 \end{cases}. \tag{5.65}$$

The gradient $\nabla P(\underline{\lambda})$ is again a cubic equation on the vector $\underline{\lambda}$, whose roots are to our knowledge not easily obtainable. We can again resort to a numerical minimisation of $P(\underline{\lambda})$ through the conjugate gradient method. Details on the application of this method to the minimisation problem above are found in Appendix G.2.

Constrained-power precoding was derived here considering that no Rake receiver is employed, but the same development applies in case Rake receivers are considered. All we have to do then is to use the equivalent channel matrix $\boldsymbol{H'}=\boldsymbol{H}^{\mathrm{T}}\boldsymbol{H}$ instead of $\boldsymbol{H}$ in the algorithm.

Simulation Results

We will now show some simulation results that allow a comparison between the linear transformation methods of Section 5.2.2 and precoding with power constraint. In the results from Fig. 5.5 to Fig. 5.9 we can see that when no power limitation is considered the performance deteriorates rapidly beyond a certain number of users because the signal-to-noise ratio is reduced as a consequence of precoding for interference elimination; and that this deterioration is more critical when channel coding is employed and, hence, the number of degrees of freedom per bit is reduced. This is exactly the situation in which the power limitation can be helpful, and, therefore, we will only show here the results that were obtained considering that a rate R=1/2 convolutional code is used for part of the spreading. To keep the simulation time short we have just considered the numerical minimisation of the modified data vector $\underline{\lambda}$, which is much faster than the minimisation of $\boldsymbol{s}$ for few users. We have also considered precoding for integrate-and-dump receivers only.

The block precoding method with power constraint described in this section has three different parameters that may affect the algorithm performance:

- the penalty factor r in (5.64), which was already introduced and indicates how strict the power constraint is.
- the power factor P, described following. Let E_{blk} be the block energy to be effectively transmitted, as defined in (5.51). We can perform the optimisation algorithm considering $E_{max}=PE_{blk}$ and then normalise the energy to E_{blk}. By doing this we can obtain a greater

reduction in the interference at the expense of a lower signal-to-noise ratio at the decoder input.

- the maximum number of iterations I.

The optimisation of r and P was made for both channels from Table 2.1 with several system configurations (number of users and signal-to-noise ratios) and I=50 iterations. From the results shown below in Fig. 5.10 and Fig. 5.11 we can see that the optimum parameter values may depend on the system configurations. The power factor P was optimised considering a value r=1 for the penalty factor. We can see in Fig. 5.10 that in noisier channels (E_b/N_0=6dB in Fig. 5.10) the signal-to-noise ratio at the receiver should not be further reduced by the precoding, i.e., a low transmit energy is required before normalisation, and in this case the power factor should be P=1. In channels with higher signal-to-noise ratio (E_b/N_0=9dB or E_b/N_0=12dB in Fig. 5.10) the reduction in the multiuser interference may compensate the decrease in the signal-to-noise, in which case a larger power factor can be preferable (P=2). If $P \geq 2$ the performance does not show a strong dependency on this parameter for the configurations investigated here. As it can be observed in Fig. 5.11, the penalty factor r has in most cases little influence on the performance, but in some configurations a 'softer' power limitation, corresponding to lower values of r, can be preferred, which allows a slight loss in the signal-to-noise ratio (transmit energy higher than PE_{blk} before normalisation) in exchange for lower multiuser interference.

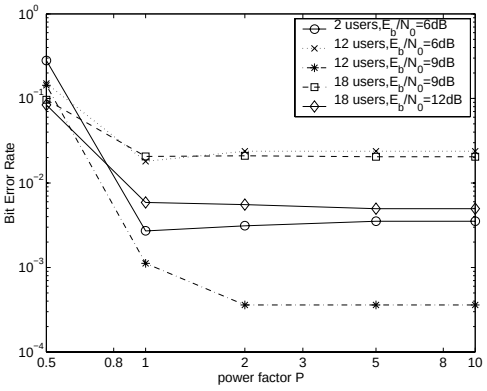

a) 2-path channel with strong LOS

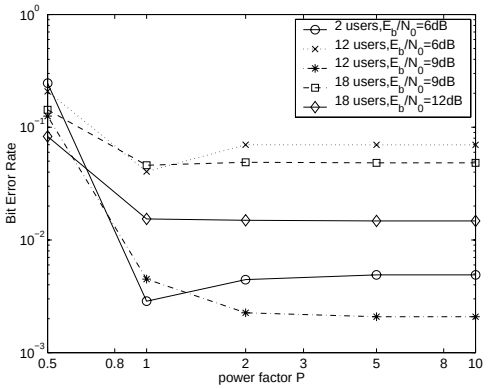

b) 6-path severe multipath channel

Fig. 5.10 - Optimisation of power factor P (r=1.0)

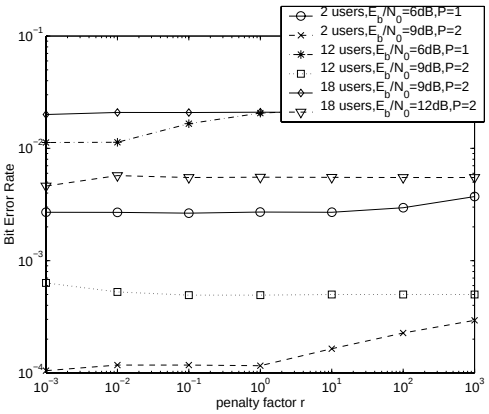

a) 2-path channel with strong LOS

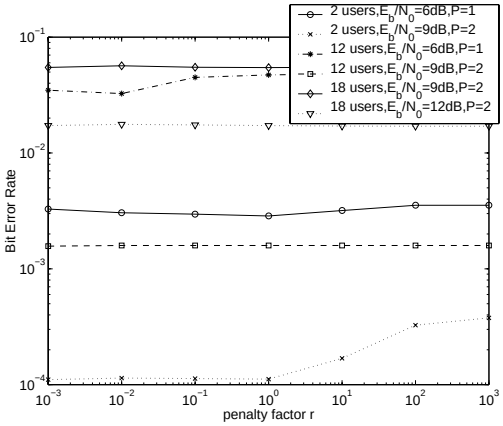

b) 6-path severe multipath channel

Fig. 5.11 - Optimisation of penalty factor r

In Fig. 5.12 and Fig. 5.13 the performance of the numerical algorithm proposed in this section is compared to the performances of conventional single-user transmission with Rake receivers and of zero-forcing joint precoding. In all cases orthogonal spreading after a convolutional code of rate R=1/2 was considered. The processing gain G=16 is the same as in the results shown in Section 5.2.4. The power factor P and the penalty factor r were chosen based on the parameter optimisation performed above. In the following simulations we will consider P=1 if E_b/N_0=6dB and P=2 if E_b/N_0=9dB. The penalty factor will be r=0,01 in all cases.

Fig. 5.12 displays the results for the 2-path channel with strong line-of-sight component. We can see that the numerical algorithm performs very well compared to the zero-forcing precoding method. The reduction in the bit error rate with a small number of users observed when the zero-forcing algorithm was employed also occurs with the numerical minimisation. This happens because with few users the zero-forcing precoding algorithm can eliminate the interference with less energy than the one needed with conventional transmission. With this traffic load the power constraint does not come into effect in the numerical method and the algorithm converges rapidly to the minimum $\boldsymbol{e}(\underline{\lambda})$=0. For instance with the examples chosen already 20 iterations can provide excellent results.

With a larger number of users the limited power method does not collapse as the zero-forcing scheme and it is always better than the pre-Rake, which was expected, since it is based on successive minimisation steps starting from a pre-Rake. The Rake receiver approach with conventional transmission has still good results to offer for a large number of users and low noise level, due to the preservation of code orthogonality without a pre-Rake. It is however reasonable to expect that the application of the precoding minimisation algorithm with power constraint considering Rake receivers should bring a great improvement compared to the conventional transmission approach. This will be however not investigated here.

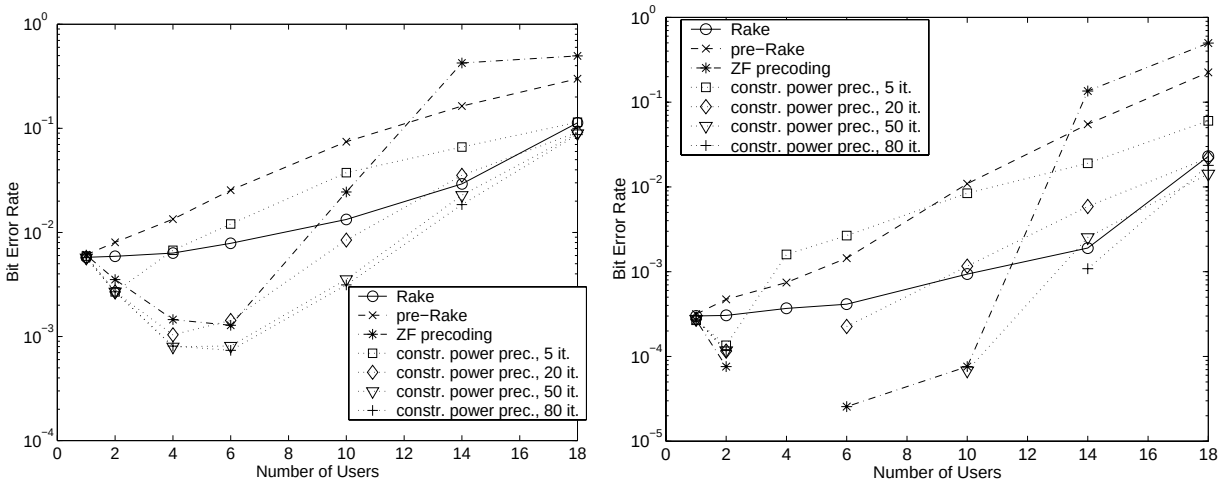

a) E_b/N_0 = 6dB *b) E_b/N_0 = 9dB*

Fig. 5.12 - Performance of Precoding with Power Constraint (2-path channel)

The results for a 6-path channel, which are shown in Fig. 5.13 are similar to the ones for a 2-path channel, but, since the severe multipath propagation destroys part of the orthogonality, the advantage of employing the precoding method with limited power compared to conventional transmission with Rake receivers is much more significant.

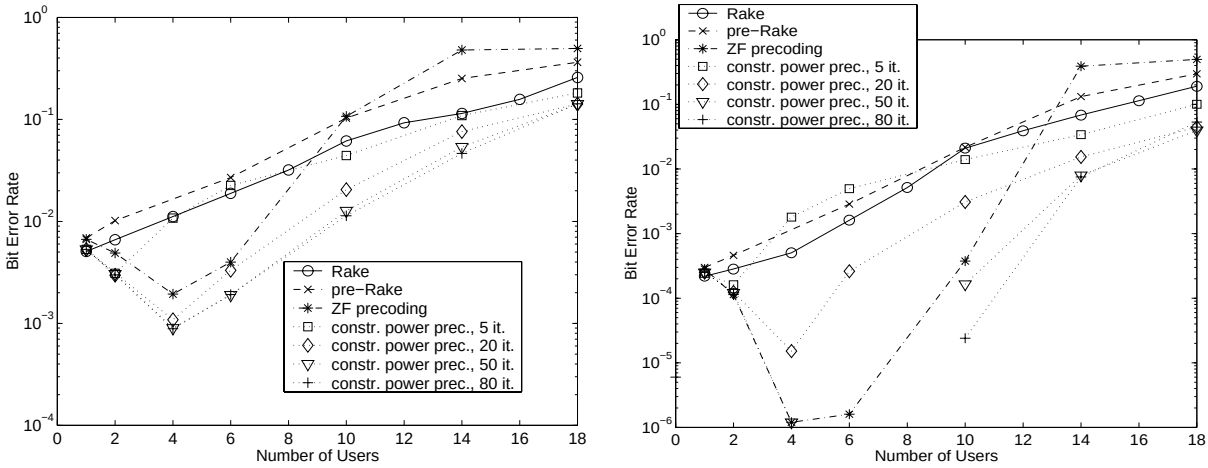

a) E_b/N_0 = 6dB *b) E_b/N_0 = 9dB*

Fig. 5.13 - Performance of Precoding with Power Constraint (6-path channel)

The capacity increase achieved with the power limited precoding is anyway quite substantial. For instance with a signal-to-noise ratio of E_b/N_0=6dB and a desired bit error rate of 10^{-2}, the capacity increases from 8 users with Rake receivers to 13 users with precoding in the 2-path channel, and from 4 to 10 users in the 6-path channel. With a signal-to-noise ratio of E_b/N_0=9dB and a desired bit error rate of 10^{-3} the capacity gains are also significant. In the 2-path channel the capacity increases from 10 to 14 users and in the 6-path channel from 5 to 13 users. Depending on the channel parameters, when joint precoding is employed we can have in the downlink nearly three times the capacity of a system using conventional transmission and Rake receivers, and this with less complex mobile terminals. Joint precoding may also help us attain very low bit error rates, down to 10^{-6} for instance with E_b/N_0=9dB in the 6-path channel, that cannot otherwise be reached with conventional transmission schemes.

All in all, the results shown here indicate that the precoding method with power constraint can be very efficient in increasing the capacity and, unlike the unconstrained linear precoding techniques, this method performs very well under any system load. We can also expect that a more careful choice of the algorithm parameters *r, P* and *I*, adapted to the system configuration, may provide even further capacity gains.

5.2.6 Implementation Issues

In this sub-section we will investigate some aspects that may be relevant for the implementation of the algorithms described in Sections 5.2.2 to 5.2.5.

Flexibility

The precoding techniques presented here provide a great amount of flexibility in that different quality requirements and different configurations can be supported.

In a heterogeneous communications system some users may require a higher signal power at the decoder input, either because a lower bit error rate is demanded by their applications or because they suffer a higher interference (near the cell border for instance). In some applications, for example in speech transmission, some bits can be more important than others and should have a greater protection against noise and interference. These different requirements can be accommodated if, instead of the condition in (5.22), we require that

$$\hat{\boldsymbol{d}} = \boldsymbol{Q}\boldsymbol{d} \tag{5.66}$$

where $\boldsymbol{Q}$ is a diagonal matrix whose elements determine the desired received levels of the various bits.

The same applies to the minimisation of the mean square error, in which case instead of (5.52), the error function to be minimised is

$$e = (\boldsymbol{Q}\boldsymbol{d} - \hat{\boldsymbol{d}})^{\mathrm{T}}(\boldsymbol{Q}\boldsymbol{d} - \hat{\boldsymbol{d}}). \tag{5.67}$$

All we have to do then in the block precoding algorithms described earlier is to substitute $\boldsymbol{d}$ for $\boldsymbol{Q}\boldsymbol{d}$.

We can also make allowance for the fact that various users may have different receiver configurations, i.e., some mobile stations may be equipped with a Rake receiver while other low-end terminals have just an integrate-and-dump receiver. We can model the use of Rake receivers at a given mobile station k by considering the equivalent channel $\boldsymbol{H}'_k=\boldsymbol{H}_k^{\mathrm{T}}\boldsymbol{H}_k$. With this in mind the different receiver configurations can be taken into account by letting

$$\boldsymbol{H}_{rec} = \begin{bmatrix} \rho_0\boldsymbol{H}_0^{\mathrm{T}} & 0 & \dots & 0 \\ 0 & \rho_1\boldsymbol{H}_1^{\mathrm{T}} & \dots & 0 \\ \dots & \dots & \dots & \dots \\ 0 & 0 & \dots & \rho_{K-1}\boldsymbol{H}_{K-1}^{\mathrm{T}} \end{bmatrix} \tag{5.68}$$

where ρ_k=0 if the k-th user has an integrate-and-dump receiver and ρ_k=1 if it has a Rake receiver, and employing the equivalent channel matrix $\boldsymbol{H}'=\boldsymbol{H}_{rec}\boldsymbol{H}$ in the optimisation process.

Complexity

We will following briefly investigate the order of complexity of the block precoding algorithms proposed above as a function of the number of users K, the number of coded bits in a block N, the number of chips in a bit M and, in the case of power constrained minimisation. the number of iterations I.

Methods without power constraint: The order of complexity is the same for all the algorithms proposed in Section 5.2.2, since the most complex operation in all those approaches is the solution of a linear system with KN variables[1], which requires $O(K^3N^3)$ operations[2]. In the zero-forcing method the system matrix to be inverted is symmetric and positive definite, and,

1. We actually do not have to invert the correlation matrix $\boldsymbol{R}$ to obtain the transformation matrix $\boldsymbol{T}=\boldsymbol{R}^{-1}$, as indicated in (5.25), (5.27) and (5.30). We can simply obtain the vector $\boldsymbol{y}$ that solves the linear system $\boldsymbol{R}\boldsymbol{y}=\boldsymbol{d}$, which requires fewer operations than matrix inversion[30].

hence, the system can be solved using Cholesky decomposition [30]. The same is not true for the Vojcic-Jang method, which has to be solved through other methods, LU-decomposition [30] for instance, which requires about twice as many operations as Cholesky decomposition.

*Minimisation of **s** with power constraint:* If we ignore the many iterations required for minimisation, then the complexity of this algorithm arises basically from the computation of $\boldsymbol{A}\boldsymbol{H}^{\mathrm{T}}\boldsymbol{C}\boldsymbol{C}^{\mathrm{T}}\boldsymbol{H}\boldsymbol{A}^{\mathrm{T}}$, which is required to obtain the function gradient. This matrix has to be obtained only once in each block and can be used for every subsequent iteration. By making use of the fact that the matrices $\boldsymbol{A}$, $\boldsymbol{H}$ and $\boldsymbol{C}$ are relatively sparse, this computation can be made with $O(KNM^2)$ operations. Within the iteration loop (see Appendix G.1) $O(N^2M^2)$ operations are required. The total complexity of the numerical algorithm is therefore $O(KNM^2+IN^2M^2)$.

Minimisation of $\underline{\lambda}$ with power constraint: The most complex part of this algorithm is the calculation of the matrix $\boldsymbol{R}^{\mathrm{T}}\boldsymbol{R}$ in (5.55) which, considering the sparseness of $\boldsymbol{R}$, requires $O(K^3N)$ operations. In each iteration of the numerical method $O(K^2N^2)$ operations have to be performed (see Appendix G.2), and the total algorithm complexity is hence $O(K^3N+IK^2N^2)$.

All the block precoding methods investigated here have a complexity that increases polynomially with the number of users and with the block size. Comparing both numerical methods we see that their complexity is similar. The difference between them is that a factor of M^2 in the complexity required for the minimisation of the transmit vector $\boldsymbol{s}$ is replaced by K^2 for the minimisation of the modified bit vector $\underline{\lambda}$. This means that the latter method is preferable if the number of users is small in relation to the number of chips per coded bit M. This is likely to be the case in systems with a high coding rate R, since $M=GR$ is directly proportional to the coding rate and hence large for large values of R.

If few iterations of the numerical methods are performed, these are clearly superior to the analytical one in terms of complexity. However, as seen in Figs., many iterations are needed if a good performance is to be achieved, and in this case there is no significant difference in the complexity of both algorithms.

The complexity of the block precoding algorithms proposed here grows very rapidly with the number of users and with the frame size, thus limiting their application in real-life systems. The complexity is also much higher if part of the spreading gain is used for coding, since for a given block of N_{inf} information bits there are $N=N_{inf}/R$ code bits to be considered at the precoding algorithm. The only exception to this is the numerical minimisation of the signal $\boldsymbol{s}$, whose complexity depends basically on the number of chips in a block NM.

5.3. Bitwise Precoding

The block precoding techniques presented in Section 5.2 can be very efficient in increasing the capacity of CDMA spread spectrum systems, but, due to their high complexity, their implementation is in practice limited to systems with a small number of users and short data blocks.

---

2. We utilise here the big "O" notation for the complexity of algorithms, which indicates their asymptotic complexity. Let $f(n)$ be the number of operations required for a certain algorithm as a function of parameter n. We can say that the algorithm has a complexity $O(g(n))$ if there are two positive constants c and N such that

   $$f(n) \le cg(n) \qquad ,\forall\ n \ge N$$

   This means that, as n increases, $f(n)$ grows no faster than $g(n)$.

We can however use the same concepts from the joint precoding methods proposed so far and perform bitwise joint precoding. If the spreading gain is large in relation to the number of paths the interference between bits caused by multipath propagation can be neglected and we can use the same algorithms from Section 5.2 for each bit at a time. The precoding has to be performed once every bit, and, considering for instance the zero forcing algorithm, $O(K^3N)$ operations are needed if the signal is precoded bitwise, which is a significant reduction in the complexity compared to the $O(K^3N^3)$ operations required by block precoding.

5.3.1 Algorithm

We can also consider the interference between the bits in our precoding scheme if there are no Rake receivers at the mobile terminals. In this case, neglecting the thermal noise, the decision vector corresponding to the n-th bit is

$$\hat{\boldsymbol{d}}(n) = \boldsymbol{C}^{\mathrm{T}}(n)\boldsymbol{H}\boldsymbol{A}^{\mathrm{T}}\boldsymbol{s}(n) + \boldsymbol{i}(n) \tag{5.69}$$

where

$$\boldsymbol{C}(n) = \begin{bmatrix} \boldsymbol{c}_0(n) & 0 & \dots & 0 \\ 0 & \boldsymbol{c}_1(n) & \dots & 0 \\ \dots & \dots & \dots & \dots \\ 0 & 0 & \dots & \boldsymbol{c}_{K-1}(n) \end{bmatrix}, \tag{5.70}$$

$\boldsymbol{H}$ is the $2MK \times 2MK$ channel matrix, $\boldsymbol{A}$ the $2M \times 2MK$ addition matrix, $\boldsymbol{s}(n)$ the transmitted signal corresponding to the n-th bit and $\boldsymbol{i}(n)$ the interference due to the other bits.

Considering that no Rake processing is made and that the channel impulse response is not longer than one bit ($L \leq M$), the inter-bit interference $\boldsymbol{i}(n)$ is caused by the previous bit only and it can be given by

$$\boldsymbol{i}(n) = \boldsymbol{C}^{\mathrm{T}}(n)\boldsymbol{H}_{prev}\boldsymbol{A}^{\mathrm{T}}\boldsymbol{s}(n-1) \tag{5.71}$$

where

$$\boldsymbol{H}_{prev} = \begin{bmatrix} \boldsymbol{H}_{prev,0} & 0 & \dots & 0 \\ 0 & \boldsymbol{H}_{prev,1} & \dots & 0 \\ \dots & \dots & \dots & \dots \\ 0 & 0 & \dots & \boldsymbol{H}_{prev,K-1} \end{bmatrix}, \tag{5.72}$$

with $\boldsymbol{H}_{prev,k}$ the $2M \times 2M$ matrix

$$\boldsymbol{H}_{prev,\,k} = \begin{bmatrix} \cdots & 0 & g_{k,\,L-1,\,R} & -g_{k,\,L-1,\,I} & \cdots & g_{k,\,1,\,R} & -g_{k,\,1,\,I} \\ \cdots & 0 & g_{k,\,L-1,\,I} & g_{k,\,L-1,\,R} & \cdots & g_{k,\,1,\,I} & g_{k,\,1,\,R} \\ \cdots & 0 & 0 & 0 & \cdots & g_{k,\,2,\,R} & -g_{k,\,2,\,I} \\ \cdots & 0 & 0 & 0 & \cdots & g_{k,\,2,\,I} & g_{k,\,2,\,R} \\ \cdots & \cdots & \cdots & \cdots & \cdots & \cdots & \cdots \\ \cdots & 0 & 0 & 0 & \cdots & g_{k,\,L-1,\,R} & -g_{k,\,L-1,\,I} \\ \cdots & 0 & 0 & 0 & \cdots & g_{k,\,L-1,\,I} & g_{k,\,L-1,\,R} \\ \cdots & 0 & 0 & 0 & \cdots & 0 & 0 \\ \cdots & \cdots & \cdots & \cdots & \cdots & \cdots & \cdots \end{bmatrix}. \tag{5.73}$$

When joint precoding is applied to the *n*-th bit we have already knowledge of the optimised signal obtained for the previous bit $\boldsymbol{s}(n\text{-}1)$ and we can take it into account in the precoding algorithm.

Suppose we want to completely eliminate the interference with no power constraint, then we must satisfy the equality

$$\hat{\boldsymbol{d}}(n) = \boldsymbol{d}(n). \tag{5.74}$$

By substituting (5.69) into (5.74) we have the following condition:

$$\boldsymbol{C}^{\mathrm{T}}(n)\boldsymbol{H}\boldsymbol{A}^{\mathrm{T}}\boldsymbol{s}(n) = \boldsymbol{d}(n) - \boldsymbol{i}(n). \tag{5.75}$$

This can be solved for example through the zero-forcing (minimum power) precoding method, by making

$$\boldsymbol{s}(n) = \boldsymbol{A}\boldsymbol{H}^{\mathrm{T}}\boldsymbol{C}(n)\underline{\lambda}(n) \tag{5.76}$$

where

$$\underline{\lambda}(n) = \left[\boldsymbol{C}^{\mathrm{T}}(n)\boldsymbol{H}\boldsymbol{A}^{\mathrm{T}}\boldsymbol{A}\boldsymbol{H}^{\mathrm{T}}\boldsymbol{C}(n)\right]^{-1}(\boldsymbol{d}(n) - \boldsymbol{i}(n)). \tag{5.77}$$

The same applies for the minimisation with power constraint, where the function to be minimised is now

$$e(\boldsymbol{s}(n)) = \left[\boldsymbol{d}(n) - \boldsymbol{i}(n) - \boldsymbol{C}^{\mathrm{T}}(n)\boldsymbol{H}\boldsymbol{A}^{\mathrm{T}}\boldsymbol{s}(n)\right]^{\mathrm{T}}\left[\boldsymbol{d}(n) - \boldsymbol{i}(n) - \boldsymbol{C}^{\mathrm{T}}(n)\boldsymbol{H}\boldsymbol{A}^{\mathrm{T}}\boldsymbol{s}(n)\right] \tag{5.78}$$

This approach cannot be carried out if a Rake receiver is employed. We should bear in mind that Rake processing is equivalent to a non-causal channel matched filtering, and thus the inter-bit interference will be caused both by the previous and by the following bit. In this case, a block precoding scheme as the ones presented in Section 5.2 must be employed if we desire to cancel out the interference.

5.3.2 Simulation Results

In Fig. 5.14 we have compared the performance of bitwise precoding through the zero-forcing method to the one of block precoding, as described in Section 5.2.2. We have simulated a system with no channel coding and the same processing gain considered so far in this chapter (G=16) with the channels from Table 2.1. It can be seen that the performance loss of bitwise precoding compared to block precoding is negligible for the 2-path channel, but more

significant for the 6-path channel. In bitwise precoding a truncated pre-Rake is applied on each bit, and the longer the multipath delay in relation to the number of chips per bit is, the greater is the performance loss due to truncation.

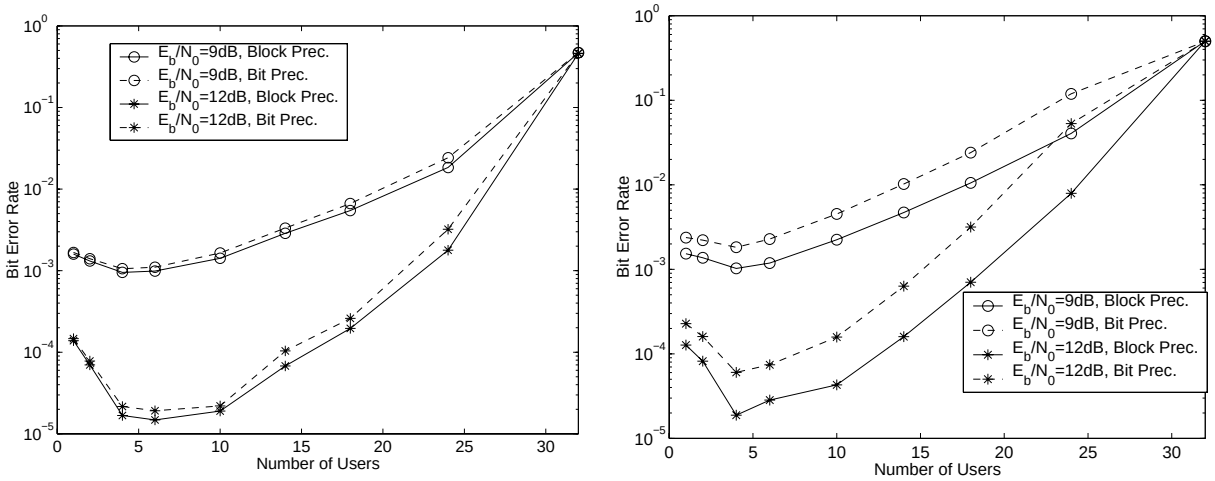

a) 2-path channel *b) 6-path channel*

Fig. 5.14 - Performance of bitwise zero-forcing precoding

The reduced complexity of bitwise precoding makes it feasible also for systems with a larger number of users, independently of the frame length. In Fig. 5.15 performance results for a system with processing gain G=128, convolutional coding of rate R=1/2 and orthogonal spreading are displayed. The 6-path channel model with signal-to-noise ratio E_b/N_0=9dB is considered. Both zero-forcing precoding and precoding with power constraint were considered. If the spreading gain is large, as in this case, the effect of pre-Rake truncation is insignificant and quite good results can be achieved with bitwise joint precoding, as we can observe in the Fig. 5.15. The same behaviour observed with block precoding can also be seen here, an initial reduction in the bit error rate for few users and the superior performance of the power constrained method for a large number of users. The capacity gain achieved through bitwise precoding is also quite substantial, for a desired bit error rate of 10^{-2} for instance the cell capacity can be increased from about 65 users with conventional transmission and a Rake receiver to over 110 users with precoding, for a target bit error rate of 10^{-3} the increase is from 35 to 90 users, i.e., a more than twofold capacity gain.

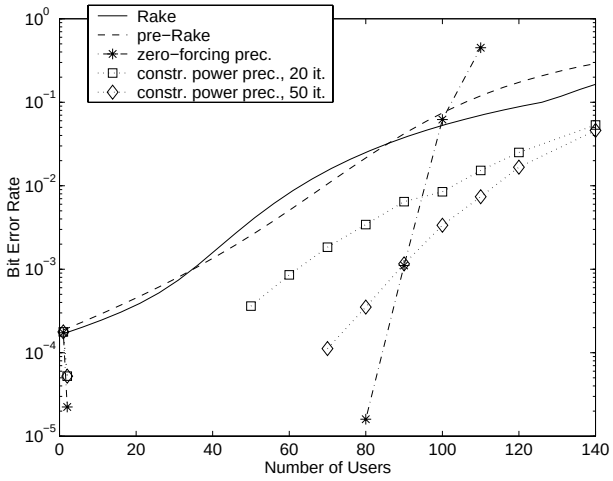

Fig. 5.15 - Performance of bitwise precoding with large spreading factor (G=128)

5.4. Precoding with Multiple Antennas

The use of multiple antennas can be considered with a few small changes in the system matrices. These will be briefly discussed in this section. We will consider here the vector notation developed for the block precoding techniques from Section 5.2 and extend it to systems employing multiple antennas at the base station transmitter.

Suppose we have L_{Tx} transmit antennas at the base station with $\boldsymbol{s}_l$ the transmitted signal at the l-th antenna. The overall transmit signal can be expressed in vector form as:

$$\boldsymbol{s}_{ma} = \begin{bmatrix} \boldsymbol{s}_0 \\ \boldsymbol{s}_1 \\ \dots \\ \boldsymbol{s}_{L_{Tx}-1} \end{bmatrix} \tag{5.79}$$

Let $\tilde{\boldsymbol{H}}_l$ be the matrix describing the channel between the l-th transmit antenna and the mobile terminals of every user, as described by (5.15). Then, if integrate-and-dump receivers are used, the vector of decision variables at the mobile terminals can be given by

$$\hat{\boldsymbol{d}} = \boldsymbol{C}^{\mathrm{T}} \boldsymbol{H}_{ma} \boldsymbol{A}_{ma}^{\mathrm{T}} \boldsymbol{s}_{ma} + \boldsymbol{C}^{\mathrm{T}} \underline{\nu}, \tag{5.80}$$

where

$$\boldsymbol{H}_{ma} = \left[\tilde{\boldsymbol{H}}_0 \; \tilde{\boldsymbol{H}}_1 \; \dots \; \tilde{\boldsymbol{H}}_{L_{Tx}-1} \right] \tag{5.81}$$

and

$$\boldsymbol{A}_{ma} = \underbrace{\begin{bmatrix} \boldsymbol{A} & 0 & \dots & 0 \\ 0 & \boldsymbol{A} & \dots & 0 \\ \dots & \dots & \dots & \dots \\ 0 & 0 & \dots & \boldsymbol{A} \end{bmatrix}}_{L_{Tx} \text{ times}}, \tag{5.82}$$

with $\boldsymbol{A}$ defined in (5.9).

The system equation (5.80) is the same as for a system employing a single transmit antenna, except for the extended channel, addition and transmit signal matrices. If we apply, for instance, the optimisation algorithm from Section 5.2.3 considering multiple antennas we will end up with the following optimum solution for the transmit signal:

$$\boldsymbol{s}_{ma} = \boldsymbol{A}_{ma}\boldsymbol{H}_{ma}^{\mathrm{T}}\boldsymbol{C}\underline{\lambda}, \tag{5.83}$$

where

$$\underline{\lambda} = \boldsymbol{R}_{ma}^{-1}\boldsymbol{d}, \tag{5.84}$$

with $\boldsymbol{R}_{ma}$ the correlation matrix

$$\boldsymbol{R}_{ma} = \boldsymbol{C}^{\mathrm{T}}\boldsymbol{H}_{ma}\boldsymbol{A}_{ma}^{\mathrm{T}}\boldsymbol{A}_{ma}\boldsymbol{H}_{ma}^{\mathrm{T}}\boldsymbol{C}. \tag{5.85}$$

The computation of the transmit signal in (5.83) and of the correlation matrix in (5.85) are indeed more complex than the ones necessary for the single antenna case, but most of the algorithm complexity arises from the matrix inversion in (5.84). By comparing the expressions for the correlation matrices with a single and with multiple antennas in (5.47) and (5.85) we see that they have the same dimension and hence the same complexity for the matrix inversion. The same applies for the other algorithms investigated in this chapter, multiple antennas can be taken into account with only a marginal increase in the computational complexity. The capacity achieved with joint precoding employing multiple antennas will be however not addressed in this work and is a matter for future studies.

5.5. Summary of Chapter 5

In this chapter we have investigated several joint precoding techniques that may help increase the capacity in the downlink of spread spectrum systems without requiring any extra complexity in the mobile terminals. This can be achieved provided channel state information is available at the base station before transmission.

We have first investigated block precoding algorithms that eliminate the interference by obtaining a linear transformation of the coded bit sequence. The optimum method was derived and it could be shown that a significant performance improvement can be obtained this way, specially with a small to moderate system load, in which case even the single-user situation can be outperformed. As the number of users approaches the degrees of freedom of the system, the interference elimination with normalised power provokes a large reduction in the signal-to-noise ratio at the receiver such that the precoding performance eventually collapses.

A solution to this problem was proposed in that a power limitation was introduced and a numerical optimisation approach to the minimisation of the mean square error was taken. We have seen that with this modification a performance improvement can be reached also for a

large number of users when the linear block precoding techniques fail. This numerical method also approaches the performance of the optimum linear precoding method for a light traffic load.

Blockwise techniques have the drawback that they are somewhat complex and hence infeasible for systems with reasonably large block sizes and many users. We can however make the complexity increase only linearly with the block size by applying the same precoding techniques bit by bit. By employing this approach we have negligible losses in relation to blockwise precoding with only a fraction of the complexity, provided the number of significant multipaths is small compared to the spreading factor. This makes the use of joint precoding feasible also for systems with larger processing gains and higher capacity, which was demonstrated here.

Unlike joint detection, which has been extensively studied, the investigation of joint precoding techniques is still in its initial steps. The performance of these algorithms in the presence of channel estimation errors and the development of robust algorithms is an important issue for future work. Another promising research field is the application of the proposed precoding schemes to systems with multiple transmit antennas at the base stations. The precoding algorithms themselves increase only marginally in complexity if multiple antennas are used, but the acquisition of reliable channel state information for each antenna element might pose some difficulties. The investigation of space-time joint precoding is an extension of the work presented in this chapter intended for the future.

6. CONCLUSION

In this work we have investigated the use of signal precoding in the downlink of direct-sequence spread spectrum systems. Pre-processing is possible if channel state information is known before transmission, which is the case for instance in TDD systems.

We have first examined individual pre-processing, in which the signal of each user is treated separately, ignoring the knowledge about other users' channels and data. The technique considered was the pre-Rake, in which the Rake processing usually performed at the mobile station receiver is transferred to the base station transmitter. This provides us with less complex mobile terminals and, in spite of that, under certain conditions the capacity can be increased compared to conventional transmission using Rake receivers, particularly in channels with severe multipath distortion. We have observed that the use of channel coding must be taken into account for a fair comparison among different techniques, and a new semi-analytical method was develop to calculate the system performance of spread spectrum systems considering error correcting codes. With this analysis method we have also investigated the optimum trade-off between the channel coding rate and orthogonal spreading, which is an issue of great importance in chip synchronous CDMA.

We have also seen that the pre-Rake acts like a channel matched pre-filter, and that with a Rake decorrelator matched to the combination of pre-Rake and multipath channel the signal-to-noise ratio at the decoder input can be enhanced, with a receiver complexity similar to the one of a conventional Rake receiver. This novel technique, which we call a post-Rake, was investigated both in a single user and in a multiuser scenario, and we observed that whereas the signal-to-noise ratio improves, the interference level increases compared to conventional methods (Rake receiver, pre-Rake only), which limits its application to situations with few users and low bit error rate.

All in all it cannot be said that there is a single optimum technique in terms of capacity among the ones mentioned so far: Rake receiver, pre-Rake and post-Rake. The optimum technique depends rather on the particular system configuration, i.e., it depends on parameters like processing gain, coding scheme, channel multipath profile, traffic load and quality requirements. For instance with high traffic loads, the Rake receiver is the best technique in terms of capacity for channels with light multipath propagation, whereas in channels with severe multipath distortion the pre-Rake performs much better. The latter technique is anyway preferable if low complexity mobile receivers are desired. With low traffic loads however, the combination of pre-Rake and post-Rake allows us to obtain much lower bit error rates than with a single Rake filter.

A higher capacity can be attained if all the users of the same cell are precoded jointly instead of applying a pre-Rake to each user separately, as we have shown in Chapter 5. The joint precoding methods investigated there make use of the knowledge of all the users' channels and codes at the base station to optimise the transmit signal in order to reduce the multiuser interference. Both block and bit precoding schemes were analysed and the latter were shown to yield quite good results with a fraction of the complexity of the former, provided the delay spread is small compared to the processing gain. We have demonstrated that using these techniques the downlink capacity can be increased up to three times compared to the one obtained with conventional transmission and Rake receivers. This can be achieved with no extra complexity at the mobile terminals, since the joint precoding algorithms are performed at

the base station only. Improved methods that combine joint precoding at the base station and multiuser detection at the mobile stations are however an interesting issue for future investigation.

Channel estimation is a major problem for signal preprocessing techniques, since they rely on the knowledge of the channel impulse response before transmission. Even though possible in TDD systems, the acquisition of this information may be difficult in rapidly changing channels. We have investigated some methods that increase the reliability of the channel state information before transmission in time variant channels and analysed the performance of the pre-Rake under these conditions. The sensitivity of joint precoding techniques to erroneous information is however yet to be investigated. Anyway, even if absolutely accurate channel state information cannot be obtained it would be a waste not to use the available information, however imprecise. The search for robust methods that provide a capacity increase also with partial channel information is also an issue for future work.

Another aspect that should be further investigated is the use of precoding techniques, either joint or individual, in systems with multiple transmit antennas. It can be expected that the new degrees of freedom provided by the spacial component of the signal will help us further increase the capacity, and the development of space-time precoding techniques is a promising field for future research.

We can conclude that the techniques investigated here show a great potential for wireless communications systems. Their application is relevant for instance in the TDD mode of third generation mobile communications systems or in WLL applications. However, much work is still to be done to improve these techniques, to assess their performance in multicell systems and to make their implementation possible in real life; and we hope to have contributed with this work to the fulfilment of this goal.

APPENDIX A. CODE PARAMETERS

In this appendix the parameters of the convolutional codes considered throughout this work are listed.

In Table A.1 the generator polynomials are given in octal form. For the codes with rate R=1/2 and R=1/4 the polynomials were taken from [27], and for the lower rate codes from [14].

Rate	*generator polynomials in octal form*	d_{free}
R=1/2	561 753	12
R=1/4	463 535 733 745	24
R=1/8	473 513 671 765 657 745 753 517	50
R=1/256	453 455 457 467 473 475 513 517 551 557 573 657 671 675 735 745 753 765 453 455 457 467 473 475 517 551 557 573 657 671 675 735 745 753 453 455 457 467 473 475 517 557 573 657 671 675 745 753 453 455 457 467 473 475 517 557 573 657 675 745 753 453 455 457 467 473 475 517 557 573 657 675 745 753 453 455 457 473 475 517 557 573 657 675 745 753 453 457 473 475 517 557 573 657 675 745 753 453 457 473 475 517 557 573 657 675 753 453 457 473 475 517 557 573 657 675 753 453 473 475 517 557 657 675 753 453 473 475 557 675 753 453 473 475 557 675 753 453 473 475 557 675 753 453 473 475 557 675 753 453 473 475 557 675 753 453 473 475 557 675 453 473 475 557 675 453 473 475 557 675 453 473 475 557 675 453 473 475 557 453 473 475 557 473 475 557 473 475 557 473 475 557 473 475 557 475 557 475 557 475 557 475 557 475 557 475 557 475 557 453 735 475 557 475 467 557 453 735 475 557 475 467 557 453	1608

Table A.1 - Maximum free distance codes with memory order m=8

The derivative of the code transfer function $T(D,I)$ was obtained recursevely by the method suggested in [15] and it is given below in Table A.2 for the first fifteen terms

.

Rate	$\left.\frac{d}{dI}T(D, I)\right\|_{I=1}$
R=1/2	$33D^{12}+281D^{14}+1997D^{16}+10454D^{18}+44839D^{20}+6603D^{22}+39069D^{24}+29104D^{26}$ $+50619D^{28}+42265D^{30}+53501D^{32}+18306D^{34}+48492D^{36}+12183D^{38}+2061D^{40}$
R=1/4	$4D^{24}+22D^{26}+38D^{28}+103D^{30}+237D^{32}+587D^{34}+1251D^{36}+2765D^{38}+6666D^{40}$ $+15909D^{42}+36505D^{44}+16295D^{46}+53201D^{48}+9660D^{50}+53119D^{52}$
R=1/8	$5D^{50}+10D^{52}+2D^{54}+16D^{56}+16D^{58}+37D^{60}+29D^{62}+50D^{64}+99D^{66}+144D^{68}+182D^{70}$ $+278D^{72}+502D^{74}+585D^{76}+1016D^{52}$
R=1/256	$D^{1608}+7D^{1610}+5D^{1628}+3D^{1630}+7D^{1720}+3D^{1780}+4D^{1784}+5D^{1790}+3D^{1866}+9D^{1876}$ $+5D^{1884}+4D^{1898}+4D^{1912}+6D^{1918}+4D^{1924}$

Table A.2 - Derivative of code transfer function (m=8, *maximum* d_{free})

As described in Section 2.2, for signal-to-noise ratios Γ less than a certain threshold Γ_{Thresh} the bit error rate was obtained from a 6th-order polynomial approximation of simulation results, such that:

$$\log_{10}(F_e(\Gamma)) = a_0 + a_1\Gamma_{dB} + a_2{\Gamma_{dB}}^2 + a_3{\Gamma_{dB}}^3 + a_4{\Gamma_{dB}}^4 + a_5{\Gamma_{dB}}^5 + a_6{\Gamma_{dB}}^6 \qquad \text{(A.1)}$$

where Γ_{dB} is the value of the signal-to-noise ratio Γ in dB.

The polynomial coefficients were chosen such that the mean square error of the logarithm of the bit error rate was minimised in relation to simulation results. The polynomial coefficients for the different codes, as well as the threshold Γ_{Thresh} are shown in Table A.3.

Rate	Γ_{Thresh}	a_0	a_1	a_2	a_3	a_4	a_5	a_6
R=1/2	3,0dB	-0,748020	-0,500368	-0,216549	-0,024265	0,006207	0,000979	-0,000058
R=1/4	3,5dB	-1,299793	-0,729030	-0,165606	-0,000427	0,002922	-0,000086	-0,000042
R=1/8	3,0dB	-1,555992	-0,774266	-0,154368	-0,002204	0,002911	0,000336	0,000011
R=1/256	2,5dB	-1,604887	-0,777223	-0,158898	-0,000507	0.005059	0.000787	0.000038

Table A.3 - Coefficients of approximation polynomial

The simulations from which the polynomials were obtained were performed over 25.000.000 bits (1.000.000 for *R*=1/256) and their results are shown in Table A.4.

Γ	*R*=1/2	*R*=1/4	*R*=1/8	*R*=1/256
-5,0dB	$4{,}980801 \times 10^{-1}$	$4{,}862879 \times 10^{-1}$	$4{,}752806 \times 10^{-1}$	
-3,0dB	$4{,}785980 \times 10^{-1}$	$4{,}299228 \times 10^{-1}$	$3{,}913424 \times 10^{-1}$	$3{,}597178 \times 10^{-1}$
-2,0dB	$4{,}469286 \times 10^{-1}$	$3{,}414609 \times 10^{-1}$	$2{,}728328 \times 10^{-1}$	$2{,}473870 \times 10^{-1}$
-1,0dB	$3{,}624890 \times 10^{-1}$	$1{,}847000 \times 10^{-1}$	$1{,}186816 \times 10^{-1}$	$1{,}046817 \times 10^{-1}$
0dB	$1{,}774763 \times 10^{-1}$	$5{,}121488 \times 10^{-2}$	$2{,}712927 \times 10^{-2}$	$2{,}390493 \times 10^{-2}$
0,5dB	$8{,}991118 \times 10^{-2}$	$1{,}933077 \times 10^{-2}$	$1{,}014594 \times 10^{-2}$	$9{,}321840 \times 10^{-3}$
1,0dB	$3{,}315082 \times 10^{-2}$	$6{,}265671 \times 10^{-3}$	$3{,}252435 \times 10^{-3}$	$3{,}193999 \times 10^{-3}$
1,5dB	$9{,}175767 \times 10^{-3}$	$1{,}738120 \times 10^{-3}$	$9{,}149200 \times 10^{-4}$	
2,0dB	$2{,}059609 \times 10^{-3}$	$4{,}299999 \times 10^{-4}$	$2{,}123599 \times 10^{-4}$	$1{,}890000 \times 10^{-4}$
2,5dB	$4{,}021999 \times 10^{-4}$	$8{,}508000 \times 10^{-5}$	$4{,}348000 \times 10^{-5}$	5.599999×10^{-5}
3,0dB	$6{,}999999 \times 10^{-5}$	$1{,}468000 \times 10^{-5}$	$9{,}999999 \times 10^{-6}$	
3,5dB	$9{,}360000 \times 10^{-6}$	$2{,}560000 \times 10^{-6}$	$2{,}520000 \times 10^{-6}$	

Table A.4 - Coding performance in AWGN channel(simulation results)

APPENDIX B. CALCULATION OF THE INTERFERENCE VARIANCE (RAKE)

Considering that the channel gains $g_{0,l}$ are constant values, we want to obtain the variance of the interference components:

$$\nu_{self} = \sqrt{\frac{E_c}{2}} \sum_{i=0}^{M-1} \sum_{\substack{\lambda=-(L-1) \\ \lambda \neq 0}}^{L-1} \sum_{l-m=\lambda}^{l,m} (g^*_{0,m} g_{0,l} a_0(i-\lambda)) \otimes c_0(i) \tag{B.1}$$

and

$$\nu_{mu} = \sqrt{\frac{E_c}{2}} \sum_{i=0}^{M-1} \sum_{k=1}^{K-1} \left[\sum_{\substack{\lambda=-(L-1) \\ \lambda \neq 0}}^{L-1} \sum_{l-m=\lambda}^{l,m} (g^*_{0,m} g_{0,l} a_k(i-\lambda)) \otimes c_0(i) + \sum_{l=0}^{L-1} (|g_{0,l}|^2 a_k(i)) \otimes c_0(i) \right] \tag{B.2}$$

Now let

$$S(a) = a_R + a_I \tag{B.3}$$

where a_R and a_I are respectively the real and imaginary parts of the complex value a. As indicated in Section 2.2, we are actually interested in the interference $S(\nu_{self}+\nu_{mu})$, but if the real and imaginary parts of the interference are independent we have

$$\mathrm{var}\{\nu_{self} + \nu_{mu}\} = \mathrm{var}\{S(\nu_{self} + \nu_{mu})\} \tag{B.4}$$

We can safely assume that all the terms in the summation over λ are statistically independent complex random variables of zero mean, and that they are identically distributed for the same value of λ. The same applies for the summation over l if random sequences are used, but not if orthogonal sequences are employed. In this case, they are not independent for different values of i and k, since by the definition of orthogonal codes if $c_0(i)$ and $c_k(i)$ are orthogonal over M samples for $k \neq 0$ we have:

$$S\left(\sum_{i=0}^{M-1} c_0(i) \otimes c_k(i) \right) = 0 \tag{B.5}$$

and consequently, since $d_k(i)$ is constant over M symbols,

$$\begin{aligned} S\left(\sum_{i=0}^{M-1} \sum_{l=0}^{L-1} (|g_{0,l}|^2 a_k(i)) \otimes c_0(i) \right) &= \sum_{l=0}^{L-1} |g_{0,l}|^2 S\left(\sum_{i=0}^{M-1} a_k(i) \otimes c_0(i) \right) \\ &= \sum_{l=0}^{L-1} |g_{0,l}|^2 d_k S\left(\sum_{i=0}^{M-1} c_k(i) \otimes c_0(i) \right) = 0 \end{aligned} \tag{B.6}$$

Hence, with the above assumptions, the variance of (B.1) and (B.2) can be given by:

$$\mathrm{var}\{\nu_{self}\} = M\frac{E_c}{2}\sum_{\substack{\lambda=-(L-1)\\ \lambda\neq 0}}^{L-1}\mathrm{var}\left\{\sum_{\substack{l,m\\ l-m=\lambda}}(g^*_{0,m}g_{0,l}a_0(i-\lambda))\otimes c_0(i)\right\} \tag{B.7}$$

and

$$\mathrm{var}\{\nu_{mu}\} = (K-1)M\frac{E_c}{2}\sum_{\substack{\lambda=-(L-1)\\ \lambda\neq 0}}^{L-1}\mathrm{var}\left\{\sum_{\substack{l,m\\ l-m=\lambda}}(g^*_{0,m}g_{0,l}a_k(i-\lambda))\otimes c_0(i)\right\} + \alpha(K-1)M\frac{E_s}{2}\mathrm{var}\left\{\sum_{l=0}^{L-1}(|g_{0,l}|^2 a_k(i))\otimes c_0(i)\right\} \tag{B.8}$$

where α=0 if orthogonal sequences are employed and α=1 if random sequences are used.
The term corresponding to the synchronised signal $a_k(i)$ is easy to calculate. As the multiplier $|g_{0,l}|^2$ has zero phase then

$$\sum_{l=0}^{L-1}(|g_{0,l}|^2 a_k(i))\otimes c_0(i) = \sum_{l=0}^{L-1}|g_{0,l}|^2 a_k(i)\otimes c_0(i) \tag{B.9}$$

where $a_k(i)\otimes c_0(i)$ are complex independent discrete random variables with probability p=1/4 of assuming the values $\pm 1\pm j$, i.e. $\mathrm{var}\{a_k(i)\otimes c_0(i)\}=2$. Hence

$$\mathrm{var}\left\{\sum_{l=0}^{L-1}(|g_{0,l}|^2 a_k(i))\otimes c_0(i)\right\} = 2\left(\sum_{l=0}^{L-1}|g_{0,l}|^2\right)^2 \tag{B.10}$$

However, the variance of $\sum_{\substack{l,m\\ l-m=\lambda}}(g^*_{0,m}g_{0,l}a_k(i-n))\otimes c_0(i)$ is not so obvious due to the off-phase component $\gamma_l=g_{0,l-\lambda}{}^*g_{0,l}$. By making $a=a_k(i)$ and $c=c_0(i)$, we want to obtain $\mathrm{var}\left\{\sum_l(\gamma_l a)\otimes c\right\}$. It is easy to see that this term has zero mean, so that

$$\mathrm{var}\left\{\sum_l(\gamma_l a)\otimes c\right\} = \mathrm{E}\left\{\left|\sum_l(\gamma_l a)\otimes c\right|^2\right\} \tag{B.11}$$

which, according to the definition of the operator $\otimes$ in (2.7) is

$$\mathrm{var}\left\{\sum_l(\gamma_l a)\otimes c\right\} = \mathrm{E}\left\{\left|\sum_l(\gamma_{l_R}a_R c_R-\gamma_{l_I}a_I c_R)\right|^2\right\} + \mathrm{E}\left\{\left|\sum_l(\gamma_{l_R}a_I c_I-\gamma_{l_I}a_R c_I)\right|^2\right\} \tag{B.12}$$

, where x_R is the real part and x_I the imaginary part of the complex value x.

We can safely assume that a_R, a_I, c_R and c_I are independent random variables with probability p=1/2 of assuming a value 1. Then, by manipulating (B.12) we come to the following expression:

$$\mathrm{var}\left\{\sum_l (\gamma_l a) \otimes c\right\} = \sum_l \sum_m \gamma_{l_R}\gamma_{m_R} \mathrm{E}\{a_R^2 c_R^2\} + \sum_l \sum_m \gamma_{l_R}\gamma_{m_I} \mathrm{E}\{a_I^2 c_R^2\} \tag{B.13}$$

$$+ \sum_l \sum_m \gamma_{l_R}\gamma_{m_R} \mathrm{E}\{a_I^2 c_I^2\} + \sum_l \sum_m \gamma_{l_I}\gamma_{m_I} \mathrm{E}\{a_R^2 c_I^2\}$$

It is clear that $\mathrm{E}\{a_R^2 c_R^2\} = \mathrm{E}\{a_I^2 c_R^2\} = \mathrm{E}\{a_I^2 c_I^2\} = \mathrm{E}\{a_R^2 c_I^2\} = 1$, and thus

$$\mathrm{var}\left\{\sum_l (\gamma_l a) \otimes c\right\} = 2\sum_l \sum_m (\gamma_{l_R}\gamma_{m_R} + \gamma_{l_I}\gamma_{m_I}) = 2\left|\sum_l \gamma_l\right|^2 \tag{B.14}$$

By substitution of the results from (B.10) and (B.14) in (B.7) and (B.8) we obtain the desired variances:

$$\mathrm{var}\{\nu_{self}\} = ME_c \sum_{\substack{\lambda = -(L-1) \\ \lambda \neq 0}}^{L-1} \left| \sum_{\substack{l,m \\ l-m=\lambda}} g_{0,m}^* g_{0,l} \right|^2 \tag{B.15}$$

and

$$\mathrm{var}\{\nu_{mu}\} = (K-1)ME_c \sum_{\substack{\lambda = -(L-1) \\ \lambda \neq 0}}^{L-1} \left| \sum_{\substack{l,m \\ l-m=\lambda}} g_{0,m}^* g_{0,l} \right|^2 \tag{B.16}$$

$$+ \alpha(K-1)ME_c \left(\sum_{l=0}^{L-1} |g_{0,l}|^2 \right)^2$$

APPENDIX C. CALCULATION OF THE INTERFERENCE VARIANCE (PRE-RAKE)

We want to obtain the variance of the multi-user interference component:

$$\nu_{mu,\,pR} = \sqrt{\frac{E_c}{2}} \sum_{i=0}^{M-1} \sum_{k=1}^{K-1} \frac{\beta_k}{\beta_0} \left[\sum_{\substack{\lambda = -(L-1) \\ \lambda \neq 0}}^{L-1} \sum_{\substack{l,\,m \\ l-m\,=\,\lambda}} (g^*_{k,\,m} g_{0,\,l} a_k(i-\lambda)) \otimes c_0(i) + \sum_{l=0}^{L-1} (g^*_{k,\,l}\, g_{0,\,l} a_k(i)) \otimes c_0(i) \right] \tag{C.1}$$

If random sequences are used then all the terms in the summation over λ are statistical independent complex random variables of zero mean, and the variance is

$$\begin{aligned} \mathrm{var}\{\nu_{mu,\,pR}\} = M \frac{E_c}{2} \sum_{k=1}^{K-1} \frac{\beta_k^2}{\beta_0^2} \sum_{\substack{\lambda = -(L-1) \\ \lambda \neq 0}}^{L-1} \mathrm{var}\left\{ \sum_{\substack{l,\,m \\ l-m\,=\,\lambda}} (g^*_{k,\,m} g_{0,\,l} a_k(i-\lambda)) \otimes c_0(i) \right\} \\ + \frac{E_c}{2} \sum_{k=1}^{K-1} \frac{\beta_k^2}{\beta_0^2} \mathrm{var}\left\{ \sum_{i=0}^{Q-1} \sum_{l=0}^{L-1} (g^*_{k,\,l}\, g_{0,\,l} a_k(i)) \otimes c_0(i) \right\} \end{aligned} \tag{C.2}$$

The calculation of the variance is similar to the one obtained for a Rake receiver in Appendix B, but the approach must be different if orthogonal sequences are used, since the synchronised terms of the interference signal $g^*_{k,\,l}\, g_{0,\,l} a_{k,\,0}(i)$ are out of phase with the sequence $c_0(i)$ of the desired user.

We can assume that the real and imaginary parts of the interference $\nu_{mu,pR}$ are independent random variables. Now let the function $S(a) = a_R + a_I$, where a_R and a_I are respectively the real and imaginary parts of the complex value a. Then

$$\mathrm{var}\{\nu_{mu,\,pR}\} = \mathrm{var}\{S(\nu_{mu,\,pR})\} \tag{C.3}$$

Suppose we have two orthogonal complex sequences $x(i)$ and $y(i)$ such that

$$S\left(\sum_{i=0}^{M-1} x(i) \otimes y(i) \right) = \sum_{i=0}^{M-1} [x_R(i) y_R(i) + x_I(i) y_I(i)] = 0 \tag{C.4}$$

If the sequence $x(i)$ is multiplied by a complex constant $Ae^{j\theta}$ before correlation with the sequence $y(i)$ we have

$$\begin{aligned} S\left(\sum_{i=0}^{M-1} (Ae^{j\theta} x(i)) \otimes y(i) \right) &= A \sum_{i=0}^{M-1} [x_R(i) y_R(i) \cos\theta - x_I(i) y_R(i) \sin\theta \\ &\qquad + x_I(i) y_I(i) \cos\theta + x_R(i) y_I(i) \sin\theta] \\ &= A \sum_{i=0}^{M-1} [x_R(i) y_I(i) + x_I(i) y_R(i)] \sin\theta \end{aligned} \tag{C.5}$$

We can assume that $x_R(i)$, $x_I(i)$, $y_R(i)$ and $y_I(i)$ are independent random variables with equal probability p=1/2 of assuming the values 1,and, hence, unit variance. With this assumption the variance from the expression in (C.5) is

$$\mathrm{var}\left\{ \sum_{i=0}^{M-1} (Ae^{j\theta}x(i)) \otimes y(i) \right\} = 2MA^2\sin^2\theta \tag{C.6}$$

With this result and the ones from (B.14) we can obtain the desired variance

$$\mathrm{var}\{\nu_{mu,\,pR}\} = ME_c \sum_{k=1}^{K-1} \frac{\beta_k^2}{\beta_0^2} \left[\sum_{\substack{\lambda=-(L-1) \\ \lambda \neq 0}}^{L-1} \left| \sum_{l-m=\lambda}^{l,\,m} g_{k,\,m}^* g_{0,\,l} \right|^2 + \alpha_k \left| \sum_{l=0}^{L-1} g_{k,\,l}^* g_{0,\,l} \right|^2 \right] \tag{C.7}$$

with

$$\alpha_k = \begin{cases} 1 & \text{, if } c_0(i) \text{ and } c_k(i) \text{ are not orthogonal} \\ \sin^2\left(\angle \sum_{l=0}^{L-1} g_{k,\,l}^* g_{0,\,l} \right) & \text{, if } c_0(i) \text{ and } c_k(i) \text{ are orthogonal} \end{cases} \tag{C.8}$$

where $\angle x$ is the phase of the complex x.

APPENDIX D. ON THE ABILITY TO PREDICT THE CHANNEL

In this appendix we will investigate the theoretical limits for channel prediction. First the channel model applied here will be described. Then we will briefly introduce the concept of differential entropy, as described in [10]. We will finally apply this concept to investigate the uncertainty of prediction in Rayleigh faded channels.

D.1. Channel Model

We assume that perfect channel estimations $g_u(n)$ are obtained on the n-th uplink frame and that these are obtained in intervals of T_{TDD}, where T_{TDD} is the TDD duplex frame length. We want to predict the channel gain channel $g_d(n)$ for a given time of the n-th downlink frame, such that δ_T is the difference between the time that the estimate $g_u(n)$ was obtained and the prediction time.

Now let $\boldsymbol{g}_u(n)$ be the vector of the past N+1 channel estimates obtained in the uplink

$$\boldsymbol{g}_u(n) = \left[\mathrm{Re}[g_u(n)]\ \mathrm{Im}[g_u(n)]\ \mathrm{Re}[g_u(n-1)]\ \mathrm{Im}[g_u(n-1)]\ \ldots\ \mathrm{Re}[g_u(n-N)]\ \mathrm{Im}[g_u(n-N)]\right]^{\mathrm{T}}, \quad \text{(D.1)}$$

which will be used for the prediction of $g_d(n)$.

Let us assume that the channel path gain $g(t)$ is a zero-mean complex Gaussian variable with equally distributed independent real and imaginary parts and complex variance var[$g(t)$]=1; i.e., the envelope $|g(t)|$ is Rayleigh distributed. We further assume that $g(t)$ is a random process with classic Doppler spread, such that its power spectral density is given by [34]:

$$S(f) = \begin{cases} \dfrac{1}{\pi f_d \sqrt{1-(f/f_d)^2}} & \text{, if } |f| < f_d \\ 0 & \text{, if } |f| \geq f_d \end{cases} \quad \text{(D.2)}$$

and autocorrelation

$$R(\tau) = J_0(2\pi f_d \tau), \quad \text{(D.3)}$$

where f_d is the Doppler spread and $J_0(\cdot)$ is the zero-order Bessel function of the first kind.

From (D.3) we can obtain the 2(N+1)×2(N+1) covariance matrix of vector $\boldsymbol{g}_u(n)$

$$\boldsymbol{R}_u = \frac{1}{2}\begin{bmatrix} 1 & 0 & J_0(2\pi f_d T_{TDD}) & 0 & J_0(4\pi f_d T_{TDD}) & 0 & \ldots \\ 0 & 1 & 0 & J_0(2\pi f_d T_{TDD}) & 0 & J_0(4\pi f_d T_{TDD}) & \ldots \\ J_0(2\pi f_d T_{TDD}) & 0 & 1 & 0 & J_0(2\pi f_d T_{TDD}) & 0 & \ldots \\ 0 & J_0(2\pi f_d T_{TDD}) & 0 & 1 & 0 & J_0(2\pi f_d T_{TDD}) & \ldots \\ J_0(4\pi f_d T_{TDD}) & 0 & J_0(2\pi f_d T_{TDD}) & 0 & 1 & 0 & \ldots \\ 0 & J_0(4\pi f_d T_{TDD}) & 0 & J_0(2\pi f_d T_{TDD}) & 0 & 1 & \ldots \\ \ldots & \ldots & \ldots & \ldots & \ldots & \ldots & \ldots \end{bmatrix} \quad \text{(D.4)}$$

Let us express the value to be predicted in vector form:

$$\boldsymbol{g}_d(n) = \begin{bmatrix} \mathrm{Re}[g_d(n)] \\ \mathrm{Im}[g_d(n)] \end{bmatrix}, \tag{D.5}$$

which, since $g_d(n)$ has the same statistics as $g_u(n)$, has the following covariance matrix

$$\boldsymbol{R}_d = \frac{1}{2}\begin{bmatrix} 1 & 0 \\ 0 & 1 \end{bmatrix}. \tag{D.6}$$

Let us now define the composite vector

$$\boldsymbol{g}_{ud}(n) = \begin{bmatrix} \boldsymbol{g}_d(n) \\ \boldsymbol{g}_u(n) \end{bmatrix}, \tag{D.7}$$

which has the $2(N+2)\times 2(N+2)$ covariance matrix

$$\boldsymbol{R}_{ud} = \begin{bmatrix} \boldsymbol{R}_d & \boldsymbol{R}'^{\mathrm{T}}_{ud} \\ \boldsymbol{R}'_{ud} & \boldsymbol{R}_u \end{bmatrix} \tag{D.8}$$

with $\boldsymbol{R}'_{ud}$ the $2(N+1)\times 2$ matrix

$$\boldsymbol{R}'_{ud} = \frac{1}{2}\begin{bmatrix} J_0(2\pi f_d \delta_T) & 0 \\ 0 & J_0(2\pi f_d \delta_T) \\ J_0(2\pi f_d (T_{IDD}+\delta_T)) & 0 \\ 0 & J_0(2\pi f_d (T_{IDD}+\delta_T)) \\ J_0(2\pi f_d (2T_{IDD}+\delta_T)) & 0 \\ 0 & J_0(2\pi f_d (2T_{IDD}+\delta_T)) \\ \cdots & \cdots \end{bmatrix} \tag{D.9}$$

D.2. Differential Entropy

Let $x_0,x_1,...,x_{N-1}$ be a set of N continuous random variables with joint probability density function $p(x_0,x_1,...,x_{N-1})$. The joint differential entropy of $x_0,x_1,...,x_{N-1}$is given by

$$h(x_0, x_1, \ldots, x_{N-1}) = -\int p(x_0, x_1, \ldots, x_{N-1}) \log p(x_0, x_1, \ldots, x_{N-1}) dx_0 dx_1 \ldots dx_{N-1} \tag{D.10}$$

and it is a measure of the degree of uncertainty in $x_0, x_1,...,x_{N-1}$.

The conditional differential entropy $h(x_0,x_1,...,x_{M-1}|x_M,x_{M+1},...,x_{N-1})$ is a measure of the degree of uncertainty in $x_0,x_1,...,x_{M-1}$ given that $x_M,x_{M+1},...,x_{N-1}$ are known. It is given by:

$$h(x_0 \ldots, x_{M-1} | x_M, \ldots, x_{N-1}) = -\int p(x_0, \ldots, x_{N-1}) \log p(x_0, \ldots, x_{M-1} | x_M, \ldots, x_{N-1}) dx_0 dx_1 \ldots dx_{N-1}$$

(D.11)

where $p(x_0,...,x_{M-1}|x_M,...,x_{N-1})$ is the conditional probability density function.

Furthermore the conditional differential entropy can also be expressed as [10]:

$$h(x_0,x_1,\ldots,x_{M-1}\big|x_M,x_{M+1},\ldots,x_{N-1}) = h(x_0,x_1,\ldots,x_{N-1}) - h(x_M,x_{M+1},\ldots,x_{N-1}) \quad \text{(D.12)}$$

If $x_0,x_1,...,x_{N-1}$ are jointly Gaussian with covariance matrix $\boldsymbol{R}$ then their joint differential entropy is given by [10]:

$$h(x_0, x_1, \ldots, x_{N-1}) = \frac{1}{2}\log[(2\pi e)^N|\boldsymbol{R}|], \quad \text{(D.13)}$$

where $|\boldsymbol{R}|$ is the determinant of $\boldsymbol{R}$.

D.3. Entropy of Channel Prediction

From (D.12) and (D.13) we obtain the conditional entropy of $\boldsymbol{g}_d(n)$ given that $\boldsymbol{g}_u(n)$ is known, which is:

$$\begin{aligned} h(\boldsymbol{g}_d(n)\big|\boldsymbol{g}_u(n)) &= h(\boldsymbol{g}_{ud}(n)) - h(\boldsymbol{g}_u(n)) \\ &= \frac{1}{2}\log[(2\pi e)^{2(N+1)}\big|\boldsymbol{R}_{ud}\big|] - \frac{1}{2}\log[(2\pi e)^{2N}\big|\boldsymbol{R}_u\big|], \end{aligned} \quad \text{(D.14)}$$

Given that N previous uplink channel values are known, this is a measure of the channel uncertainty at the prediction time in the downlink, and hence a measure of our ability to obtain reliable channel estimates for the downlink at the base station.

In Fig. D.1 the conditional entropy $h(\boldsymbol{g}_d(n)\big|\boldsymbol{g}_u(n))$ is plotted as a function of the product $T_{TDD}f_d$ for several values of the time difference δ_T for N=8.

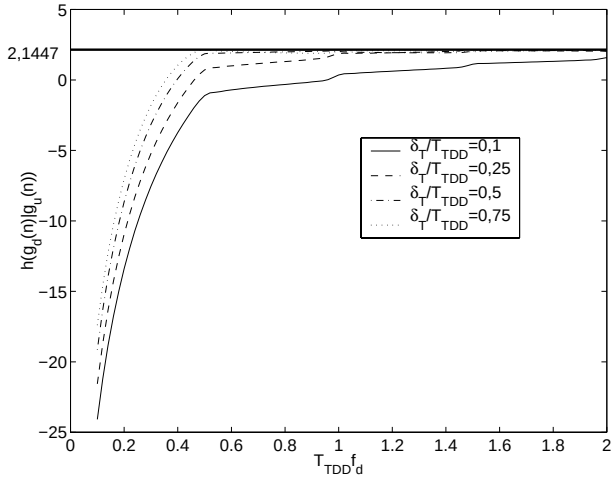

Fig. D.1 - Entropy of Channel Prediction

As $T_{TDD}f_d$ increases the correlation between channel samples diminishes and the channel prediction becomes more difficult. The conditional entropy tends asymptotically to 2,1447, which is the entropy of a complex normal random variable with unit variance if no other information is available. As $T_{TDD}f_d$ tends to zero the entropy tends rapidly to -∞, which means that the channel $g_d(n)$ can be estimated with more certainty if the correlation between samples increases. The uncertainty of the channel prediction also decreases if the time difference δ_T between the prediction time and the last available sample is reduced.

We can view the channel coefficients obtained at the uplink as a sampling of the channel with sampling rate T_{TDD}. The channel gain is a band-limited process with maximum frequency f_d, and, hence, according to the Nyquist theorem [31] it can be ideally reconstructed if $T_{TDD} \leq \frac{1}{2 f_d}$. Consistently with this, it can be seen that in all curves for the prediction entropy there is a turning point at $T_{TDD}f_d$=0,5. For $T_{TDD}f_d$<0,5 it is possible to decrease substantially the prediction entropy with small reductions of $T_{TDD}f_{dc}$, whereas for $T_{TDD}f_d$>0,5 the prediction entropy is always high.

APPENDIX E. THE RLS KALMAN ALGORITHM

The Recursive Least Squares(RLS) Kalman algorithm will be recalled in this appendix, following the description in [31]. Its application to our channel prediction problem will be stressed.

We suppose that the number of paths and their delays are constant and, therefore, we must predict the path amplitudes only. This assumption is consistent if only the fast fading is considered. This can be done for each path separately and the path index l will be dropped from the time-variant channel coefficients $g_l(t)$ to simplify the notation. Let $g_u(n)$ be the channel gain when the training sequence is transmitted in the uplink period of frame n:

$$g_u(n) = g(nT_{TDD} + T_{tr}) \tag{E.1}$$

where T_{tr} is the time delay between the beginning of a TDD frame and the uplink training sequence.

We assume that ideal channel estimation can be performed on reception. Then, based on the set of estimates $\{g_u(0),g_u(1),...,g_u(n)\}$ we want to predict the channel gain for the downlink period of the n-th frame, at a time T_{dl} after the beginning of the TDD frame:

$$g_d(n) = g(nT_{TDD} + T_{dl}) \tag{E.2}$$

The prediction $\hat{g}_d(n)$ can be made for instance with a Finite Impulse Response (FIR) filter of N-th order, which can be expressed in vector form as:

$$\hat{g}_d(n) = \boldsymbol{h}^{\mathrm{T}}(n-1)\boldsymbol{g}_u(n) \tag{E.3}$$

where $\boldsymbol{g}_u(n)$ is the vector of the past N+1 channel estimates obtained in the uplink

$$\boldsymbol{g}_u(n) = \left[g_u(n)\ g_u(n-1)\ \ldots\ g_u(n-N)\right]^{\mathrm{T}} \tag{E.4}$$

and $\boldsymbol{h}(n)$ is the vector of filter coefficients.

The filter coefficients are chosen such that the time-average weighted square error

$$E = \sum_{n=0}^{m} w^{m-n}\left|g_d(n) - \boldsymbol{h}^{\mathrm{T}}(m)\boldsymbol{g}_u(n)\right|^2 \tag{E.5}$$

is minimised, where $0<w<1$ is the forgetting factor.

Now let $\boldsymbol{R}(n)$ be the correlation matrix

$$\boldsymbol{R}(n) = \sum_{m=0}^{n} w^{n-m}\boldsymbol{g}_u{}^{*}(m)\boldsymbol{g}_u{}^{\mathrm{T}}(m) \tag{E.6}$$

and

$$\boldsymbol{P}(n) = \boldsymbol{R}^{-1}(n). \tag{E.7}$$

Starting with initial values $\boldsymbol{h}(-1)$ and $\boldsymbol{P}(-1)$ for the coefficients vector and for the inverse of the correlation matrix respectively, this minimisation can be achieved if at each prediction the following steps are carried out [31]:

- compute prediction value according to (E.3)

- calculate error:

$$e(n) = \hat{g}_d(n) - g_d(n) \tag{E.8}$$

The real value of the downlink channel $g_d(n)$ is in fact not known by the base station, unless some feedback loop is provided. In our implementation the value of $g_d(n)$ was approximated by interpolation of the measured uplink channel in the following frame $g_u(n+1)$ with the past 4 values. Interpolation was made using the method of Lagrange polynomials [30]. Since $g_u(n+1)$ has to be known, this and the following steps have to be carried out in the $(n+1)$-th frame.

- compute the Kalman gain vector:

$$\boldsymbol{K}(n) = \frac{\boldsymbol{P}(n-1)\boldsymbol{g}_u^{\mathrm{T}}(n)}{w + \boldsymbol{g}_u^{\mathrm{T}}(n)\boldsymbol{P}(n-1)\boldsymbol{g}_u^{*}(n)} \tag{E.9}$$

- update the inverse of the correlation matrix

$$\boldsymbol{P}(n) = \frac{1}{w}[\boldsymbol{P}(n-1) - \boldsymbol{K}(n)\boldsymbol{g}_u^{\mathrm{T}}(n)\boldsymbol{P}(n-1)] \tag{E.10}$$

- update the filter coefficients

$$\boldsymbol{h}(n) = \boldsymbol{h}(n-1) + \boldsymbol{K}(n)e(n) \tag{E.11}$$

For our simulations we have chosen an 8-tap filter with initial values $\boldsymbol{h}(-1)=[1,0,0...,0]^{\mathrm{T}}$ and $\boldsymbol{P}(-1)=100\boldsymbol{I}$, where $\boldsymbol{I}$ is the identity matrix; and the forgetting factor was $w=0{,}95$. These parameters were however not optimised to our particular application. The prediction was made once every frame and we tried to predict the channel gains corresponding to the middle of the downlink frame.

APPENDIX F. CONDITIONS FOR OPTIMISATION USING LAGRANGE MULTIPLIERS

We want to obtain the minimum $\boldsymbol{s}_{min}$ of the function $E(\boldsymbol{s}) = \boldsymbol{s}^{\mathrm{T}}\boldsymbol{s}$ with NK constraints given by $\boldsymbol{g}(\boldsymbol{s}) = \boldsymbol{C}^{\mathrm{T}}\boldsymbol{H}\boldsymbol{A}^{\mathrm{T}}\boldsymbol{s} - \boldsymbol{d} = 0$, where the vector $\boldsymbol{s}$ has $2MN$ elements. In order that this problem be solvable by the method of Lagrange multipliers the following conditions are sufficient [43]:

- $K<2M$
- The second derivatives of the functions $f(\boldsymbol{s}_{min})$ and $g_k(\boldsymbol{s}_{min})$ exist and are continuous, where $g_k(\boldsymbol{s}_{min})$ is the k-th component of $\boldsymbol{g}(\boldsymbol{s})$. This is true in our problem, since:

$$\begin{aligned} \nabla^2 E(\boldsymbol{s}) &= 2\boldsymbol{I} \\ \nabla^2 g_k(\boldsymbol{s}) &= 0 \end{aligned} \tag{F.1}$$

  with $\boldsymbol{I}$ the identity matrix, which are continuous for every $\boldsymbol{s}\in\Re^{2MN}$.

- The following condition must be satisfied:

$$\mathrm{Rank}(\nabla \boldsymbol{g}(\boldsymbol{s}_{min})) = NK \tag{F.2}$$

  In our case we have:

$$\nabla \boldsymbol{g}(\boldsymbol{s}) = \boldsymbol{A}\boldsymbol{H}^{\mathrm{T}}\boldsymbol{C} = \left[\boldsymbol{H}_0^{\mathrm{T}}\boldsymbol{C}_0 \;\; \boldsymbol{H}_1^{\mathrm{T}}\boldsymbol{C}_1 \;\; \cdots \;\; \boldsymbol{H}_{K-1}^{\mathrm{T}}\boldsymbol{C}_{K-1}\right] \tag{F.3}$$

  for every $\boldsymbol{s}\in\Re^{2MN}$. From the definitions of $\boldsymbol{H}_k$ and $\boldsymbol{C}_k$ in Section 5.2.1 it can be seen that $\mathrm{Rank}(\boldsymbol{H}_k^{\mathrm{T}}\boldsymbol{C}_k)=N$. It can be safely assumed that the spreading sequences of the K different users are linearly independent and hence $\mathrm{Rank}(\boldsymbol{A}\boldsymbol{H}^{\mathrm{T}}\boldsymbol{C})=NK$.

- Let

$$F(\boldsymbol{s}) = E(\boldsymbol{s}) - \sum_{k=0}^{KN-1} \lambda_k g_k(\boldsymbol{s}) \tag{F.4}$$

  Then the matrix $\nabla^2 F(\boldsymbol{s}_{min})$ must have only positive eigenvalues. It is easy to verify that in our problem we have

$$\nabla^2 F(\boldsymbol{s}) = \nabla^2 E(\boldsymbol{s}) = 2\boldsymbol{I} \tag{F.5}$$

  where $\boldsymbol{I}$ is the $2MN\times 2MN$ identity matrix, which has a KN-fold eigenvalue $\mu=1>0$ for every $\boldsymbol{s}\in\Re^{2MN}$.

Since all the above conditions can be satisfied, a strict constrained minimum of the function $E(\boldsymbol{s})$ can be obtained by solving:

$$\begin{aligned} \nabla F(\boldsymbol{s}_{min}) &= 0 \\ \boldsymbol{g}(\boldsymbol{s}_{min}) &= 0 \end{aligned} \tag{F.6}$$

Furthermore, since the eigenvalues of $\nabla^2 F(\boldsymbol{s}_{min})$ are positive for every $\boldsymbol{s} \in \Re^{2MN}$, the function $F(\boldsymbol{s})$ is strictly convex and we can guarantee that a global minimum can be found this way.

APPENDIX G. NUMERICAL OPTIMISATION OF THE TRANSMIT SIGNAL

G.1. Direct minimisation of the signal vector

We start with any initial value for the $2MN\times1$ vector to be optimised $\boldsymbol{s}_1$ and any strictly positive definite $2MN\times2MN$ matrix $\boldsymbol{B}_0$, for example the identity matrix. We have chosen the initial $\boldsymbol{s}_1$ to be the signal vector obtained with a pre-Rake

$$\boldsymbol{s}_1 = \boldsymbol{A}\boldsymbol{H}^{\mathrm{T}}\boldsymbol{C}\boldsymbol{d}. \tag{G.1}$$

The iterative minimisation procedure is described by the following steps:

I. calculate the direction of minimisation

$$\boldsymbol{g}_i = \boldsymbol{B}_{i-1}\nabla P(\boldsymbol{s}_i) \tag{G.2}$$

where $\nabla P(\boldsymbol{s}_i)$ can be obtained from (5.60).

II. find the usability limit a_i in the direction $\boldsymbol{g}_i$ (see Appendix G.1.1).

III. update vector $\boldsymbol{s}$

$$\boldsymbol{s}_{i+1} = \boldsymbol{s}_i + a_i\boldsymbol{g}_i \tag{G.3}$$

IV. calculate new matrix $\boldsymbol{B}$

$$\boldsymbol{B}_i = \boldsymbol{B}_{i-1} + a_i\frac{\boldsymbol{g}_i\boldsymbol{g}_i^{\mathrm{T}}}{(\nabla P(\boldsymbol{s}_i))^{\mathrm{T}}\boldsymbol{B}_{i-1}\nabla P(\boldsymbol{s}_i)} - \frac{\boldsymbol{B}_{i-1}\boldsymbol{y}_i\boldsymbol{y}_i^{\mathrm{T}}\boldsymbol{B}_{i-1}}{\boldsymbol{y}_i^{\mathrm{T}}\boldsymbol{B}_{i-1}\boldsymbol{y}_i} \tag{G.4}$$

where

$$\boldsymbol{y}_i = \nabla P(\boldsymbol{s}_i) - \nabla P(\boldsymbol{s}_{i+1}) \tag{G.5}$$

The vector $\boldsymbol{s}_i$ converges quadratically to the function minimum. The search can be interrupted if $\|\nabla P(\boldsymbol{s}_i)\| < \varepsilon$, with ε an arbitrary small value.

G.1.1 Finding the Usability Limit

Definition

Let $F(\boldsymbol{x})$ be a function to be minimised over several iterations. In the i-th step of the minimisation, starting from $\boldsymbol{x}_i$ we try to minimise $F(\boldsymbol{x})$ in the direction $\boldsymbol{g}_i$, i.e., we search the optimum $\boldsymbol{x}_{i+1}=\boldsymbol{x}_i+a\boldsymbol{g}_i$.

The direction $\boldsymbol{g}_i$ is a usable direction at $\boldsymbol{x}_i$ if there is a real-valued $a^*>0$ such that $F(\boldsymbol{x}_i+a\boldsymbol{g}_i)<F(\boldsymbol{x}_i)$ for all $0<a<a^*$. The maximum $\bar{a}$ of all possible a^* is the usability limit. In other words, $\bar{a}$ is the line minimum of $F(a)$ over $\Re^+$, which can be found by solving the following equation:

$$\frac{\partial}{\partial a}F(\boldsymbol{x}_i + a\boldsymbol{g}_i) = \boldsymbol{g}_i^{\mathrm{T}}\nabla F(\boldsymbol{x}_i + a\boldsymbol{g}_i) = 0 \tag{G.6}$$

Application to Minimisation Problem

In our particular minimisation problem we want to find a such that

$$\frac{\partial}{\partial a}P(\boldsymbol{s}_i + a\boldsymbol{g}_i) = 0 \tag{G.7}$$

The function to be minimised can be expressed as a function of the step a

$$P(a) = e(a) + \begin{cases} r[G(a)]^2 & \text{,if } G(a) > 0 \\ 0 & \text{,if } G(a) \le 0 \end{cases} \tag{G.8}$$

where

$$e(a) = e(\boldsymbol{s}_i + a\boldsymbol{g}_i) = e(\boldsymbol{s}_i) - 2a\boldsymbol{g}_i^{\mathrm{T}}\boldsymbol{D}\boldsymbol{d} + 2a\boldsymbol{g}_i^{\mathrm{T}}\boldsymbol{D}\boldsymbol{D}^{\mathrm{T}}\boldsymbol{s}_i + a^2\boldsymbol{g}_i^{\mathrm{T}}\boldsymbol{D}\boldsymbol{D}^{\mathrm{T}}\boldsymbol{g}_i \tag{G.9}$$

with $\boldsymbol{D}=\boldsymbol{A}\boldsymbol{H}^{\mathrm{T}}\boldsymbol{C}$, and

$$G(a) = G(\boldsymbol{s}_i) + 2a\boldsymbol{s}_i^{\mathrm{T}}\boldsymbol{g}_i + a^2\boldsymbol{g}_i^{\mathrm{T}}\boldsymbol{g}_i . \tag{G.10}$$

The partial derivative of P in relation to a is

$$\frac{\partial P}{\partial a} = 2\boldsymbol{g}_i^{\mathrm{T}}\boldsymbol{D}(\boldsymbol{D}^{\mathrm{T}}\boldsymbol{s}_i - \boldsymbol{d} + a\boldsymbol{D}^{\mathrm{T}}\boldsymbol{g}_i) + \begin{cases} 4r[G(a)](\boldsymbol{s}_i^{\mathrm{T}} + a\boldsymbol{g}_i^{\mathrm{T}})\boldsymbol{g}_i & \text{,if } G(a) > 0 \\ 0 & \text{,if } G(a) \le 0 \end{cases} . \tag{G.11}$$

The usability limit a is the root of (G.11), which is a cubic function on a if $G(a)>0$, and can be solved as indicated in [43].

G.2. Minimisation of the Modified Data Vector $\underline{\lambda}$

We choose as initial value $\underline{\lambda}_1=\boldsymbol{d}$ and the minimisation process follows the same steps I to IV in Appendix G.1 by substituting $\underline{\lambda}_i$ for $\boldsymbol{s}_i$ in equations (G.2) to (G.5). The gradient $\nabla P(\underline{\lambda})$ can be obtained from (5.65).

G.2.1 Finding the Usability Limit

We are searching now the value of a such that

$$\frac{\partial}{\partial a}P(\underline{\lambda}_i + a\boldsymbol{g}_i) = 0$$

The function to be minimised can be still expressed by (G.8), but now

$$e(a) = e(\underline{\lambda}_i) - 2a\boldsymbol{d}^{\mathrm{T}}\boldsymbol{R}\boldsymbol{g}_i + 2a\boldsymbol{g}_i^{\mathrm{T}}\boldsymbol{R}^{\mathrm{T}}\boldsymbol{R}\underline{\lambda}_i + a^2\boldsymbol{g}_i^{\mathrm{T}}\boldsymbol{R}^{\mathrm{T}}\boldsymbol{R}\boldsymbol{g}_i \tag{G.12}$$

and

$$G(a) = G(\underline{\lambda}_i) + 2a\boldsymbol{g}_i^{\mathrm{T}}\boldsymbol{R}\underline{\lambda}_i + a^2\boldsymbol{g}_i^{\mathrm{T}}\boldsymbol{R}\boldsymbol{g}_i \tag{G.13}$$

where $\boldsymbol{R}$ is given by (5.47).

The partial derivative of P in relation to a is now

$$\frac{\partial P}{\partial a} = 2\boldsymbol{g}_i^{\mathrm{T}}\boldsymbol{R}(\boldsymbol{R}\underline{\lambda}_i - \boldsymbol{d} + a\boldsymbol{R}\underline{\lambda}_i) + \begin{cases} 4r[G(a)](\underline{\lambda}_i^{\mathrm{T}} + a\boldsymbol{g}_i^{\mathrm{T}})\boldsymbol{R}\boldsymbol{g}_i & \text{,if } G(a) > 0 \\ 0 & \text{,if } G(a) \le 0 \end{cases} . \tag{G.14}$$

The usability limit a is now the root of (G.14), which is also a cubic function on a if $G(a)>0$.

REFERENCES

[1] J.B. Andersen, J. Jensen, S.H. Jensen and F. Frederiksen, "Prediction of Future Fading Based on Past Measurements", *Proc. of VTC-Fall '99*, pp. 151-155, Amsterdam, Sep. 1999

[2] G. Auer, G.J.R. Povey and D.I. Laurenson, "Mobile Channel Estimation for Decision Directed Rake Receivers Operating in Fast Fading Radio Channels", *Proc. of ISSSTA'98*, pp.576-579, Sun City, South Africa, Sep. 1998

[3] P.W. Baier, M. Meurer, T. Weber and H. Tröger, "Joint Transmission (JT), an Alternative Rationale for the Downlink of Time Division CDMA Using Multi-Element Transmit Antennas", *Proc. of ISSSTA 2000*, pp. 1-5, New Jersey, USA, Sep. 2000

[4] A.N. Barreto and J.C. Brandão, "The impact of soft-handoff on the downlink capacity of mobile CDMA systems", *Proc. of Brazilian Telecomm. Symposium (SBT'97),* pp. 465-468, Recife, Brazil, Sep. 1997

[5] A.N. Barreto and G. Fettweis, "On The Downlink Capacity of TDD CDMA Systems Using a Pre-Rake", *Proc. of Global Comm. Conf. (Globecom'99)*, pp. 117-121, Rio de Janeiro, Brazil, Dec. 1999

[6] A.N. Barreto and G. Fettweis, "Performance Improvement on DS-Spread Spectrum Systems using a pre- and a post-Rake", *Proc. of Int'l Zurich Seminar on Broadband Comm. (IZS2000)*, Zurich, Switzerland, Feb. 2000

[7] A.N. Barreto, M. Mecking and G. Fettweis, "A Flexible Air interface for Integrated Broadband Mobile Systems", *Proc. of Vehicular Technology Conference (VTC2000)*, pp.1899-1903, Tokyo, Japan, May 2000

[8] M. Brandt-Pearce and A. Dharap, "Transmitter-Based Multiuser Interference Rejection for the Downlink of a Wireless CDMA System in a Multipath Environment", *IEEE Journal on Sel. Areas of Comm.*, pp. 407-417, March 2000

[9] P. Chaudhury, W. Mohr and S. Onoe, "The 3GPP Proposal for IMT-2000", *IEEE Comm. Mag.*, pp. 72-81, Dec. 1999

[10] T. Cover, J.A. Thomas, "*Elements of Information Theory*", John Wiley and Sons, New York, USA, 1991

[11] R. Esmailzadeh and M. Nakagawa, "Pre-Rake Diversity Combination for Direct Sequence Spread Spectrum Mobile Communications Systems", *IEICE Trans. on Comm.*, pp. 1008-1015, Aug. 1993

[12] R. Esmailzadeh, E. Sourour and M. Nakagawa, "Pre-Rake Diversity Combining in Time Division Duplex CDMA Mobile Communications", *IEEE Trans. on Vehicular Tech.*, pp. 795-801, May 1999

[13] T. Eyceoz, A. Duel-Hallen and H. Hallen, "Deterministic Channel Modeling and Long Range Prediction of Fast Fading Mobile Radio Channels", *IEEE Comm. Letters*, pp. 254-256, Sep. 1998

[14] P. Frenger, P. Orten and T. Ottoson, "Code-Spread CDMA using Maximum Free Distance Low-Rate Convolutional Codes", *IEEE Trans. on Comm.*, pp.?, Jan. 2000

[15] B. Friedrichs, "*Kanalcodierung*", Springer, Berlin, 1996

[16] R.G. Gallager, "*Information Theory and Reliable Communication"*, John Wiley and Sons, New York, 1968

[17] K.S. Gilhousen et al., "On the Capacity of a Cellular CDMA System", *IEEE Trans. on Vehicular Technology,* pp. 303-312, May 1991

[18] S. Haykin, "*Adaptive Filter Theory*", Prentice Hall, Upper Saddle River, NJ, USA, 1991

[19] http://www.3GPP.org

[20] J.Y.N. Hui, "Throughput Analysis for Code Division Multiple Accessing of the Spread Spectrum Channel", *IEEE Journal on Sel. Areas in Comm.*, pp. 482-486, Jul. 1984

[21] J. Hwang and J.H. Winters, "Sinusoidal Modeling and Prediction of Fast Fading Processes", *Proc. of GLOBECOM '98*, pp. 892-896, Sydney, Australia, Nov. 1998

[22] D. Hunold, A.N. Barreto, M. Bronzel and G. Fettweis, "Investigations on Capacity in the Integrated Broadband Mobile System (IBMS) Using a Wireless Network Simulator", *Proc. of MoMuC '98*, pp. 325-336, Berlin, Oct. 1998

[23] T.A. Kadous, E. Sourour and S.E. El-Khamy, "Comparison between Various Diversity Techniques of the Pre-Rake Combining System in TDD/CDMA", *Proc. of VTC'97*, pp.2210-2214, Phoenix, USA, May 1997

[24] A. Klein and P.W. Baier, "Linear Unbiased Data Estimation in Mobile Radio Systems Applying CDMA", *IEEE Journal on Sel. Areas in Comm.*, pp. 1058-1066, Sep. 1993

[25] W.C. Lee, "*Mobile Communications Design Fundamentals*", John Wiley & Sons, New York, USA,1993

[26] F.Li, H. Xiao and J. Yang, "On Channel Estimation for Rake Receiver in a Mobile Multipath Fading Channel", *Proc. of ICASSP'94, vol IV,* pp. 577-580, Adelaide, Australia, Apr. 1994

[27] S. Lin, D.J. Costello, Jr., "*Error Control Coding - Fundamentals and Applications*", Prentice Hall, Englewood Cliffs, NJ, USA, 1983

[28] S. Moshavi, "Multi-User Detection for DS-CDMA Communications", *IEEE Comm. Mag,* pp. 124-136, Oct. 1996

[29] A. Papoulis, "*Probability, Random Variables, and Stochastic Processes*", McGraw-Hill, Boston, USA, 1991

[30] W.H. Press, S.A. Teukolsky, W.T. Vetterling, B.P. Flannery, "*Numerical Recipes in C*", Cambridge University Press, Cambridge, UK, 1992

[31] J. G.Proakis, "*Digital Communications*", McGraw-Hill, New York, USA, 1995

[32] T. Rappaport, "*Wireless Communications: Principles & Practice*", Prentice-Hall, Upper Saddle River, NJ, USA, 1996

[33] H. Sari, F. Vanhaverbeke and M. Moeneclaey, "Extending the Capacity of Multiple Access Channels", *IEEE Comm. Mag.*, pp. 74-83, Jan. 2000

[34] B. Sklar, "Rayleigh Fading Channels in Mobile Digital Communication Systems. Part I : Characterization", *IEEE Comm. Mag.*, pp. 136-146, Sep. 1997

[35] Tdoc 3GPP TSGR1#6(99)918, "*Tx Diversity with Joint Predistortion*", ftp://ftp.3gpp.org/TSG_RAN/WG1_RL1/TSGR1_06/Docs/Pdfs/r1-99918.PDF

[36] TIA/EIA-IS95B, "*Mobile Station-Base Station Compatibility Standard for Dual-Mode Wideband Spread Spectrum Cellular Systems"*, July 1997

[37] A.J. Viterbi, “Very Low Rate Convolutional Codes for Maximum Theoretical Performance of Spread-Spectrum Multiple-Access Channels”, *IEEE Journal on Sel. Areas in Comm.*, pp 641-649, May 1990

[38] A.M. Viterbi and A.J. Viterbi, “Erlang capacity of a power controlled CDMA system”, *IEEE Journal on Sel. Areas in Comm.*, pp. 892-900, Aug. 1993

[39] A.J. Viterbi, “*CDMA: Principles of Spread Spectrum Communication”*, Addison-Wesley, Reading, MA, USA, 1995

[40] B.R. Vojcic, W.M. Jang, “Transmitter Precoding in Synchronous Multiuser Communications”, *IEEE Trans. on Comm.*, pp. 1346-1355, Oct. 1998

[41] L. Wilhelmsson and K.Sh. Zigangirov, “Coordinated Pre-coding for the Forward-link in DS-CDMA”, *Proc. of GLOBECOM ’97*, pp. 1509-1513, Phoenix, USA, Nov. 1997

[42] J. Yang, M. Rajan, “Microcell Performance Evaluation in IS-95 Based CDMA Networks”, *Proc. of Int’l Conference on Universal Personal Comm. (ICUPC ‘98)*, pp. 899-903, Florence, Italy, Oct. 1998

[43] E. Zeidler et al., “*Teubner-Taschenbuch der Mathematik*”, Teubner Verlag, Leipzig 1996

[44] E. Zeidler et al., “*Teubner-Taschenbuch der Mathematik - Teil II*”, Teubner Verlag, Leipzig 1995

LIST OF FREQUENTLY USED SYMBOLS AND ACRONYMS

Symbols

$\boldsymbol{A}$	addition matrix
$a(\cdot)$, $a_k(\cdot)$	complex scrambled sequence (of k-th user)
$\boldsymbol{C}$, $\boldsymbol{C}_k$	spreading marix (of k-th user)
$c(\cdot)$, $c_k(\cdot)$	scrambling sequence (of k-th user)
d, $d(\cdot)$, $d_k(\cdot)$	coded bits (of k-th user) repeated M times
$\boldsymbol{d}$, $\boldsymbol{d}_k$	vector of trnasmitted bits ((of k-th user)
E_b	energy of a data bit
E_c	chip energy
f_c	carrier frequency
f_d	Doppler spread
G	processing gain (chips/data bit)
$\boldsymbol{g}$	channel gains vector
$g_{l,}$ $g_{k,l}$	gain of l-th path (of k-th user)
$\boldsymbol{H}$, $\boldsymbol{H}_k$	channel matrix (of k-th user)
$h(.)$	channel impulse response
i	discrete-time index
I	number of iterations
$\boldsymbol{I}$	identity matrix
I_0, $I_{0,\,pR,}$ $I_{0,\,pRp}$	power spectral density of interference (with a pre-Rake or with a post-Rake)
Im[·]	imaginary part of
K	number of users
K_{ort}	number of orthogonal users
k	user index
L	number of resolvable paths
l	path index
M	chips per coded bit
m	Rake finger index
m_o	memory order of convolutional code
N	noise variance or number of coded bits in a block (it should be clear from the context)
N_0	power spectral density of complex Gaussian white noise
$O(\cdot)$	order of complexity

R	coding rate
$\boldsymbol{R}$	correlation matrix
Re[·]	real part of
$\Re$	set of real numbers
$r_k(\cdot)$, $r_{k,\,pR}(\cdot)$	discrete-time received signal of k-th user (with pre-Rake)
$s(\cdot)$, $s_{pR}(\cdot)$	discrete-time transmitted signal (with pre-Rake)
$\boldsymbol{s}$	transmit signal vector
$\boldsymbol{T}$	transformation matrix
T_c	chip period
T_{coh}	coherence time
T_{TDD}	TDD duplex frame duration
t	time variable
V	velocity
v	decision variable
var{·}	variance of
$x(\cdot)$, $x_k(\cdot)$	discrete-time spread signal
$\boldsymbol{x}$, $\boldsymbol{x}_k$	spread signal vector
$y(\cdot)$, $y_{pRp}(\cdot)$	output of Rake receiver or received signal with a pre-Rake (with post-Rake)
z, z_k	complex output of integrate-and-dump at receiver (of k-th user)
α, α_k	orthogonality factor (of k-th user)
β, β_k	pre-Rake normalisation factor (of k-th user)
Γ	bit-energy-to-noise-spectral-density ratio
γ_l, $\gamma_{k,l}$	l-th tap gain of convolution of channel and pre-Rake (of k-th user)
$\delta(\cdot)$	Dirac impulse
λ	discrete delay index
λ_c	carrier wavelength
ν, $\underline{\nu}$	Gaussian noise, Gaussian noise vector
.*	complex conjugate of
$\lvert\cdot\rvert$	magnitude of a complex number
$\lVert\cdot\rVert$	norm of a vector
$\angle\cdot$	phase of a complex number
$\overline{\cdot}$	mean value of
$\cdot\otimes\cdot$	separate multiplication of real and imaginary parts of two complex numbers

Acronyms

AWGN	Additive White Gaussian Noise
BER	Bit Error Rate
CDMA	Code Division Multiple Access
CSI	Channel State Information
DS-SS	Direct Sequence Spread-Spectrum
FDD	Frequency Division Duplexing
FDMA	Frequency Division Multiple Access
FH-SS	Frequency Hopping Spread Spectrum
LOS	Line-of-Sight
MC-SS	Multi Carrier Spread Spectrum
QoS	Quality of Service
QPSK	Quaternary Phase Shift Keying
RLS	Recursive Least Squares
SNR	Signal-to-Noise Ratio
TDD	Time Division Duplexing
TDMA	Time Division Multiple Access
WLL	Wireless Local Loop